

PROJECT ADMINISTRATION DATA SHEET



ORIGINAL



REVISION NO. _____

Project No. E-18-626DATE 9/2/82Project Director: Dr. James F. BenzelSchool/Dept. Ceramic EngineeringSponsor: U.S. Department of the Interior Bureau of MinesType Agreement: Contract No. J0123041Award Period: From 8/20/82 To 5/19/83 (Performance) 8/19/83 (Reports)Sponsor Amount: \$37,000

Contracted through:

Cost Sharing: \$16,600 (E-18-316)

GTRI/CIT

Title: Fundamental Investigation of Phosphate Bonding

ADMINISTRATIVE DATA

OCA Contact Faith G. Costello x4820

1) Sponsor Technical Contact:

Rustu KalyoncuTech. Proj. officerTuscaloosa Research CenterUniv. of ALABAMA

(address to be provided in notification letter)

PH: (205) 229-2971

2) Sponsor Admin/Contractual Matters:

Oliver H. Snyder, III, Contracting OfficerU.S. Bureau of MinesBranch of Procurement Washington2401 E Street NWWashington, D.C. 20241

(202) 634-4700

Security Classification: n/aDefense Priority Rating: n/a

RESTRICTIONS

See Attached Gov't Supplemental Information Sheet for Additional Requirements.

Travel: Foreign travel must have prior approval - Contact OCA in each case. Domestic travel requires sponsor approval where total will exceed greater of \$500 or 125% of approved proposal budget category.

Equipment: Title vests with Sponsor; however, none proposed

COMMENTS:



COPIES TO:

Administrative Coordinator
Research Property Management
Accounting
Procurement/EES Supply Services
FORM OCA 4:781Research Security Services
Reports Coordinator (OCA)
Legal Services (OCA)
LibraryEES Public Relations (2)
Computer Input
Project File
Other _____

SPONSORED PROJECT TERMINATION/CLOSEOUT SHEETDate 7/3/84Project No. E-18-626School/Lab ~~XXX~~ Ceramic Engineering

Includes Subproject No.(s) _____

Project Director(s) Dr. James F. BenzelGTRI / ~~GPI~~Sponsor U. S. Department of the Interior Bureau of MinesTitle Fundamental Investigation of Phosphate BondingEffective Completion Date: 8/20/83 (Performance) 11/20/83 (Reports)

Grant/Contract Closeout Actions Remaining:

- ☐ None
- ☐ Final Invoice or Final Fiscal Report
- ☐ Closing Documents
- ☐ Final Report of Inventions
- ☒ Govt. Property Inventory & Related Certificate
- ☐ Classified Material Certificate
- ☐ Other _____

Continues Project No. _____ Continued by Project No. _____

COPIES TO:

Project Director
Research Administrative Network
Research Property Management
Accounting
Procurement/EES Supply Services
Research Security Services
Reports Coordinator (OCA)
Legal Services

Library
GTRI
Research Communications (2)
Project File
Other I. Newton

FUNDAMENTAL INVESTIGATION OF PHOSPHATE BONDING

QUARTERLY PROGRESS REPORT NO. 1

20 AUGUST - 30 NOVEMBER 1982

Submitted to:

U. S. Bureau of Mines
2401 E Street
Washington, D.C. 20241

Contract No. J0123041

Submitted by:

James F. Benzel
School of Ceramic Engineering
Georgia Institute of Technology
Atlanta, Georgia 30332

Fundamental Investigation of Phosphate Bonding

Quarterly Progress Report No. 1
20 August - 30 November 1982

I. Introduction

Since Kingery's (Ref. 1) literature review in 1950, the amount of published information on phosphate bonding has been greatly expanded. Chvatal's 1975 review (Ref. 2), which concentrated primarily on the 1965 to 1975 literature, contained 222 references. Most of the effort represented by these publications has been devoted towards empirically investigating phosphate bonding materials and development of useful refractory products.

The effect of variables, such as temperature, soaking time, particle size, concentration of bonding agent and source of raw materials on the form, and relative abundance of the reaction products present in a number of phosphate bonded systems, have been investigated. However, there is still little fundamental physiochemical information about phosphate bonding in the literature. This is not surprising when the complexity of the multistep reactions, the difficulty in differentiation between the many possible reaction products and the fine grain sized polycrystalline nature of materials being bonded are taken into consideration.

Thus, it appears that fundamental investigations on phosphate bonding should be performed on simple model systems. This study involves the use of single crystals to accomplish this goal. The major portion of this investigation will be carried out using single crystals of materials (i.e. alumina, quartz, magnesia, magnesium aluminate spinel and stabilized

zirconia) and phosphate binding agents (i.e. orthophosphoric acid, mixtures of chromic and orthophosphoric acid, monoaluminum phosphate and sodium phosphate glasses) commonly incorporated in phosphate bonded refractories. However, materials, such as fused silica and single crystals of materials not normally used in refractories, such as magnesium fluoride and silicon metal, will also be utilized.

The reaction of phosphate bonding agents with different crystallographic faces of single crystals will be studied after various heat treatments. The effect of interatomic spacing and atomic planar density of the material being bonded will be investigated by rejoining single crystals, cleaved or cut along low order planes, such as 100, 110, or 111, with various phosphate bonding agents.

The effect of interfacial crystallographic misorientations (tilt, twist and combinations of both) on the strength of phosphate bonds will be investigated using phosphate bonded bicrystals. It is anticipated that there is a relationship between the strength of phosphate bonding and the degree of mismatch between the bonded faces.

An attempt will be made to evaluate the effect of the atomic structure of the material being bonded on the strength of the resulting phosphate bond formation. The role of the anion in phosphate bonding will also be investigated.

II. Status of Investigation

A. Single Crystal and Raw Material Procurement

Single crystals of alumina, magnesia, magnesium aluminate and quartz are on hand. Fused silica rods, phosphoric acid, chromic acid, sodium dihydrogen phosphate and one long chain phosphate glass have also been delivered. Some of the required diamond saw blades have also been

received. It is expected that most of the needed single crystals, diamond saw blades and chemicals will be delivered during the second quarter.

B. Single Crystal Orientation

Many of the experiments to be carried out during this investigation require the orientation of single crystals. The orientation of single crystals involves two basic tasks. First, an unknown orientation must be determined and the crystal must then be rotated to the desired orientation.

Preuss (Ref. 3) has developed two Fortran IV computer programs designed to reduce the time required to accomplish single crystal orientations, using the conventional Laue back reflection method (Ref. 4). The unknown orientation is first determined using a program called PLOMAC (Ref. 5). A second program named COL (Ref. 6) is then used to plot the back reflection Laue pattern for the desired orientation. These two programs then allow the amount of rotation required to translate the crystal to the desired orientation (Ref. 7) to be calculated. Crystals of alumina, magnesia and quartz have been successfully oriented using $\text{CuK}\alpha$ radiation. Optimum conditions for producing back reflection Laue patterns using 3000 speed Type 57 Polaroid film have been determined: 35 kV, 20 ma and 10-20 minute exposure times.

C. Formation of Bicrystals

Preliminary attempts to form alumina, magnesia and quartz bicrystals by phosphate bonding have been successful. Bicrystals have been produced using both phosphoric acid and sodium dihydrogen phosphate as the bonding agent. Samples cured at 1093°C for four hours were strong enough to be easily handled except for the quartz ones which broke during the β to α inversion at 570°C . During these preliminary experiments, neither bond thickness nor crystal orientation was controlled.

D. Reaction of Phosphate Bonding Agents with Different Crystallographic Faces of Single Crystals

A drop of phosphoric acid (61 w/o P_2O_5) or a 1:1 mixture of phosphoric acid (61 w/o P_2O_5) and chromic acid (61 w/o CrO_3) was placed on lapped surfaces of alumina, fused silica and quartz specimens. The alumina and quartz specimens were single crystals. The acid solutions were placed on the (0001) face of the quartz crystals. The orientation of the alumina crystals was not determined, but was perpendicular to the surface of an as grown rod.

The acid solutions were dried at about 80°C for at least six hours and then fired at 370, 815 or 1093°C. After cooling, a diamond saw cut was made about two-thirds of the way through the sample in the face opposite from the one on which the reaction had taken place. The reaction face was then fractured by gently tapping a wedge placed in the cut. The fractured samples were then mounted on SEM stubs and sputtered with gold.

The alumina, fused silica and quartz samples reacted with phosphoric acid at 815°C and the alumina crystal reacted with the chromic-phosphoric acid mixture at 815°C were examined with an SEM. The surface of the alumina-phosphoric acid reaction area was made up primarily of dendrites, which appeared to be crystalline. Below the dendrites, there was a layer that contained a small amount of porosity and may have been amorphous. Beneath this layer, there may be a very thin layer of crystalline material. However, the structure observed could also have been the result of the acid roughening the surface of the alumina crystal. In some places, a crack between the amorphous layer and the alumina or between the thin crystalline layer and the amorphous layer was observed.

The reaction products formed when the acid mixture was reacted with an alumina crystal were friable and appeared to be very porous. The SEM showed

the top surface of these reaction products to consist of many small needle-like crystals. It also appeared that some of the reaction layer was either broken off or crushed during the cutting and mounting procedures. Below this surface, a very porous amorphous appearing layer was present. This layer appeared to be tightly adherent to the surface of the alumina crystal.

The top surface of the phosphoric acid-quartz reaction products appeared to be composed primarily of plate-like crystals. The material below this surface was granular in nature and appeared to be tightly bonded to the surface of the quartz. The surface of the phosphoric acid-fused silica reaction products was composed of amorphous looking spheres and plate-like crystals that appeared to have grown out of the spheres. Below the surface, the coating was made up of the amorphous spheres with voids between the spheres. Some cracks developed in the quartz crystal when it was cooled through the β to α transition. The fused silica surface appeared to have been attacked much more severely than either the quartz or the alumina crystals. In one of these attacked areas, small plate-like crystals were observed. The limited observations described above appear to indicate that the observation of fractured surfaces instead of polished surfaces (Ref. 8) may give a better understanding of phosphoric acid-oxide reaction phases and morphologies.

III. Future Work

During the second quarter, the work on the reaction of phosphate bonding agents with different crystallographic faces of single crystals will be continued. X-ray and electron diffraction investigations will be made in an attempt to identify the crystalline appearing morphologies that are observed.

The effect of interatomic spacing and atomic planar density of the materials being phosphate bonded will also be investigated. Single crystals

of materials, such as alumina, magnesia and quartz, will be cleaved or cut along low order planes, such as 100, 110 or 111, and then rejoined with various phosphate bonding agents to form bicrystals. The strength and morphology of these bonds will be determined.

IV. References

1. W. D. Kingery, "Fundamental Study of Phosphate Bonding in Refractories: I. Literature Review," J. Am. Ceram. Soc., (33) 239-41 (1950).
2. T. Chvatal, "The Position of Refractory Phosphate Bonding Today," Sprechsaal Keram. Glas. Baustoffe, (108) 576, 78, 80, 82-89 (1975).
3. E. Preuss, B. Krahe-Urban and R. Butz, Laue Atlas, John Wiley and Sons, London, pp 60-67 (1974).
4. B. D. Cullity, Elements of X-ray Diffraction, Addison-Wesely Publishing Co., London, pp 239-59 (1978).
5. E. Preuss, "Plot Program for Laue Patterns and Stereographic Projections," Computer Physics Comm., (18) 261-275 (1979).
6. E. Preuss, "Calculation of Crystal Orientation Using Laue Patterns," *ibid*, 277-280.
7. E. Preuss, "A Simplified Procedure for Orientation of Single Crystals of Any Structure," Acta Cryst., (A29) 86-90 (1978).
8. M. J. O'Hara, J. J. Duga and H. D. Sheets, Jr., "Studies in Phosphate Bonding," Bull. Am. Ceram. Soc., (51) 590-95 (1972).

FUNDAMENTAL INVESTIGATION OF PHOSPHATE BONDING

QUARTERLY PROGRESS REPORT NO. 2

1 DECEMBER 1982 - 28 FEBRUARY 1983

Submitted to:

U. S. Bureau of Mines
2401 E Street
Washington, D.C. 20241

Contract No. J0123041

Submitted by:

James F. Benzel
School of Ceramic Engineering
Georgia Institute of Technology
Atlanta, Georgia 30332

Fundamental Investigation of Phosphate Bonding

Quarterly Progress Report No. 2
1 December 1982 - 28 February 1983

I. Introduction

Since Kingery's (Ref. 1) literature review in 1950, the amount of published information on phosphate bonding has been greatly expanded. Chvatal's 1975 review (Ref. 2), which concentrated primarily on the 1965 to 1975 literature, contained 222 references. Most of the effort represented by these publications has been devoted towards empirically investigating phosphate bonding materials and development of useful refractory products.

The effect of variables, such as temperature, soaking time, particle size, concentration of bonding agent and source of raw materials on the form, and relative abundance of the reaction products present in a number of phosphate bonded systems, have been investigated. However, there is still little fundamental physiochemical information about phosphate bonding in the literature. This is not surprising when the complexity of the multistep reactions, the difficulty in differentiation between the many possible reaction products and the fine grain sized polycrystalline nature of materials being bonded are taken into consideration.

Thus, it appears that fundamental investigations on phosphate bonding should be performed on simple model systems. This study involves the use of single crystals to accomplish this goal. The major portion of this investigation will be carried out using single crystals of materials (i.e. alumina, quartz, magnesia, magnesium aluminate spinel and stabilized zirconia) and phosphate binding agents (i.e. orthophosphoric acid, mixtures of chromic and orthophosphoric acid, monoaluminum phosphate and sodium

phosphate glasses) commonly incorporated in phosphate bonded refractories. However, materials, such as fused silica and single crystals of materials not normally used in refractories, such as magnesium fluoride and silicon metal, will also be utilized.

The reaction of phosphate bonding agents with different crystallographic faces of single crystals will be studied after various heat treatments. The effect of interatomic spacing and atomic planar density of the material being bonded will be investigated by rejoining single crystals, cleaved or cut along low order planes, such as 100, 110, or 111, with various phosphate bonding agents.

The effect of interfacial crystallographic misorientations (tilt, twist and combinations of both) on the strength of phosphate bonds will be investigated using phosphate bonded bicrystals. It is anticipated that there is a relationship between the strength of phosphate bonding and the degree of mismatch between the bonded faces.

An attempt will be made to evaluate the effect of the atomic structure of the material being bonded on the strength of the resulting phosphate bond formation. The role of the anion in phosphate bonding will also be investigated.

II. Status of Investigation

A. Single Crystal Orientation

The computer program, PLOMAC (Ref. 3), was modified to plot Laue patterns of sapphire (alumina) and quartz more accurately. The (hk.l) of the desired plane, along with the lattice parameters (a, b, c) and (α , β , γ) of the crystal are fed into the program and the program calculates the coordinates and intensities for the Laue pattern. The Laue pattern can then be plotted manually or by using a Calcomp plotter.

B. Reaction of Phosphate Bonding Agents with Different Crystallographic Faces of Single Crystals of Alumina

A drop of 85% Phosphoric Acid (61% P_2O_5) was placed on lapped surfaces of alumina specimens. The orientations of these surfaces were determined to be (0001), (11 $\bar{2}$ 0), and (11 $\bar{0}$ 0). The acid solutions were dried at 80°C for four hours and then fired to 1500°F for four hours. After cooling in the furnace to room temperature, the reaction face was fractured by gently tapping a wedge placed in a diamond saw cut made in the back face before firing. The fractured samples were then mounted on SEM stubs and sputtered with gold.

The morphology of these alumina samples were examined with the SEM. At 100X, the (0001) face appeared to be primarily covered with whitish, star-shaped crystals on a gray crystalline background. A few grayish, star-shaped crystals were also observed. At higher magnifications, these star-shaped crystals were observed to be composed of dendrites (see Figures 1 and 2). These types of crystal morphologies were also seen on (1120) and (1100) faces. However, a smaller percentage of these surfaces were covered with the star-shaped crystals.

EDAX analysis of the whitish star-shaped crystals indicated that their Al:P ratio was 1:3. This suggests that they are composed of aluminum meta phosphate ($Al(PO_4)_3$). This phase is reported to be the major phase present on the surfaces of alumina (Ref. 1) that had been heat treated above 500°C.

EDAX analysis of the grayish star-shaped crystals and the grayish crystalline background material indicated an Al:P ratio of approximately 1:1.07, which suggests they are composed of monoaluminum phosphate ($AlPO_4$). This compound can exist in several polymorphic forms (berlinite, cristoballite, or tridymite). The different growth morphologies may



Figure 1. Whitish Star-Shaped Dendritic Crystal Produced by Reacting H_3PO_4 with (0001) Face of Alumina at 1500°F (610X).

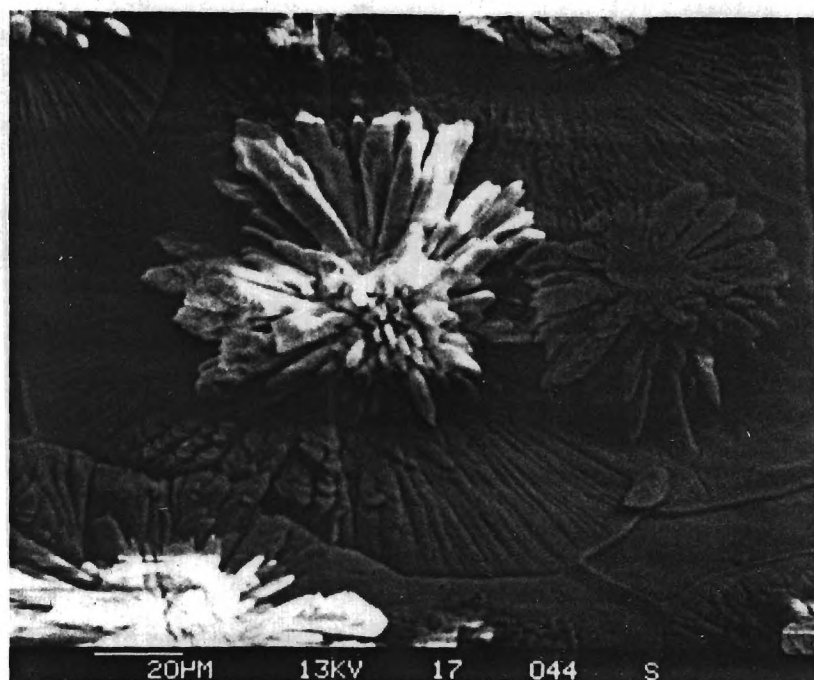


Figure 2. Whitish and Grayish Star-Shaped Dendritic Crystals Produced by Reacting H_3PO_4 with (0001) Face of Alumina at 1500°F (600X).

indicate the presence of two of these polymorphs. In addition to the slightly different growth morphologies of the $\text{Al}(\text{PO}_4)_3$ and AlPO_4 (MAP) dendritic structures, at higher magnifications (Figures 3 and 4) it can clearly be seen that the MAP crystals contain much more porosity. The flat interlocking MAP crystals covering the surface of the alumina appear to have nucleated at a central location and then to have grown outward until they encountered another group of crystals growing in a different direction.

Similar morphologies were seen on the $(1\bar{1}00)$ and $(11\bar{2}0)$ faces. However, it appeared that the whitish dendritic stars occurred much less frequently than on the (0001) face. This is probably due to the fact that the (0001) face has a different atomic packing factor than the $(1\bar{1}00)$ and $(11\bar{2}0)$ faces.

C. Formation of Bicrystals of Alumina

The sapphire single crystals used for this part of the study had zero porosity and very low dislocation density, and well oriented faces ($\pm 30'$). Preliminary attempts to form bicrystals were made using 85% H_3PO_4 (61% P_2O_5) as the bonding agent with bond thicknesses of 0.002 to 0.007" (before firing). In general, the strength of the bicrystals, bonded at 1500°F, was low and decreased as the thickness of the bond was increased. Since the separation of the bicrystals before bonding could not be accurately controlled below 0.002" (using feeler gauges), a new series of bicrystals were formed under varying loads during the heat treatment process. These bicrystals were strong enough to be easily handled. Examination of these samples in the SEM indicated that their bond thicknesses were all less than 0.002".

Three series of bicrystals were formed at 750°F, 1500°F and 2000°F. In each series, (0001) faces were bonded to (0001) faces and

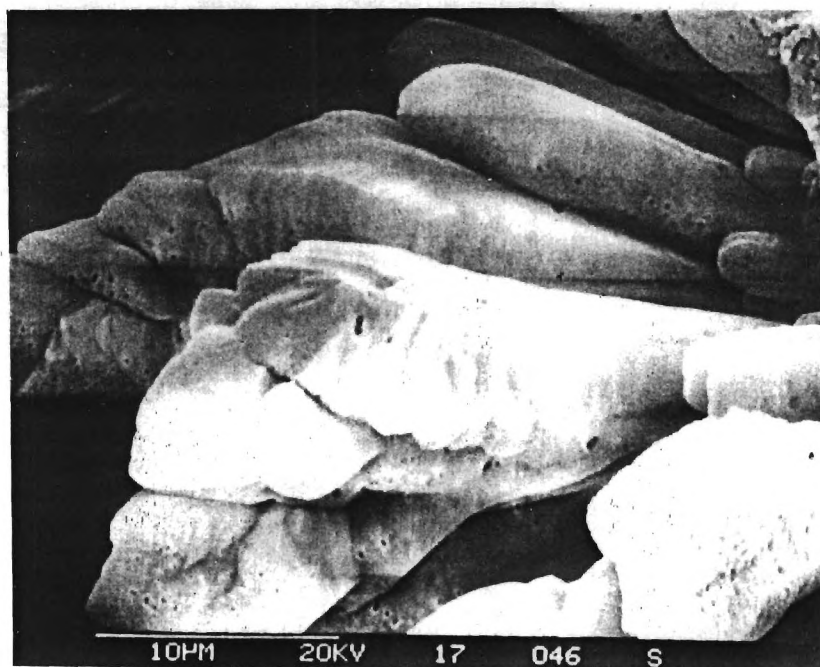


Figure 3. Structure of Aluminum Meta Phosphate ($\text{Al}(\text{PO}_4)_3$) Dendrites (3200X).

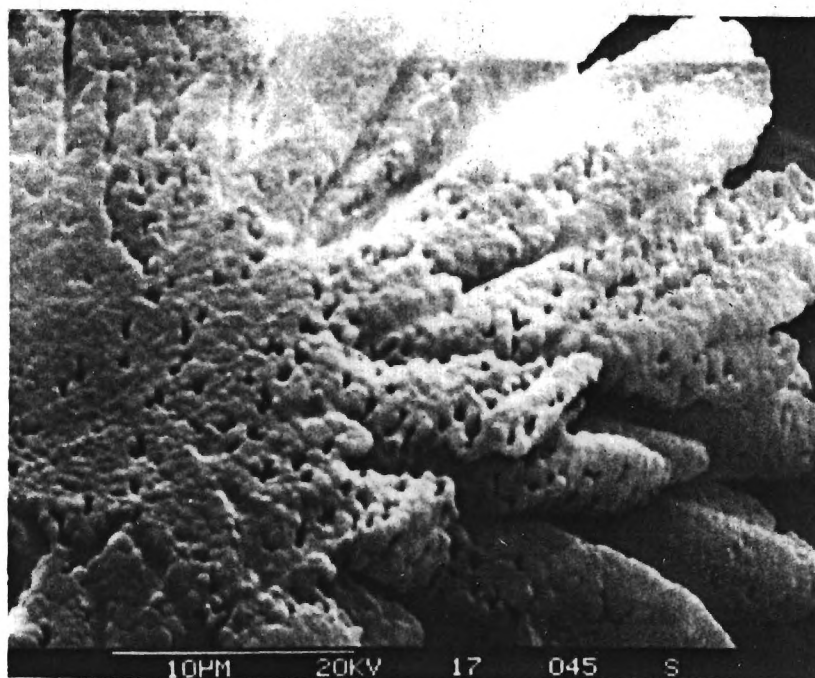


Figure 4. Porous Morphology of Monoaluminum Phosphate (AlPO_4) Dendritic Structure (3200X).

(11 $\bar{2}$ 0) faces were joined to (11 $\bar{2}$ 0) faces using three different bonding agents and various loads. The three bonding agent solutions used were 85% H_3PO_4 (61.1% P_2O_5), $\text{NaH}_2\text{PO}_4 \cdot \text{H}_2\text{O}$ (30% P_2O_5) and Glass H (NaPO_3)₂₀ (30% P_2O_5).

The tensile strength of the bonds were determined using an Instron Universal Testing Machine. The results are given in Table I. These results show that there is a positive relationship between bond strength and firing temperature. In general, the strength of the (0001) bicrystals were stronger than the (11 $\bar{2}$ 0) bicrystals. The samples prepared with H_3PO_4 as the bonding agent were the weakest and those prepared with Glass H were the strongest. In every case where a comparison was possible, the samples cured under the higher load (200 gms) were stronger.

D. Morphology of Fractured Samples

The bicrystals heat treated to 1500°F were selected for morphological study after strength testing. The fracture morphologies of Glass H and $\text{NaH}_2\text{PO}_4 \cdot \text{H}_2\text{O}$ bonded bicrystals were basically the same (Figures 5 and 6), and showed that the bond is formed from interlocking cones that join the two faces of the bicrystals together. It also can be seen that voids existed between many of the cones and that the direction of fracture was parallel to the bicrystal faces. The fracture morphology of H_3PO_4 bonded bicrystals was entirely different from what was observed when H_3PO_4 was fired on the surface of a crystal. In general, the H_3PO_4 bond appeared to be very porous and none of the dendritic structures seen on the crystal surfaces were observed.

III. Future Work

During the next quarter, the effect of firing temperature,

Table I. Tensile Strength of Phosphate Bonded Bicrystals

Heat Treatment Temperature (°F)	Bonding Agent	Load Applied During Firing (gms)	Bicrystal Faces Bonded	Tensile Strength (kgf/cm ²)
750	NaH ₂ PO ₄ ·H ₂ O	200	(0001)	20.9
750	Glass H	100	(0001)	19.3
1500	H ₃ PO ₄	200	(0001)	21.5
1500	NaH ₂ PO ₄ ·H ₂ O	100	(0001)	77
1500	NaH ₂ PO ₄ ·H ₂ O	200	(0001)	83
2000	NaH ₂ PO ₄ ·H ₂ O	100	(0001)	65
2000	NaH ₂ PO ₄ ·H ₂ O	200	(0001)	89
2000	NaH ₂ PO ₄ ·H ₂ O	100	(11 $\bar{2}$ 0)	16.5
2000	NaH ₂ PO ₄ ·H ₂ O	200	(11 $\bar{2}$ 0)	29
2000	Glass H	100	(0001)	64
2000	Glass H	200	(0001)	16.0
2000	Glass H	200	(11 $\bar{2}$ 0)	17.5

Bicrystals that broke due to handling were not reported.

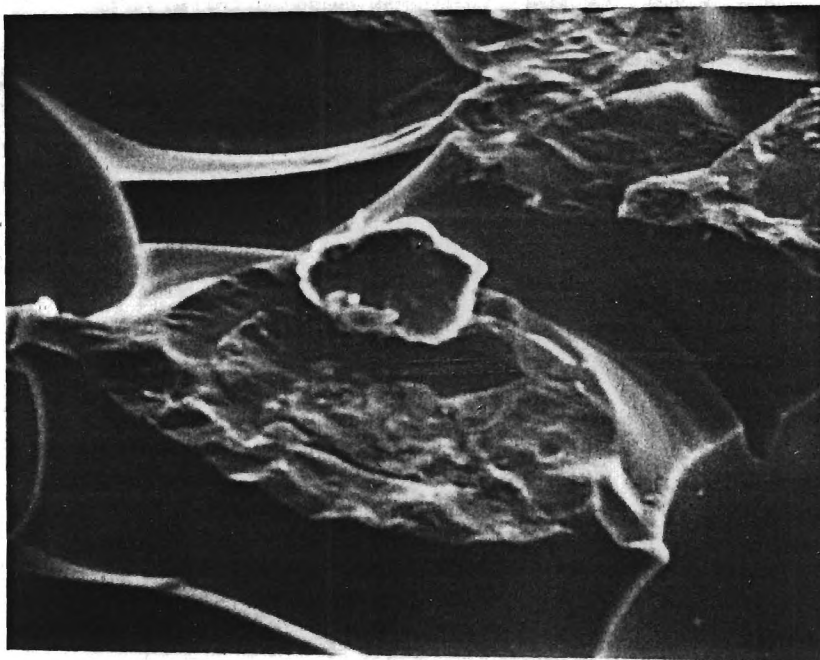


Figure 5. Fracture Morphology of $\text{NaH}_2\text{PO}_4 \cdot \text{H}_2\text{O}$ Bond Between (0001) Faces of Alumina Single Crystals Fired at 1500°F (1200X).

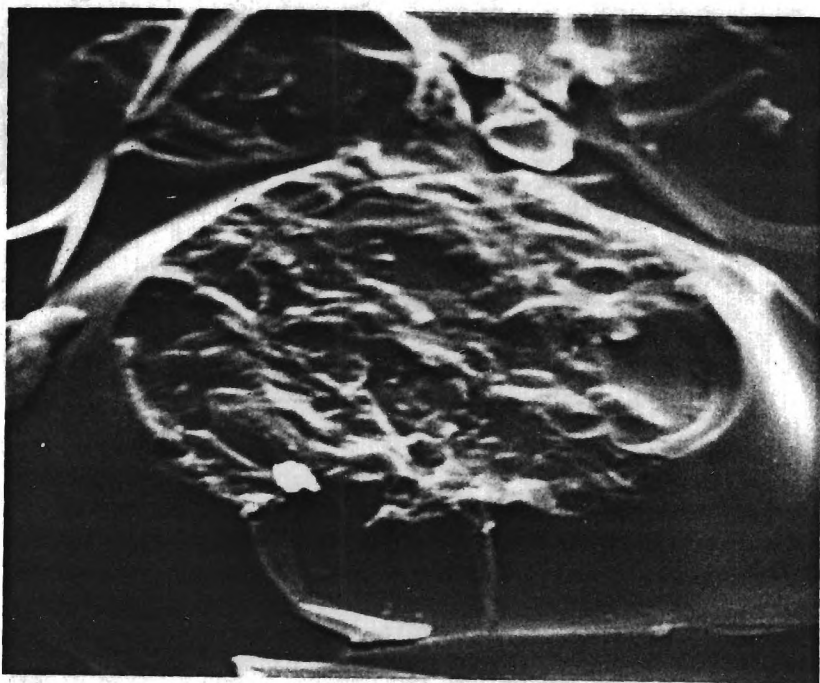


Figure 6. Fracture Morphology of Glass H Bond Between (0001) Faces of Alumina Single Crystals Fired at 1500°F (1200X).

concentration and composition of bonding agents and load on the bond strength of alumina, quartz fused, quartz, and silicon will be investigated. In addition, the effect of crystallographic mismatch on the phosphate bond between single crystals will be investigated.

IV. References

1. W. D. Kingery, "Fundamental Study of Phosphate Bonding in Refractories: I. Literature Review," J. Am. Ceram. Soc., (33) 239-41 (1950).
2. T. Chvatal, "The Position of Refractory Phosphate Bonding Today," Sprechsaal Keram. Glas. Baustoffe, (108) 576, 78, 80, 82-89 (1975).
3. E. Preuss, "Plot Program for Laue Patterns and Stereographic Projections," Computer Physics Comm., (18) 261-275 (1979).

FUNDAMENTAL INVESTIGATION OF PHOSPHATE BONDING

QUARTERLY FINANCIAL REPORT

1 DECEMBER 1983 - 28 FEBRUARY 1983

Submitted to:

U. S. Bureau of Mines
2401 E Street
Washington, D.C. 20241

Contract No. J0123041

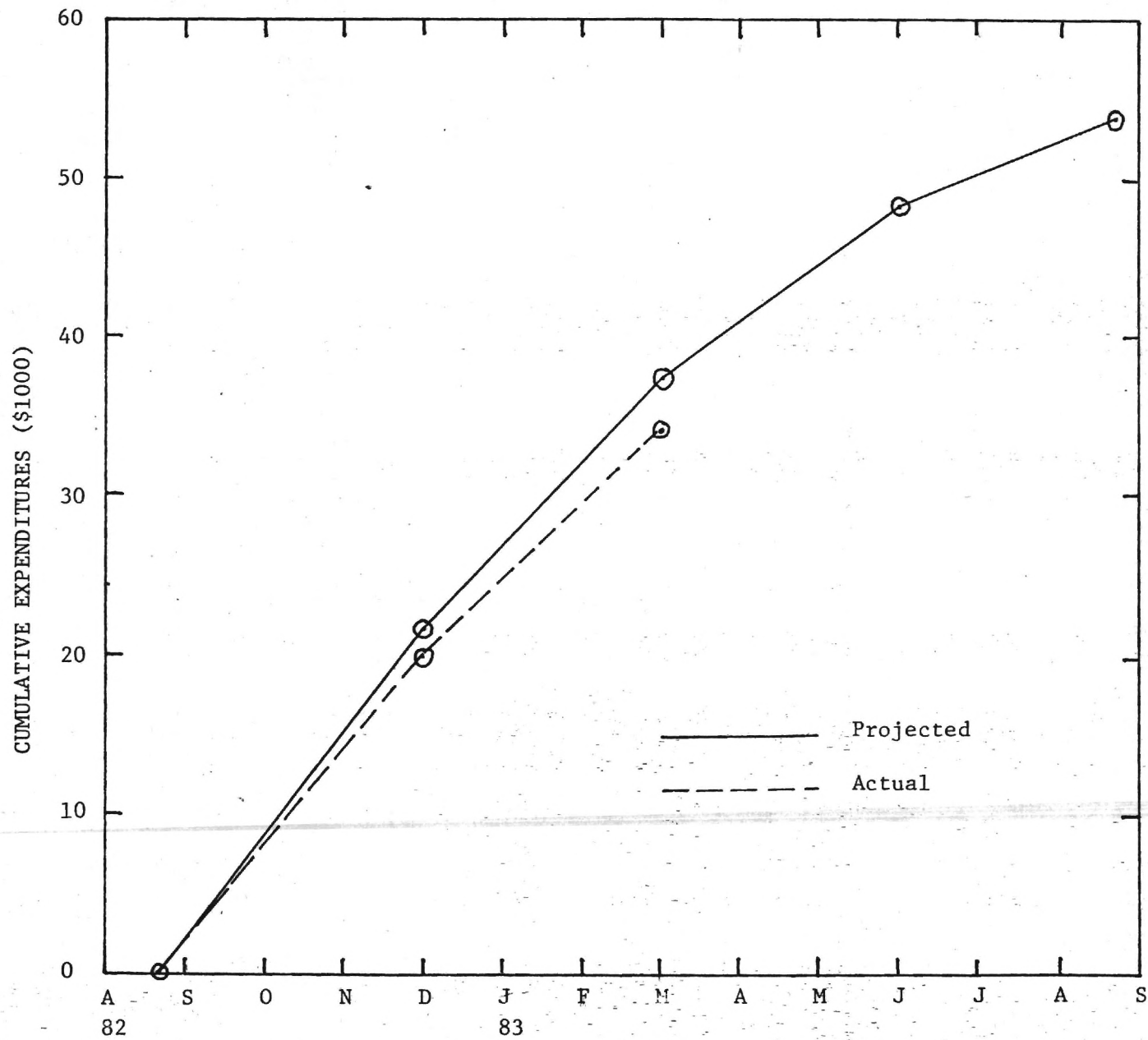
Submitted by:

James F. Benzel
School of Ceramic Engineering
Georgia Institute of Technology
Atlanta, Georgia 30332

Quarterly Financial Report
U. S. Bureau of Mines Contract J0123041
1 December 1982 - 1 February 1983

	<u>Current Quarter Expenditures</u>		<u>Cummulative Expenditures</u>	
	<u>U. S. Bureau of Mines</u>	<u>Georgia Institute of Technology</u>	<u>U. S. Bureau of Mines</u>	<u>Georgia Institute of Technology</u>
Personal Services	\$ 3,777	\$ 3,874	\$ 10,113	\$ 7,693
Fringe Benefits	437	292	1,393	1,307
Materials and Operating Expenses	1,611	60	2,717	346
Travel	-----	-----	-----	-----
Overhead	<u>2,449</u>	<u>1,995</u>	<u>6,413</u>	<u>4,412</u>
Total Expended	\$ 8,274	\$ 6,221	\$ 20,636	\$ 13,758
Total Budget			<u>\$ 37,000</u>	<u>\$ 16,600</u>
Unexpended Balance			\$ 16,364	\$ 2,842

CUMULATIVE EXPENDITURES FOR U. S. BUREAU OF MINES CONTRACT J0123041





College of Engineering
School of Ceramic Engineering

September 30, 1983

MEMORANDUM

TO: Office of Contract Administration

FROM: James F. Benzel, Professor *JFB*
School of Ceramic Engineering

SUBJECT: E-18-626 Quarterly Progress and Quarterly Financial Reports
(Third Quarter)

Attached are seven copies of the above reports. I have distributed copies to those people in Ceramic Engineering who need them. The sponsor requires five copies as shown below:

- A. U.S. Bureau of Mines 1 copy
Branch of Procurement, Washington
Columbia Plaza, 5th Floor
Washington, D.C. 20241
Attn: Contracting Officer
Contract No. J0123041
- B. U.S. Bureau of Mines 2 copies
2401 E Street, N.W.
Washington, D.C. 20241
Attn: Dr. M. A. Schwartz, 7020
- C. Dr. Rustu Kalyoncu 2 copies
U.S. Bureau of Mines
University of Alabama
Box L
Tuscaloosa, AL 35486

JFB:cm
Attachments

FUNDAMENTAL INVESTIGATION OF PHOSPHATE BONDING

QUARTERLY PROGRESS REPORT NO. 3

1 MARCH 1983 - 31 May 1983

Submitted to:

U. S. Bureau of Mines
2401 E Street
Washington, D.C. 20241

Contract No. J0123041

Submitted by:

James F. Benzel
School of Ceramic Engineering
Georgia Institute of Technology
Atlanta, Georgia 30332

Fundamental Investigation of Phosphate Bonding

Quarterly Progress Report No. 3

1 March 1983 - 31 May 1983

I. Introduction

Since Kingery's (Ref. 1) literature review in 1950, the amount of published information on phosphate bonding has been greatly expanded. Chvatal's 1975 review (Ref. 2), which concentrated primarily on the 1965 to 1975 literature, contained 222 references. Most of the effort represented by these publications has been devoted towards empirically investigating phosphate bonding materials and development of useful refractory products.

The effect of variables, such as temperature, soaking time, particle size, concentration of bonding agent and source of raw materials on the form, and relative abundance of the reaction products present in a number of phosphate bonded systems, have been investigated. However, there is still little fundamental physiochemical information about phosphate bonding in the literature. This is not surprising when the complexity of the multistep reactions, the difficulty in differentiation between the many possible reaction products and the fine grain sized polycrystalline nature of materials being bonded are taken into consideration.

Thus, it appears that fundamental investigations on phosphate bonding should be performed on simple model systems. This study involves the use of single crystals to accomplish this goal. The major portion of this investigation will be carried out using single crystals of materials (i.e. alumina, quartz, magnesia, magnesium aluminate spinel and stabilized zirconia) and phosphate binding agents (i.e. orthophosphoric acid, mixtures of chromic and orthophosphoric acid, monoaluminum phosphate and sodium

phosphate glasses) commonly incorporated in phosphate bonded refractories. However, materials, such as fused silica and single crystals of materials not normally used in refractories, such as magnesium fluoride and silicon metal, will also be utilized.

The reaction of phosphate bonding agents with different crystallographic faces of single crystals will be studied after various heat treatments. The effect of interatomic spacing and atomic planar density of the material being bonded will be investigated by rejoining single crystals, cleaved or cut along low order planes, such as 100, 110, or 111, with various phosphate bonding agents.

The effect of interfacial crystallographic misorientations (tilt, twist, and combinations of both) on the strength of phosphate bonds will be investigated using phosphate bonded bycrystals. It is anticipated that there is a relationship between the strength of phosphate bonding and the degree of mismatch between the bonded faces.

An attempt will be made to evaluate the effect of the atomic structure of the material being bonded on the strength of the resulting phosphate bond formation. The role of the anion in phosphate bonding will also be investigated.

II. Status of Investigation

A. Single Crystal Orientation

X-ray techniques and computer plotting programs for accurately determining the orientation of cubic and hexagonal single crystals have been completed.

B. Tensile Testing of Alumina Bicrystals

During this report period, a major effort was made to improve the method used to load the bonded bicrystals. The results reported earlier were

performed using a loading jig which had a double flexible joint at the top and a reservoir of Wood's metal at the bottom. The samples were tested by super-gluing the bicrystals to two attachment rods. One of these rods was threaded into the bottom of the flexible joint. The Wood's metal was then melted with a gas torch and the cross head lowered until the lower rod was partially submerged in the molten metal. The metal was then allowed to solidify around the bottom rod. This system was designed to minimize misalignment so the bicrystal would be loaded in pure tension. However, as the molten metal solidified and then cooled, it tended to misalign the lower rod and to also stress the bicrystal, causing many of them to fail.

To overcome these problems, a new loading system was developed. This system utilized two steel cables to transmit the tensile force from the Instron to the two eyelets attached to aluminum loading blocks to which the bicrystal had been super-glued.

This new loading system was used to test a series of $(11\bar{2}0)$ bicrystals bonded with $\text{NaH}_2\text{PO}_4 \cdot \text{H}_2\text{O}$ (30% P_2O_5). These bicrystals were placed under a 100 gram weight and allowed to cure at room temperature for at least 24 hours. They were then fired at 1500°F for four hours. Their room temperature strengths are listed in Table I.

Based on the fact that all of these samples were stronger than any previously tested, our visual observation that the new system produced much better alignment during loading was confirmed. A second series of similar bicrystals was prepared (A-7 to A-8) using a 200 gram load during the 24 hour room temperature curing cycle. These bicrystals were prepared from crystals that had been previously used. Before being rebonded, they were lightly ground on 180, 240, 600 grit SiC paper and were then

Table I. Tensile Strength of Alumina Bicrystals Bonded with NaH_2PO_4 and Fired at 1500°F for Four Hours.

Sample Number	Load Applied During Curing(gms)	Bicrystal Faces Bonded	Crystal Conditions	Tensile Strength (kg/cm^2)
A-1	100	(11 $\bar{2}$ 0)	New	100.9
A-2	100	(11 $\bar{2}$ 0)	New	90.5
A-3	100	(11 $\bar{2}$ 0)	New	93.5
A-4	100	(11 $\bar{2}$ 0)	New	106.0
A-5	100	(11 $\bar{2}$ 0)	New	117.6
A-6	100	(11 $\bar{2}$ 0)	New	101.6
				$\bar{x} = 101.7$
				$s = 10.1$
A-7	200	(11 $\bar{2}$ 0)	Used	32.5
A-8	200	(11 $\bar{2}$ 0)	Used	33.7
A-9	200	(11 $\bar{2}$ 0)	Used	42.2
A-10	200	(11 $\bar{2}$ 0)	Used	64.0
A-11	200	(11 $\bar{2}$ 0)	Used	42.9
A-12	200	(11 $\bar{2}$ 0)	Used	40.7
				$\bar{x} = 42.7$
				$s = 11.3$
B-1	100	(0001)	Used	13.0
B-2	100	(0001)	Used	35.4
B-3	100	(0001)	Used	26.1
B-4	100	(0001)	Used	41.5
B-5	100	(0001)	Used	15.3
				$\bar{x} = 26.3$
				$s = 12.4$
B-7	100	(0001)	New	41.5
B-8	100	(0001)	New	85.3
B-9	100	(0001)	New	43.3
B-10	100	(0001)	New	66.8
B-11	100	(0001)	New	98.4
B-12	100	(0001)	New	56.2
				$\bar{x} = 65.3$
				$s = 22.9$

lightly polished using 1, 0.5 and 0.3 μm alumina to remove any contamination. The tensile strengths of these samples are also listed in Table I. These samples were significantly weaker than the first set.

In an attempt to determine if this strength decrease was the result of reusing the alumina crystals or was due to the increased load during curing, two additional series of bicrystals bonded with $\text{NaH}_2\text{PO}_4 \cdot \text{H}_2\text{O}$ were prepared and fired. All of these samples were (0001) bicrystals cured under a 100 gram load and fired at 1500°F for four hours. The B-1 to B-5 samples were prepared from used crystals and the B-7 to B-12 samples from new crystals. Their tensile strengths are listed in Table I. Even though the new (0001) bicrystals were much weaker than the $(11\bar{2}0)$ bicrystals produced from unused crystals, it appears that reusing the alumina crystals decreases the strength of alumina bicrystals.

Additional (0001) and $(11\bar{2}0)$ bicrystals were produced from new crystals using Glass H (30% P_2O_5) as the bonding agent. These samples were cured under 100 gram loads and fired at 1500°F. Their tensile strengths are listed in Table II. These results indicate that both $(11\bar{2}0)$ and (0001) bicrystals bonded with Glass H are weaker than the same type of bicrystals bonded with NaH_2PO_4 .

C. Morphology of Fractured Samples

Examination of the bonded areas of fractured samples indicates that the thickness of the bond varies from one side to the other. The apparent cause of this is the uneven distribution of weight during the room temperature curing cycle. This technique is being modified in an attempt to eliminate this problem.

Table II. Tensile Strength of Alumina Bicrystals Bonded With Glass
H and Fired at 1500°F for Four Hours.

Sample Number	Load Applied During Curing(gms)	Bicrystals Faces Bonded	Tensile Strength (kgf/cm ²)
H-1	100	(11 $\bar{2}$ 0)	16.2
H-2	100	(11 $\bar{2}$ 0)	20.7
H-3	100	(11 $\bar{2}$ 0)	26.6
H-4	100	(11 $\bar{2}$ 0)	17.7
H-5	100	(11 $\bar{2}$ 0)	20.7
H-6	100	(11 $\bar{2}$ 0)	20.7
			$\bar{X} = 20.4$
			$S = 3.6$
G-2	100	(0001)	43.9
G-3	100	(0001)	34.0
G-5	100	(0001)	29.2
G-6	100	(0001)	17.2
			$\bar{X} = 31.1$
			$S = 11.1$

III. Future Work

During the final quarter our effort will be primarily devoted to producing bicrystals with uniform bond thicknesses across their entire cross-sections. If this is accomplished it should reduce the scatter in the data considerably. In addition, bicrystals containing rotational mismatches will be evaluated and the final report written.

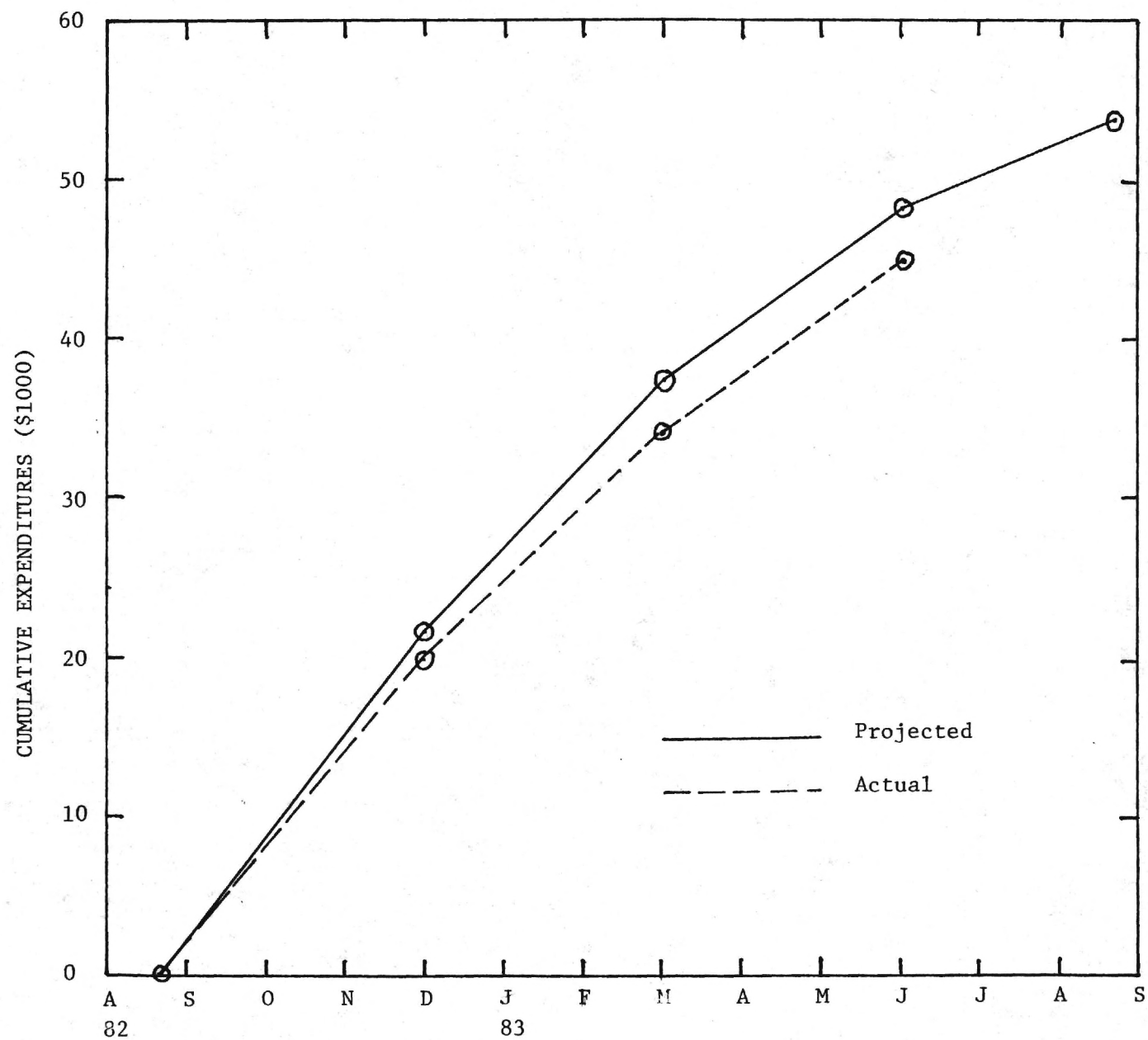
IV. References

1. W. D. Kingery, "Fundamental Study of Phosphate Bonding in Refractories: I. Literature Review," J. Am. Ceram. Soc., (33) 239-41 (1950).
2. T. Chvatal, "The Position of Refractory Phosphate Bonding Today," Sprechsaal Keram. Glas. Baustoffe, (108) 576, 78, 80, 82-89 (1975).
3. E. Preuss, "Plot Program for Laue Patterns and Stereographic Projections," Computer Physics Comm., (18) 261-275 (1979).

Quarterly Financial Report
U.S. Bureau of Mines Contract J0123041
1 March 1983 - 31 May 1983

	<u>Current Quarter Expenditures</u>		<u>Cummulative Expenditures</u>	
	<u>U.S. Bureau of Mines</u>	<u>Georgia Institute of Technology</u>	<u>U.S. Bureau of Mines</u>	<u>Georgia Institute of Technology</u>
Personal Services	\$ 2,431	\$ 1,307	\$ 12,544	\$ 9,000
Fringe Benefits	373	274	1,766	1,581
Materials and Operating Expenses	1,466	----	4,183	346
Travel	529	----	529	----
Overhead	<u>2,046</u>	<u>746</u>	<u>8,459</u>	<u>5,158</u>
Total Expended	\$ 6,845	\$ 2,327	\$ 27,481	\$ 16,085
Total Budget			<u>\$ 37,000</u>	<u>\$ 16,600</u>
Unexpended Balance			\$ 9,519	\$ 515

CUMULATIVE EXPENDITURES FOR U. S. BUREAU OF MINES CONTRACT J0123041



FUNDAMENTAL INVESTIGATION OF PHOSPHATE BONDING

QUARTERLY FINANCIAL REPORT

20 AUGUST - 30 NOVEMBER 1982

Submitted to:

U. S. Bureau of Mines
2401 E Street
Washington, D. C. 20241

Contract No. J0123041

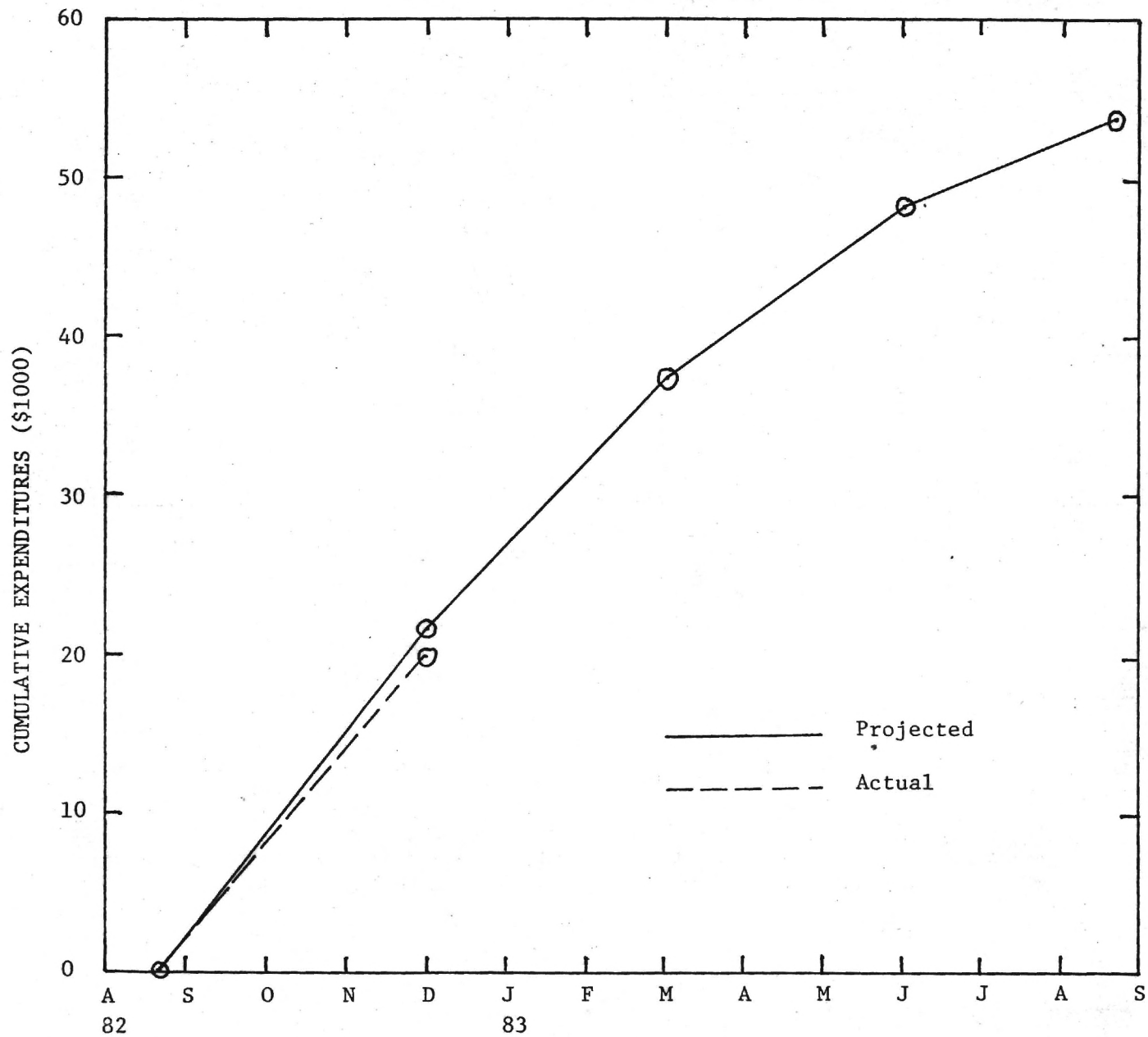
Submitted by:

James F. Benzel
School of Ceramic Engineering
Georgia Institute of Technology
Atlanta, Georgia 30332

Quarterly Financial Report
U. S. Bureau of Mines Contract J0123041
20 August - 30 November 1982

	<u>Current Quarter Expenditures</u>		<u>Cummulative Expenditures</u>	
	<u>U. S. Bureau of Mines</u>	<u>Georgia Institute of Technology</u>	<u>U. S. Bureau of Mines</u>	<u>Georgia Institute of Technology</u>
Personal Services	\$ 6,336	\$ 3,819	\$ 6,336	\$ 3,819
Fringe Benefits	956	1,015	956	1,015
Materials and Operating Expenses	1,106	286	1,106	286
Travel	-----	-----	-----	-----
Overhead	<u>3,964</u>	<u>2,417</u>	<u>3,964</u>	<u>2,417</u>
Total Expended	\$ 12,362	\$ 7,537	\$ 12,362	\$ 7,537
Total Budget			<u>\$ 37,000</u>	<u>\$ 16,600</u>
Unexpended Balance			\$ 24,638	\$ 9,063

CUMULATIVE EXPENDITURES FOR U. S. BUREAU OF MINES CONTRACT J0123041



FUNDAMENTAL INVESTIGATION OF PHOSPHATE BONDING

Prepared for

UNITED STATES DEPARTMENT OF THE INTERIOR
BUREAU OF MINES

By

GEORGIA INSTITUTE OF TECHNOLOGY
SCHOOL OF CERAMIC ENGINEERING
ATLANTA, GEORGIA 30332

FINAL REPORT

On

USBM Contract No. J0123041
(Fundamental Investigation of Phosphate Bonding)

December 1983

NOTICE

The views and conclusions contained in this document are those of the authors and should not be interpreted as necessarily representing the official policies or recommendations of the Interior Department's Bureau of Mines or of the U.S. Government.

FOREWARD

This report was prepared by the School of Ceramic Engineering, Georgia Institute of Technology, Atlanta, Georgia 30332 under USBM Contract J0123041. The contract was initiated under the Bureau of Mines Metallurgy Program. It was administered under the technical direction of Metallurgy with Dr. Martin H. Stanczyk, acting as the Technical Project Officer. Mr. Oliver H. Snyder III was the Contract Administor for the Bureau of Mines.

This report is a summary of the work recently completed on this contract during the period 20 August 1982 to 20 October 1983. This report was submitted by the authors on 20 November 1983. Portions of this report will be used as part of a Ph.D. dissertation to be submitted during 1984.

Please note that in our opinion, no patentable features of phosphate bonding are disclosed herein. Reference to specific brands, equipment, or trade names in this report is made to facilitate understanding and does not imply endorsement by the Bureau of Mines or the authors.

TABLE OF CONTENTS

	Page
Foreward	2
List of Figures	4
List of Tables	6
SECTION I	
Introduction	7
SECTION II	
Background	9
SECTION III	
Experimental Program	24
A. Single Crystal Orientation	24
B. Reaction of Phosphate Bonding Agents with Different Crystallographic Faces of Single Crystals and Fused Silica	25
C. Development of Methods to Form Phosphate Bonding Bicrystals and Tensile Testing Procedures	41
SECTION IV	
Summary	63
Section V	
References	

LIST OF FIGURES

	Page
1. Dendrite Crystals on Surface of Alumina Crystal Reacted with H_3PO_4 at 1500°F (400X).	27
2. Reaction Product Layer Below Dendrites (2500X).	27
3. Reaction Product Layer Formed on Surface of Alumina Crystal Reacted with Chromic Phosphoric Acid Mixture at 1500°F (3500X)	28
4. Top Surface of Reaction Products on (0001) Face of Quartz Crystal Reacted with Phosphoric Acid at 1500°F (2500X).	28
5. Reaction Product Layer Formed on Surface of a Fused Silica Rod Reacted with Phosphoric Acid at 1500°F (1500X).	30
6. Plate-Like Crystals Growing Out of Spheres Shown in Figure 5 (1500X)	30
7. Whitish Star-Shaped Dendritic Crystals on Surface of Reaction Products Produced by Reacting H_3PO_4 with (0001) Face of Alumina at 1500°F (610X)	31
8. Whitish and Grayish-Shaped Dendritic Crystals Produced by Reacting H_3PO_4 with (0001) Face of Alumina Crystal at 1500°F (600X)	31
9. Structure of Aluminum Meta Phosphate $[Al(PO_4)_3]$ Dendrites (3200X)	33
10. Porous Morphology of Monoaluminum Phosphate ($AlPO_4$) Dendritic Structure (3200X).	33
11. Nearly Equiaxed Crystals Covering ($\bar{1}\bar{1}00$) Face of Alumina Crystal Reacted with H_3PO_4 (1000X).	35
12. Fractured Alumina Crystal with Equiaxed Crystals on ($\bar{1}\bar{1}00$) Face (250X)	35
13. Dendritic Structure on Face of ($\bar{1}\bar{1}02$) Alumina Crystal Reacted with H_3PO_4 at 1500°F (1250X).	36
14. Aluminum Phosphate Reaction Products on Surface of ($\bar{1}\bar{1}\bar{2}2$) Face of Alumina Crystal Reacted with H_3PO_4 at 1500°F (250X) . .	36

LIST OF FIGURES (Continued)

	Page
15. Higher Magnification of Surface Shown in Figure 14 (1100X). . .	37
16. Surface of Reaction Products on a Random Plane of an Alumina Crystal Reacted with H_3PO_4 at 1500°F (250X)	37
17. Same as Figure 16 Except Random Plane was Different (250X).	38
18. Plate-Like Structure Covering Surface of Grains Shown in Figure 17 (1600X).	38
19. Surface of Reaction Product Layer Formed on the Surface of an Alumina Cutting Tool Reacted with H_3PO_4 at 1500°F (500X).	40
20. Plate-Like Grains on Different Area of Alumina Cutting Tool Shown in Figure 19 (900X).	40
21. Fracture Morphology of $NaH_2PO_4 \cdot H_2O$ Bond Between (0001) Faces of Alumina Crystals Fired at 1500°F (1200X)	45
22. Fracture Morphology of Glass H Bond Between (0001) Faces of Alumina Single Crystals Fired at 1500°F (1200X).	45
23. Average Tensile Strength Factorial Design (2 x 2) Showing Effect of Crystal Condition and Bicrystal Faces Bonded with Sodium Dihydrogen Phosphate (30% P_2O_5) and Cured Under a Load of 100 Grams	52
24. Average Tensile Strength Factorial Design (2 x 2 x 2) Showing the Effect of Bonding Agent, Curing Load and Bicrystal Faces Bonded.	53
25. Effect of Rotational Mismatch on the Tensile Strength of (1120) Alumina Bicrystals	60

LIST OF TABLES

	Page
I. Tensile Strength of Phosphate Bonded Alumina Bicrystals . . .	43
II. Tensile Strength of Alumina Bicrystals Bonded with NaH_2PO_4 and Fired at 1500°F for Four Hours	46
III. Tensile Strength of Alumina Bicrystals Bonded with Glass H and Fired at 1500°F for Four Hours	48
IV. Tensile Strength of Phosphate Bonded Alumina Bicrystals Cured Under a Distributed Load	50
V. Effect of Curing Time on the Tensile Strength of Sodium Dihydrogen Phosphate Bonded Alumina Bicrystals	55
VI. Effect of Surface Finish on the Tensile Strength of Alumina Bicrystals Bonded with Sodium Dihydrogen Phosphate	57
VII. Effect of Surface Finish and Crystal Faces Bonded on the Average Tensile Strength of Bicrystals Bonded with Sodium Dihydrogen Phosphate (20% P_2O_5)	58
VIII. Effect of Rotational Mismatch on the Tensile Strength of (11 $\bar{2}$ 0) Alumina Bicrystals with Sodium Dihydrogen Phosphate (20% P_2O_5)	59
IX. Effect of Rotational and Tilt Mismatch on the Tensile Strength of Alumina Bicrystals Bonded with Sodium Phosphate (20% P_2O_5)	62

SECTION I

Introduction

Phosphoric acid and acid phosphate compounds were first used as binders for dental materials and refractories shortly after the turn of the century. In addition to a wide variety of oxides and silicates, a number of other materials such as glasses, metal halides, metal hydrates and metals have been formed into shapes using phosphate binders.

Almost all of the phosphate bonding investigations reported to date utilized finely powdered materials or mixtures of fine grained materials and polycrystalline aggregates. The only known exception has been the use of a phosphate binder system to join moderately large mica single crystals to produce larger and thicker mica sheets for electronic applications.

The objective of this investigation was to achieve a better understanding of the mechanisms of phosphate bonding. The uniqueness of the experiments is that they were based on studying the joining together of two single crystals by phosphate bonding rather than studying the properties of polycrystalline masses held together by phosphate bonds. The use of single crystals in these experiments allowed the elimination of variables such as surface area and particle shape and also permitted the investigation of the effect crystallographic orientation plays in phosphate bonding.

The availability of this type of fundamental information could lead to the production of better and longer-lasting refractories. Since many of the currently used phosphate bonded refractories contain alumina, chrome oxide and zirconia, improving their service life would reduce the necessity for importation of bauxite, chrome ore and zirconia-bearing minerals.

SECTION II

Background

In 1950, Kingery published a comprehensive literature review (Ref. 1) and a fundamental study (Ref. 2) on the phosphate bonding of refractories. The purpose of this section is to summarize the fundamental information cited or reported in these two papers and to outline subsequent progress that has been made toward understanding phosphate bonding.

Kingery's literature search (Ref. 1) indicated that three major methods of forming phosphate bonds had been identified. They were: (1) reaction of phosphoric acid with siliceous materials, (2) reaction of phosphoric acid with oxides, and (3) the direct addition or formation in situ of acid phosphates. Cold setting (room temperature) as well as heat setting refractory bonds were described but very little fundamental information about these materials was found in the pre-1950 patent or general literature.

Dental literature indicated that zinc oxide based cements were crystalline (Refs. 3 and 4) and that the bond was primarily dibasic zinc phosphate ($\text{ZnHPO}_4 \cdot 3\text{H}_2\text{O}$). A hard white dental cement formed from powdered alumina-lime-silica glass and phosphoric acid (Refs. 3 and 5) was reported to be bonded by an amorphous silica gel formed by a solution of about 30% of the glass.

Kingery's systematic study (Ref. 2) of a large number of metal oxide-phosphoric acid reactions at room temperature indicated three distinct classes of reactions: (1) acidic and chemically inert oxides do not react,

(2) strongly basic oxides react violently to form porous friable structures, and (3) weakly basic and amphoteric oxides react but not all of them form bonded structures.

All of the reactions in the third classification which produced cement-like materials contained mono- and di-basic phosphates [$M_x(H_2PO_4)_y$ and $M_x(HPO_4)_y$], whereas no acid phosphates were detected in the similar non-cohesive mixtures. This led Kingery to conclude that acid phosphates act as the bonding media in cold-setting phosphate cements. He also concluded, because of the number of different oxides involved, that this was a general property of hydrogen phosphates rather than one particular chemical compound.

Comparison of bars (90 w/o fused Al_2O_3 and 10 w/o kaolin) bonded with phosphoric acid or phosphoric acid containing one of a number of cation additions (Ref. 3) indicated that small weakly basic or amphoteric ions such as Al^{+++} , Be^{++} , Fe^{+++} and Mg^{++} increased the bonding power of phosphoric acid and that large or strongly basic ions such as Ba^{++} , Ca^{++} and Th^{+++} decrease its effectiveness. Based on these results, Kingery concluded that weakly basic cations having a moderately small ionic radii were necessary to optimize the bond strength by allowing the formation of a somewhat variable and flexible partially non-ordered or glassy structure. The larger more basic cations tend to have higher coordination numbers which prevent the formation of flexible connected polyhedra structures, resulting in more ordered structures which results in lower bond strengths.

Heat treatment of bars (92.85 w/o fused Al_2O_3 and 7.15 w/o ball clay) bonded with 7.15 w/o mono-aluminum phosphate (Ref. 2) to various temperatures

produced the unusual result that all of their room temperature MOR's were greater than their dried strength. This lack of a temperature zone of weakness was attributed to the gradual loss of combined water and the gradual crystallization of the hydration products over a wide temperature range with no sharp rupturing effects.

The first step in this process is the loss of combined water, which leads to the formation of an amorphous phase containing three moles of water ($\text{Al}_2\text{O}_3 \cdot \text{P}_2\text{O}_5 \cdot 3\text{H}_2\text{O}$). This material crystallizes over a fairly wide temperature range (260-500°C) as additional water is lost. The resulting compound [aluminum metaphosphate, $\text{Al}(\text{PO}_3)_3$] also forms a bond with the aggregate.

When Kingery (Ref. 2) reacted aluminum hydrate ($\text{Al}_2\text{O}_3 \cdot x\text{H}_2\text{O}$) with phosphoric acid no crystalline reaction products were detected. Thus, at room temperature, the bonding phase must have been amorphous. However, continuous rate of weight loss measurements on heating clearly showed the characteristic peaks for mono-aluminum phosphate. This suggests that the amorphous bonding phase may contain more water of hydration than mono-aluminum phosphate and that it crystallizes below 200°C as the result of a gradual dehydration process which results in the formation of mono-aluminum phosphate.

In 1952, Kingery (Ref. 6) demonstrated that mortars formed from fire clay grog, kaolin, and either mono-aluminum or mono-magnesium phosphate bonds produced excellent joints between half fire bricks fired at temperatures between 105°C and 1500°C for five hours. The transverse strength of neat mortar bars bonded with mono-aluminum phosphate and cured at 105°C increased almost linearly as the percent phosphate bond was increased from 2 to 12 w/o.

Gitzen et al. (Ref. 7) in studying the phosphate bonding of sintered alumina grog found that higher bond strength was obtained with phosphoric acid than with the various forms of aluminum phosphate. Forming the acid in place by adding water to dry mixes containing phosphorous pentoxide (P_2O_5) also produced excellent bonding. The use of dry diammonium phosphate $(HN_4)_2HPO_4$ to produce phosphoric acid *in situ* resulted in weaker bond strength and production of ammonia during the casting operation.

When castables were prepared using tabular alumina and phosphoric acid, it was necessary to heat-set them by heating at 600 to 800°F. These authors (Ref. 7) thought the bonding process consisted of dehydration of orthophosphoric acid (H_3PO_4) at 416°F to form pyrophosphoric acid ($H_4P_2O_7$) which on continued heating at 600 to 800°F reacts with the alumina to form aluminum phosphate ($AlPO_4$). They attributed the loss of strength observed between 2000 and 2800°F to decomposition of aluminum phosphate to alumina and P_2O_5 . By substituting Bayer alumina for some of the tabular alumina, they produced castables which developed an initial cold-set at room temperature.

To investigate the effect of the inversion of the α - β cristobalite form of aluminum phosphate, test bars of an alumina ramming mix bonded with phosphoric acid were heat treated 20 hours at 2400°F (Ref. 7). No decrease in strength occurred even after the bars were cycled through the inversion temperature 300 times.

Sheets et al. (Ref. 8) suggested the following scenario for the phosphate bonding of alumina:

"Initially, a trivalent phosphate anion is present. As the acid reacts with the alumina, covalent polymerization occurs.

This results in bivalent PO_4 units which will become 'ends' in chain polymerizations. Two of these can fuse to form a tetravalent pyrophosphate.

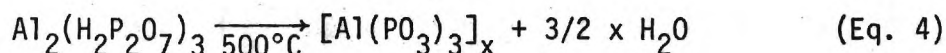
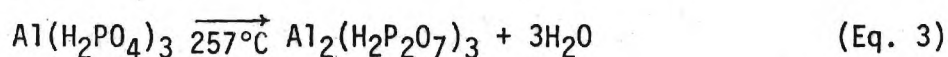
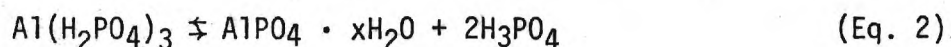
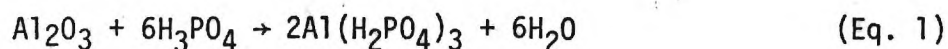
As the reaction proceeds, PO_4 units form with only one formal charge remaining. These units may be called 'middles.' One unit, terminated by two of the previously formed 'ends' gives a family of linear polyphosphates.

The next step in the development of the bond comes from PO_4 groups having no formal charge but capable of forming 'branches.' Branching, such as is proposed here, could give rise to a sheet structure.

The foregoing, 'ends,' 'middles,' and 'branches' involve only the phosphorous and oxygen atoms. To explain the unusual properties of phosphated-bonded alumina, one would expect the Al atom to become involved in these reactions. Structural chemists believe in the formation of 'super branches' which are capable of 3 dimensional growth. Thus, phosphate bonding can be viewed as a heteropolyanionization process leading to the formation of a strong oxygen polyhedral structure."

Rickles' (Ref. 9) investigation of the reaction between aluminum hydroxide and phosphoric acid (25-90°C) determined that the reaction products of this system were a mixture of amorphous mono-aluminum phosphate and a crystalline solid having the chemical composition $3\text{Al}_2\text{O}_3 \cdot 2\text{P}_2\text{O}_5 \cdot 8\text{H}_2\text{O}$. A direct correlation between the amount of amorphous mono-aluminum phosphate and bond strength was found. This was attributed to its non-uniform structure and bonding. When the molar ratio of $\text{Al}(\text{OH})_3$ to H_3PO_4 was 1:3 only amorphous mono-aluminum phosphate was formed. The addition of alumina to the reaction mixture in the ratio of 3:7 with respect to aluminum hydroxide [$\text{Al}_2\text{O}_3:\text{Al}(\text{OH})_3$] produced the highest tensile strength and decreased porosity. He also determined that the reaction between zirconium oxide and phosphoric acid produced zirconium pyrophosphate which maintained high strength at 1300°C.

Lyons et al. (Ref. 10) suggested the following reaction sequence for phosphoric acid with high-alumina refractory mixes:



The $\text{Al}(\text{H}_2\text{PO}_4)_3$ is water soluble and is the bonding phase (Ref. 11) in two senses: (1) its sticky, viscous nature at room temperature, and (2) as a precursor to $\text{Al}_2(\text{H}_2\text{P}_2\text{O}_7)_3$ and $[\text{Al}(\text{PO}_3)_3]_x$ in the cured refractory.

If the reaction can be slowed or stopped after reaction (Eq. 1) the refractory mixes would remain workable over a long period of time and would provide a large amount of $\text{Al}(\text{H}_2\text{PO}_4)_3$ that is the precursor to the binding material $[\text{Al}(\text{PO}_3)_3]_x$. Addition of oxalic acid to act as a sequestering agent to hold aluminum in a soluble form extended the storage life of ramming and plastic mixes to six months and longer (Ref. 11). These experiments confirmed the theory that the setting of phosphate-bonded alumina refractories is caused by the precipitation of insoluble aluminum phosphates.

Lyon et al. (Ref. 12) investigated the bonding of magnesia refractories with sodium phosphate glasses cured at 250°F. They found that as the average chain length (6-50) of the glass and the amount of bond added

were increased, room temperature MOR's increased and hot MOR's decreased. The shorter chain length (1-3) crystalline sodium phosphates gave poorer cold and hot MOR's than the glassy phosphates.

It was believed (Ref. 12) that glassy phosphate bonding was the result of degrading these materials to orthophosphoric acid or to ortho-salts during the curing cycle. The acid component then reacts with the magnesia to form the bond.

Samples of MgO mixed with the phosphate glasses and sufficient water to form a paste were heat treated and x-ray diffraction patterns run. Similar patterns were obtained for samples heat treated at the same temperature irrespective of the glass chain length. The 125°F patterns contained lines for magnesium orthophosphate, which confirmed the degradation of the glasses. The 950°F material was composed mainly of amorphous material and the 2200°F samples showed strong crystalline orthophosphate lines plus a large amount of noncrystalline material. These results suggest that the bonding of MgO between 500 and 2200°F is the result of amorphous phosphate glasses. As 2200-2300°F is reached the glasses begin crystallizing to form $Mg_3(PO_4)_2$. Lyon et al. (Ref. 12) concluded that the loss of strength observed in this temperature range indicated that $Mg_3(PO_4)_2$ is not a bonding agent.

Bremser and Nelson (Ref. 13) used a mixture of ammonium dihydrogen phosphate and monofluorophosphoric acid to produce low temperature bonding (260°C) of stabilized and unstabilized zirconia. The MOR's of the calcia stabilized bars were higher than those of unstabilized bars from room temperature to ~1200°C where a liquid formed in the stabilized bars.

X-ray diffraction indicated that after being heated to 1240°C the unstabilized bars contained only monoclinic zirconia and zirconium pyrophosphate. However, analysis of the stabilized zirconia bars indicated that most of the cubic zirconia had reverted to the monoclinic form and that $\text{CaZr}(\text{PO}_3)_2$ was present in addition to zirconium pyrophosphate.

A sharp decrease in the MOR of the stabilized bars was observed between 200 and 400°C but between 400 and 600°C the strength returned to about its original value (3500 psi). A second decrease in strength occurred between 600 and 900°C; however, the strength again recovered (3000 psi) at 1000°C. Above 1000°C the strength decreased with increasing temperature until liquid formed at about 1200°C. The strength of the unstabilized bars remained fairly constant (1500-1900 psi) from room temperature to 1100°C. Between 1100 and 1240°C there was some decrease in strength; however, the specimens showed brittle fracture. The irregular nature of the MOR - temperature curve for the calcia stabilized zirconia bars was attributed to the formation of one or more intermediate calcium compounds which result in the formation of a double phosphate of calcium and zirconium $[\text{CaZr}(\text{PO}_4)_2]$ at about 1200°C.

Reaction studies (Ref. 13) showed the following reaction series for unstabilized zirconia reacted with monofluorophosphoric acid alone or in the presence of ammonium dihydrogen phosphate: the acid dissociates releasing fluorine, which leads to the formation of an intermediate zirconium pyrophosphate. Zirconium pyrophosphate (ZrP_2O_7) is stable to 1380°C where it begins to lose P_2O_5 forming zirconyl pyrophosphate $[(\text{ZrO})_2\cdot\text{P}_2\text{O}_7]$, which is stable to 1600°C.

Foessel and Treffner (Ref. 14), using a glassy sodium polyphosphate

(chain length of 21), a lime-bearing addition as a second binder, and selected magnesite aggregates produced refractories having 2700°F MOR's greater than 2000 psi. By adjusting the $\text{CaO}:(\text{P}_2\text{O}_5 + \text{SiO}_2)$ ratio of a mix composition containing an aggregate which had low strength at 2700°F, they produced brick with hot MOR's above 3500 psi at 2700°F. The optimum $\text{CaO}:(\text{P}_2\text{O}_5 + \text{SiO}_2)$ ratio was around 1:1. Bricks of this type were at least twice as strong as direct bonded magnesite-chrome bricks up to 2850°F.

Similar results were obtained in magnesite-chrome refractories. However, it was found that as the MgO content decreased the optimum $\text{CaO}:(\text{P}_2\text{O}_5 + \text{SiO}_2)$ ratio increased from about 1:1 to about 1.25:1 for 60% MgO class brick. Conventional and high fired phosphate-bonded compositions were also superior to phosphate-free equivalents.

The rather narrow limits of the $\text{CaO}:(\text{P}_2\text{O}_5 + \text{SiO}_2)$ ratio for maximum hot MOR (Ref. 14) in magnesite refractories suggested that the bond might consist of a single well-defined compound. Venable and Treffner (Ref. 15) investigated this theory by reacting a glassy long-chain sodium polyphosphate polymer with the various components present in these magnesite refractories. They concluded that sodium dicalcium orthophosphate ($\text{Na}_2\text{O} \cdot 2\text{CaO} \cdot \text{P}_2\text{O}_5$) was the major high temperature bonding complex in these compositions.

Exploratory experiments (Ref. 15) showed that $\text{Na}_2\text{O} \cdot 2\text{CaO} \cdot \text{P}_2\text{O}_5$ softened to a viscous liquid between 1500 and 1600°C. However, before complete melting occurred sodium was lost and the bond composition shifted toward highly refractory whitlockite ($3\text{CaO} \cdot \text{P}_2\text{O}_5$), melting point 1775°C. The presence of silica results in the formation of calcium silicophosphates

at the expense of the sodium calcium phosphate bonding phase. Therefore, for high hot strengths in unburned magnesite brick the silica content should be kept low and the $\text{CaO}:\text{P}_2\text{O}_5$ should be approximately equal to unity.

O'Hara et al. (Ref. 16) summarized the phase conversions reported (Refs. 17-22) for an aluminum-phosphate binder (see Figure 1) with a $\text{P}_2\text{O}_5:\text{Al}_2\text{O}_3$ molar ratio of ≈ 2.3 . It was generally agreed that the major phase in this binder system is $\text{AlH}_3(\text{PO}_4)_2 \cdot 3\text{H}_2\text{O}$, which on heat treatment is converted to the berlinite and cristobalite forms of AlPO_4 and variscite $[\text{Al}(\text{H}_2\text{PO}_4)_3]$. Variscite is a highly hygroscopic phase which becomes amorphous above 570°F . Hydrated aluminum phosphates crystallize from the amorphous phase and gradually dehydrate between 930 and 1470°F to form $\text{Al}(\text{PO}_3)_3$ which in turn forms a metaphosphate glass between 2000 and 2370°F . The glass decomposes above 2370°F to form AlPO_4 with vaporization of P_2O_5 . Aluminum orthophosphate is isostructural with silica and its common polymorphs.

The physiochemical changes produced by heat treatment of chromium phosphates and chromium aluminum phosphate binders indicate that they differ from aluminum phosphate binders by retaining an amorphous phase over a larger temperature range (Refs. 23-24). They also may produce stronger bonds (Ref. 25).

The diametral tensile strength of alumina specimens bonded with phosphoric acid or a mixture of phosphoric acid and chromic acid (Ref. 16) were similar and increased with acid content for curing temperatures of 700 and 1500°F . The strength of specimens fired at 2000°F did not vary with acid content but those containing chromium were ≈ 2.5 times stronger.

Chromic acid containing specimens that had been cured at 700°F had lower overall thermal expansion when heated to 1500 or 2000°F than specimens bonded only with phosphoric acid. The isothermal expansion (1500°F for 4 hours) of the chromium containing specimen was also much lower. The sluggish isothermal expansion was attributed to the transformation of the berlinite to the tridymite form of AlPO_4 (1470°F). Cooling curves for specimens not containing chromic acid showed inversions corresponding to the β to α inversions of the tridymite and cristobalite forms of AlPO_4 for specimens heated to 1500 and 2000°F, respectively.

These findings suggest that the reason phosphoric acid bonded alumina specimens fired to 2000°F are weaker than ones bonded with a mixture of chromic and phosphoric acids is that the presence of chromium ions reduce the amount of AlPO_4 formed which prevents the structure from being disrupted when it is cooled through the β to α inversions.

O'Hara and his coworkers (Ref. 16) investigated the microstructure of these types of bonds by placing a drop of phosphoric acid or a mixture of phosphoric and chromic acid on the polished surface of polycrystalline alumina specimens which were then cured or fired. Sections of these specimens were then examined using a scanning electron microscope.

Their micrographs indicate that the aluminum-phosphate bond material developed at 700°F consisted of three distinct types: (1) a fine particle crystalline material at the bond-substrate interface and at phase boundaries, (2) an intermediate phase of larger particle size, and (3) an outer phase which appeared to be amorphous.

The specimen heated to 2000°F showed only two distinct phases (1) a fine particle crystalline phase at the bond-substrate interface and

(2) an outer layer that appeared to be glassy. There was a large separation between the bond and the substrate. They suggest that the devitrification of the bond near the substrate interface is due to a gradient in the bond composition. The higher alumina content of the bond material near the interface would most likely form AlPO_4 , whereas, bond material farther away from the substrate might form $\text{Al}(\text{PO}_3)_3$.

The specimen produced by heating a mixture of the two acids (1:1 weight ratio of P_2O_5 to CrO_3) on a substrate to 2000°F produced a different reaction product morphology. Only one phase was observed. It consisted of a uniform agglomerate of small, most likely crystalline, particulate material. No attempt was made to identify any of the observed phases.

In a review, Cassidy (Ref. 26) discussed several of the new phosphate bonds that have been developed. Aluminum chlorophosphate hydrate (Ref. 27) is a dry powder developed especially for use in castable refractories. It is highly soluble in water and decomposes to form AlPO_4 on heating without formation of any intermediate metaphosphates. The simple thermochemistry of aluminum chlorophosphate hydrate allows it to be used in refractories which are subjected to rapid heating. Mixtures of aluminum phosphate and urea phosphate (Ref. 28) have been used as a dry bond for heat setting alumina castables.

Fisher (Ref. 29) found that at temperatures up to 2000°F increasing the level of phosphate binder present in high alumina plastics produced increases in their hot MOR's. At higher test temperatures this trend was still measurable but was much less pronounced. He also determined

that bauxite based phosphate bonded plastics were as strong at 2000°F and stronger at 2500°F than similar tabular alumina plastics.

The type of phosphate binder used did not have a significant effect on the level of hot MOR achieved between 1500 and 2500°F. This was unexpected in view of the different way in which they form the bond during the curing process. The hydrated aluminum phosphate $[AlH_3(PO_4)_2 \cdot 3H_2O]$ was formed with all three types of binder, but its mode of formation varied. In the phosphoric-acid-bonded plastics, the alumina required to form this compound is supplied by solution of fine grained alumina. In the plastics bonded with stoichiometric aluminum phosphate this compound can be formed directly from the binder so there is essentially no reaction between the binder and the alumina. The acid-rich aluminum phosphate should react mildly with the alumina since it contains the ingredients for both the hydrated aluminum phosphate and free phosphoric acid.

Gonzalez and Halloran (Ref. 30) determined that the reaction products of orthophosphoric acid and alumina at temperatures up to 500°C consisted of a mixture of aluminum phosphates that vary depending on the type of alumina, concentration, reactions time and temperature. The extent of the reaction and the relative yield of each aluminum phosphate were shown to be related to the relative activity of the system. The relative activity (S_R) is given by the total surface area of the alumina per mole of P_2O_5 in the system. The fraction of alumina reacted increased with increasing relative activity and temperature.

Mixes with low relative activity values tend to yield aluminum phosphates with low Al:P ratios [i.e., $Al(H_2PO_4)_3$, $AlH_2P_3O_{10} \cdot 2H_2O$ and $Al(PO_3)_3$]. In contrast, phosphates with high Al:P ratios (i.e., the

polymorphs of AlPO_4) are formed in mixes of high relative activity.

Condensed phosphates such as $\text{Al}(\text{PO}_3)_3$ were shown to react with excess alumina at temperatures between 500 and 700°C. Thus, reaction products in the vicinity of alumina particles would be expected to form AlPO_4 by solidstate reaction.

Alum-derived alumina containing metastable $\gamma\text{-Al}_2\text{O}_3$ reacted in high $\text{Al}_2\text{O}_3:\text{P}_2\text{O}_5$ ratio mixes to form large amounts of the cristobalite form of AlPO_4 at 150°C. In contrast, mixes of identical composition prepared from alum-derived $\alpha\text{-Al}_2\text{O}_3$ reacted at a slower rate and produced only amorphous reaction products.

Since Kingery's (Ref. 1) literature review in 1950 the amount of published information on phosphate bonding has been greatly expanded. Chvatal's (Ref. 31) 1975 review which concentrated primarily on the 1965-1975 literature contained 222 references. Most of the effort represented by these publications has been devoted towards empirically investigating phosphate bonding materials and development of useful refractory products.

The effect of variables such as temperature, particle size, concentration, source of raw materials and time on the form and relative abundance of the reaction products present in a number of phosphate bonded systems have been investigated. However, there is still little fundamental physiochemical information about phosphate bonding in the literature. This is not surprising when the complexity of the multistep reactions, the difficulty in differentiation between the many possible reaction products and the fine grain sized polycrystalline nature of materials being bonded are taken into consideration.

Thus it appears that fundamental investigations on phosphate bonding should be performed on simple model systems. This investigation involves the use of single crystals to accomplish this goal.

SECTION III

Experimental Program

This section describes the methods developed to orient single crystals; the experiments carried out to investigate the reaction of phosphate bonding agents with fused silica and different crystallographic faces of single crystals; the development of methods to form phosphate bonded bicrystals and tensile testing procedures, the formation and testing of aligned bicrystals of alumina and the investigation of the effect of rotational mismatch on the fired tensile strength of alumina bicrystals.

A. Single Crystal Orientation

Many of the experiments carried out during this investigation required the determination of the crystal faces which were to be bonded together or reacted with phosphate bonding agents. Preuss (Ref. 32) developed two Fortran IV computer programs designed to reduce the time required to accomplish single crystal orientations, using the conventional Laue back reflection method (Ref. 33). A program called PLOMAX (Ref. 34) was used to plot the back reflection Laue pattern for any desired orientation. The unknown orientation was then determined using a program named COL (Ref. 35) to analyze the Laue data. The two programs then allow the calculation of the amount of rotation necessary to translate the crystal to the desired orientation (Ref. 36). These two programs were modified so they would run on our Cyber 730 computer system. Crystals of alumina, magnesia, and quartz were successfully oriented using this technique.

The optimum time for producing the required back reflection Laue patterns using CuK_α radiation (35 kV and 20 mA) and 3000 speed, Type 57 Polaroid film was found to be between 10 and 20 minutes.

The crystal faces referred to in the remainder of this report were all determined or checked using the above procedure. The sapphire single crystals (Ref. 37) were purchased in the form of square rods with the sides consisting of (0001) and (11 $\bar{2}$ 0) faces and the ends being (11 $\bar{2}$ 0) faces. The back reflection Laue patterns for at least one face from each rod was determined to make sure that the orientation was the one desired.

B. Reaction of Phosphate Bonding Agents with Different Crystallographic Faces of Single Crystals and Fused Silica

O'Hara et al (Ref. 16) investigated the microstructures formed when a drop of phosphoric acid or a mixture of phosphoric and chromic acid was placed on the polished surface of polycrystalline alumina specimens and fired (see the Background Section for a summary of their work). Similar experiments utilizing single crystals and fused silica rods were carried out during this investigation.

A drop of phosphoric acid (61 % P_2O_5) or a 1:1 mixture of phosphoric acid (61 % P_2O_5) and chromic acid (61 % CrO_3) was placed on lapped surfaces of alumina, fused silica and quartz specimens. The alumina and quartz specimens were single crystals. The acid solutions were placed on the (0001) face of the quartz crystals. The orientation of the alumina crystals were not determined, but was perpendicular to the surface of the grown rod (1/4" diameter).

The acid solutions were dried at about 80°C for at least six hours and then fired at 1500°F (815°C). After cooling, a diamond saw cut was made about two-thirds of the way through the sample in the face opposite from the one on which the reaction had taken place. The reaction face was then fractured by gently tapping a wedge placed in the cut.

The alumina, fused silica and quartz samples reacted with phosphoric acid at 1500°F and the alumina crystal reacted with the chromic-phosphoric acid mixture at 1500°F were coated with gold and examined with an SEM.

The surface of the alumina-phosphoric acid reaction area was made up primarily of dendrites (Fig. 1), which appeared to be crystalline. Below the dendrites, there was a layer that contained a small amount of porosity (Fig. 2). Beneath this layer, there may be another very thin layer of material. However, the structure observed could also have been the result of acid roughening of the surface of the alumina crystal. In some locations, a crack between the porous layer and the thin layer or the roughened alumina crystal were observed (Fig. 2).

The reaction products formed when the chromic acid mixture was reacted with an alumina crystal were friable and appeared to be very porous. The top surface of these reaction products consisted of many small, needle-like crystals. It also appeared that some of the reaction layer was either broken off or crushed during the cutting and mounting procedure. Below this surface, a very porous amorphous appearing layer was present (Fig. 3). This layer appeared to be tightly adherent to the surface of the alumina crystal as no cracks were observed.

The top surface of the phosphoric acid-quartz reaction products appeared to be composed primarily of plate-like crystals (Fig. 4). The



Figure 1. Dendrite Crystals on Surface of Alumina Crystal Reacted with H_3PO_4 at 1500°F (400X).

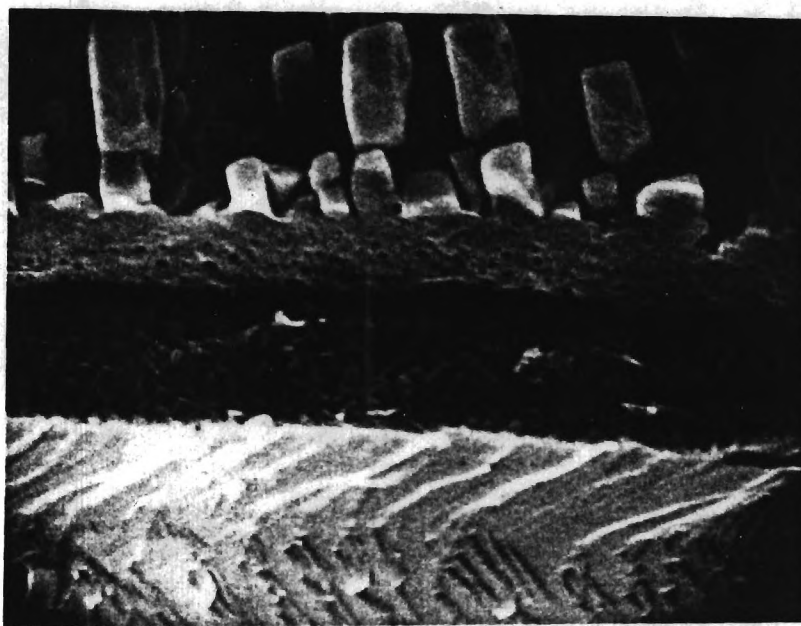


Figure 2. Reaction Product Layer Below Dendrites (2500X).

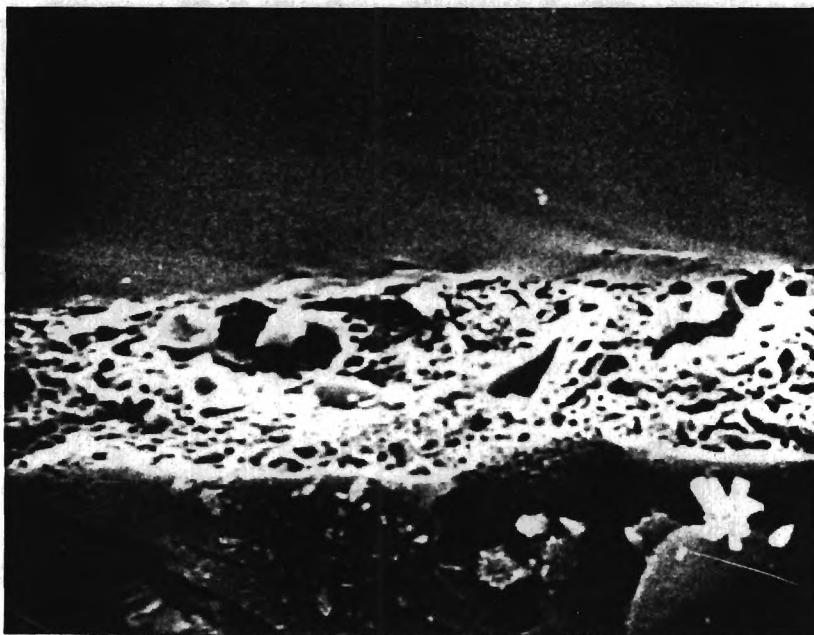


Figure 3. Reaction Product Layer Formed on Surface of Alumina Crystal Reacted with Chromic Phosphoric Acid Mixture at 1500°F. (3500X).



Figure 4. Top Surface of Reaction Products on (0001) Face of Quartz Crystal Reacted with Phosphoric Acid at 1500°F (2500X).

material below this surface was granular in nature and appeared to be tightly bonded to the surface of the quartz.

Some cracks developed in the quartz crystal when it was cooled through the β to α transition. The surface of the phosphoric acid-fused silica reaction products was composed of amorphous looking spheres (Fig. 5) and plate-like crystals that appeared to have grown out of the spheres (Fig. 6). Below the surface, the coating was made up of the amorphous spheres with voids between the spheres. The surface of the fused silica sample appeared to have been attacked much more severely than either the quartz or the alumina single crystals.

After the square alumina rods that were to be used for forming the phosphate bonded bicrystals were received, additional reaction experiments were performed. The surfaces of these rods contained (0001), (11 $\bar{2}$ 0), and (1 $\bar{1}$ 00) faces. Drops of phosphoric acid were reacted with samples of each face at 1500°F in the same manner as described above. After cooling in the furnace to room temperature, the reaction face was fractured by gently tapping a wedge placed in a diamond saw cut made in the back face before firing. The fractured samples were then mounted on SEM stubs and sputtered with gold.

The morphology of these alumina samples were examined with the SEM. At 100X, the (0001) face appeared to be primarily covered with whitish, star-shaped crystals on a gray crystalline background. A few grayish, star-shaped crystals were also observed to be composed of dendrites (see Figs. 7 and 8). These types of crystal morphologies were also seen on (11 $\bar{2}$ 0) and (1 $\bar{1}$ 00) faces. However, a smaller percentage of these surfaces were covered with the star-shaped crystals.



Figure 5. Reaction Product Layer Formed on Surface of a Fused Silica Rod Reacted with Phosphoric Acid at 1500°F (1500X).

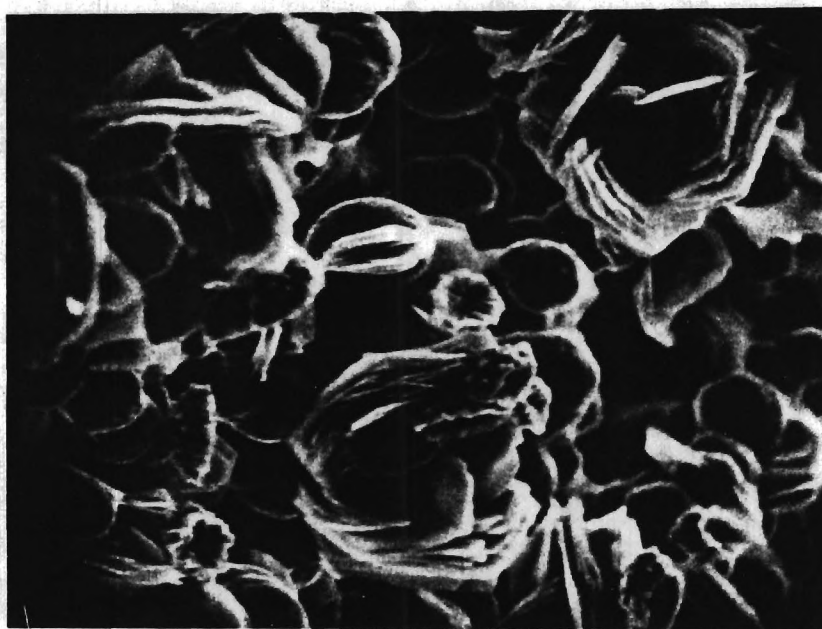


Figure 6. Plate-Like Crystals Growing Out of Spheres Shown in Figure 5 (1500X).



Figure 7. Whitish Star-Shaped Dendritic Crystals on Surface of Reaction Products Produced by Reacting H_3PO_4 with (0001) Face of Alumina at 1500°F (610X).

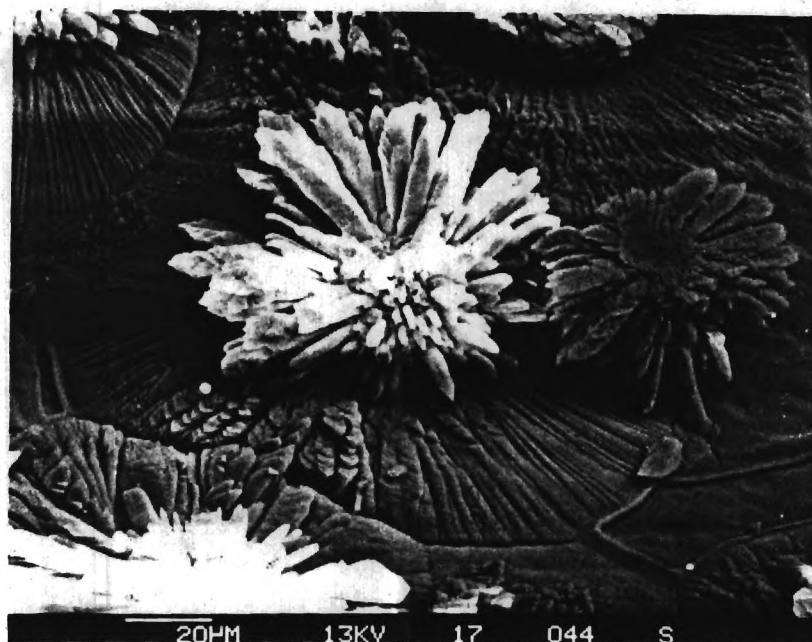


Figure 8. Whitish and Grayish-Shaped Dendritic Crystals Produced by Reacting H_3PO_4 with (0001) Face of Alumina Crystal at 1500°F (600X).

EDAX analysis of the whitish star-shaped crystals indicated that their Al:P ratio was 1:3. This suggests that they are composed of aluminum meta phosphate ($\text{Al}(\text{PO}_4)_3$). This phase is reported to be the major phase present on the surfaces of the alumina (Ref. 1) that had been heat treated above 500°C (932°F).

EDAX analysis of the grayish star-shaped crystals and the grayish crystalline background material indicated an Al:P ratio of approximately 1:1 (1:1.07), which suggests they are composed of monoaluminum phosphate (AlPO_4). This compound can exist in several polymorphic forms (berlinite, cristobalite, or tridymite forms). The different growth morphologies of the gray MAP may indicate the presence of two of these polymorphs. In addition to the slightly different growth morphologies of the $\text{Al}(\text{PO}_4)_3$ and AlPO_4 (MAP) dendritic structures, at higher magnifications (Figs. 9 and 10) it can clearly be seen that the MAP crystals contain much higher porosity. The flat interlocking MAP crystals covering the surface of the alumina appear to have nucleated at a central location and then to have grown outward until they encountered another group of crystals growing in a different direction.

Similar morphologies were seen on the (1 $\bar{1}$ 00) and (11 $\bar{2}$ 0) faces. However, it appeared that the whitish dendritic stars occurred much less frequently than on the (0001) face. This may be due to the fact that the (0001) face has a higher aluminum packing factor than the (1 $\bar{1}$ 00) and (11 $\bar{2}$ 0) faces.

The higher concentration of aluminum ions on the (0001) face appears to increase the amount of aluminum in the reaction products so that more AlPO_4 and less $\text{Al}(\text{PO}_4)_3$ is produced. Whereas, the elongated MAP crystals covering the (0001) surface appear to be grown out from a central

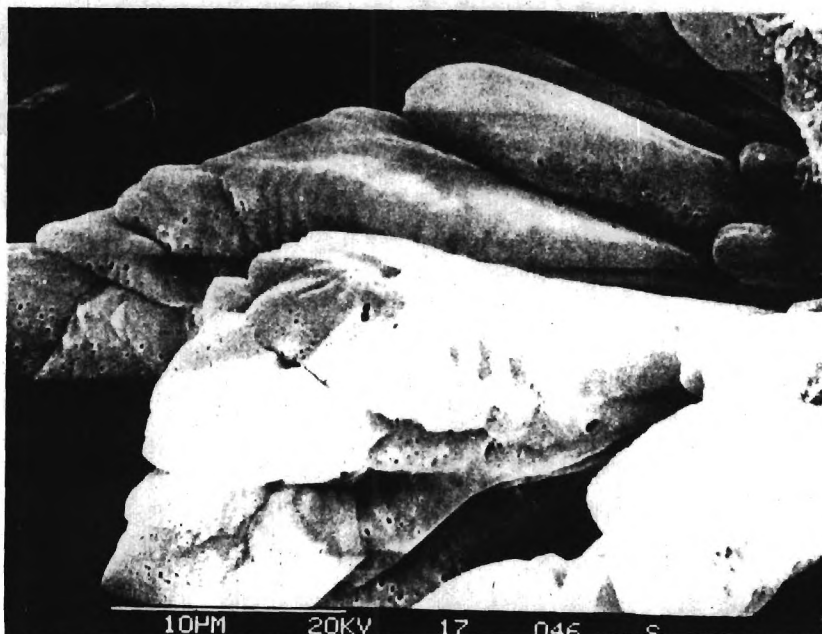


Figure 9. Structure of Aluminum Meta Phosphate $[Al(PO_4)_3]$ Dendrites (3200X).



Figure 10. Porous Morphology of Monoaluminum Phosphate ($AlPO_4$) Dendritic Structure (3200X).

location (Figures 7 and 8), those covering the $(1\bar{1}00)$ surface appeared to be more nearly equiaxed (Figures 11 and 12).

Alumina samples were cut from the sapphire rods so that $(1\bar{1}02)$, $(11\bar{2}2)$ and two random faces were exposed. The random faces were cut in such a manner that it is unlikely they correspond to any low index face. A drop of phosphoric acid was placed on each of these faces and they were then dried and fired at 1500°F as described above. The reaction products on the $(1\bar{1}02)$ faces had morphologies similar to those observed on the (0001) faces, except that the star-like dendritic structures (Figure 13) appeared to contain more branching (less needle like). The aluminum phosphate structure formed on the $(11\bar{2}2)$ face did not contain any of the star-like dendritic structures. This face was covered with roughly equiaxed grains (Figure 14) that had a plate-like or even cubic substructure on portions of its surface (Figure 15).

The structures formed on the two randomly oriented faces did not contain any of the large star-like dendritic structures (Figures 16 and 17). However, a few small dendrites were observed on one of them (Figure 16). Since these faces were prepared so that they most likely do not correspond to any low index face, it is reasonable to assume that they have relatively low aluminum packing densities. The fact that no large dendrite structures were formed suggests that large dendritic structures most likely only form on faces with high aluminum packing densities. The roughly equiaxed major grains shown in Figure 17 are also covered with a plate-like substructure (Figure 18).

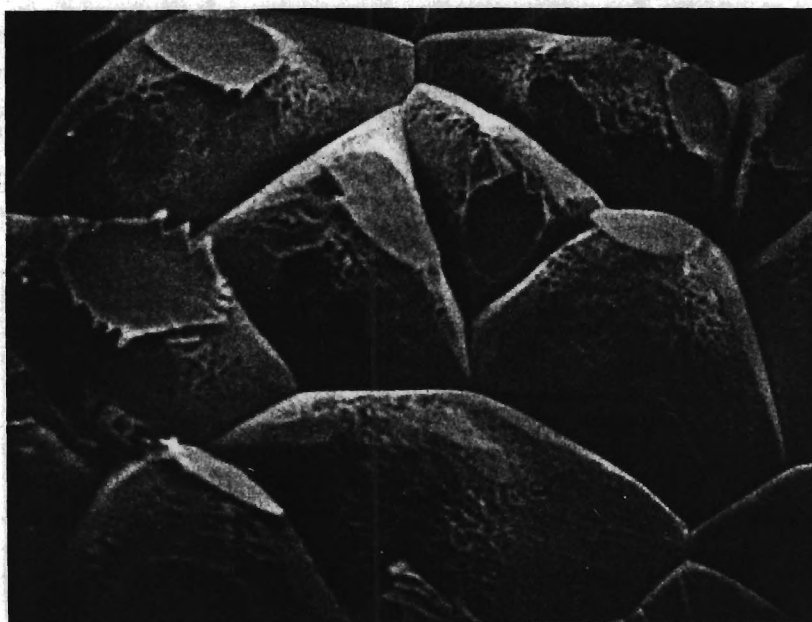


Figure 11. Nearly Equiaxed Crystals Covering ($1\bar{1}00$) Face of Alumina Crystal Reacted with H_3PO_4 (1000X).



Figure 12. Fractured Alumina Crystal with Equiaxed Crystals on ($1\bar{1}00$) Face (250X).

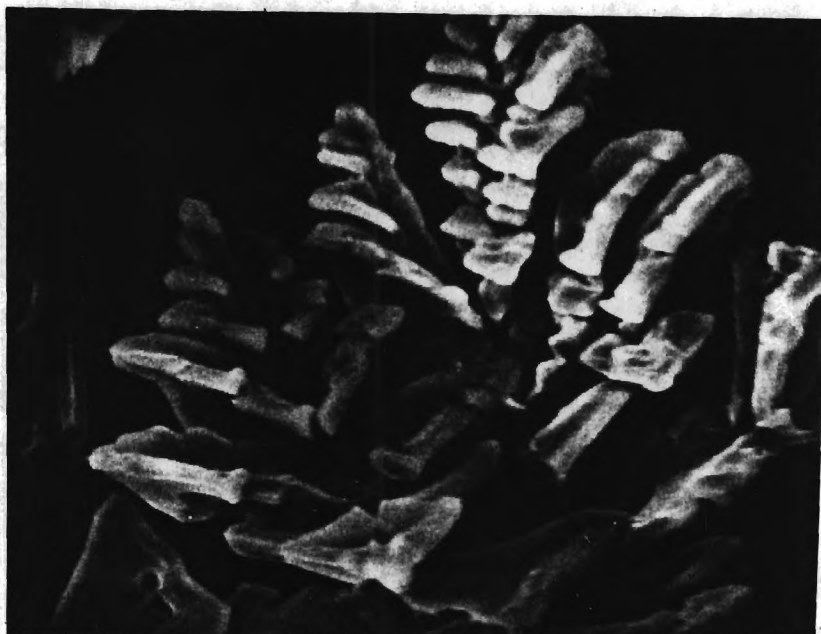


Figure 13. Dendritic Structure on Face of $(1\bar{1}02)$ Alumina Crystal Reacted with H_3PO_4 at $1500^\circ F$ (1250X).



Figure 14. Aluminum Phosphate Reaction Products on Surface of $(11\bar{2}2)$ Face of Alumina Crystal Reacted with H_3PO_4 at $1500^\circ F$ (250X).

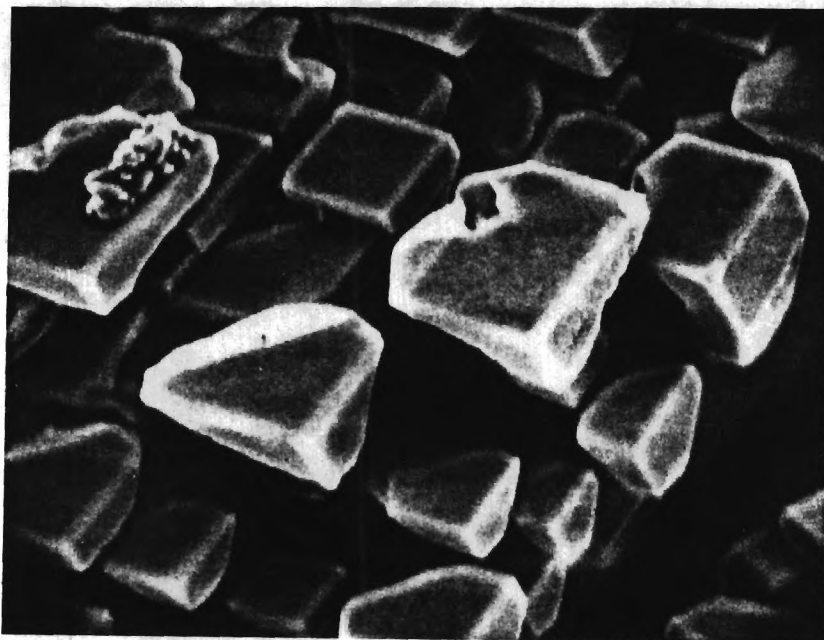


Figure 15. Higher Magnification of Surface Shown in Figure 14 (1100X).

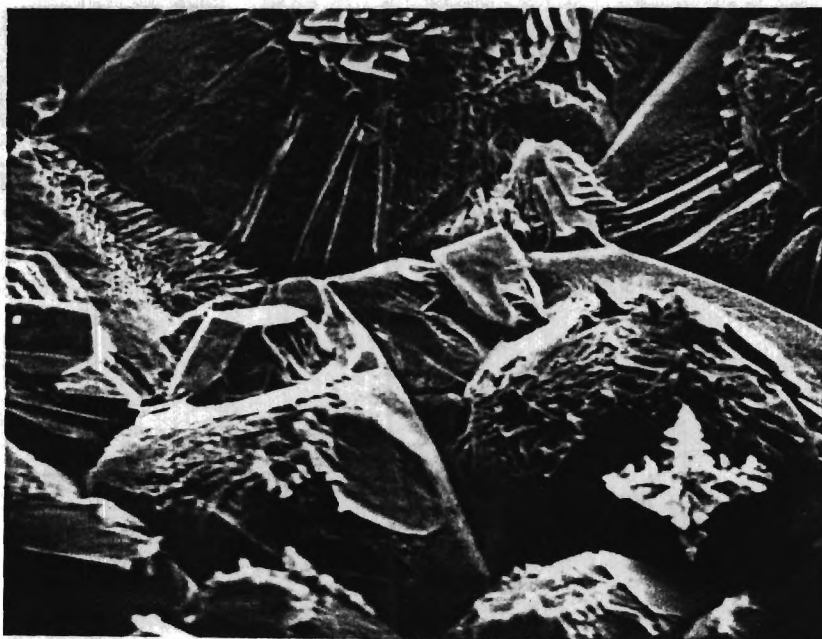


Figure 16. Surface of Reaction Products on a Random Plane of an Alumina Crystal Reacted with H_3PO_4 at 1500°F (250X).

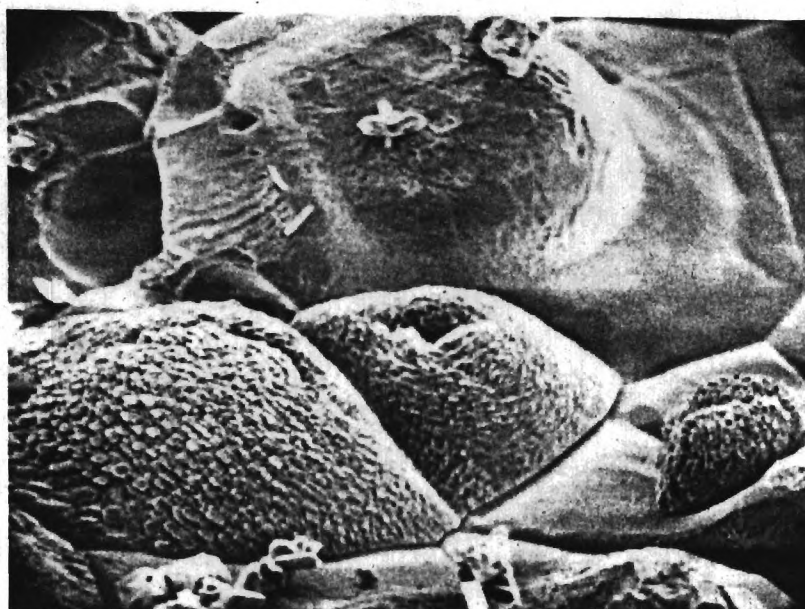


Figure 17. Same as Figure 16 Except Random Plane was Different (250X).

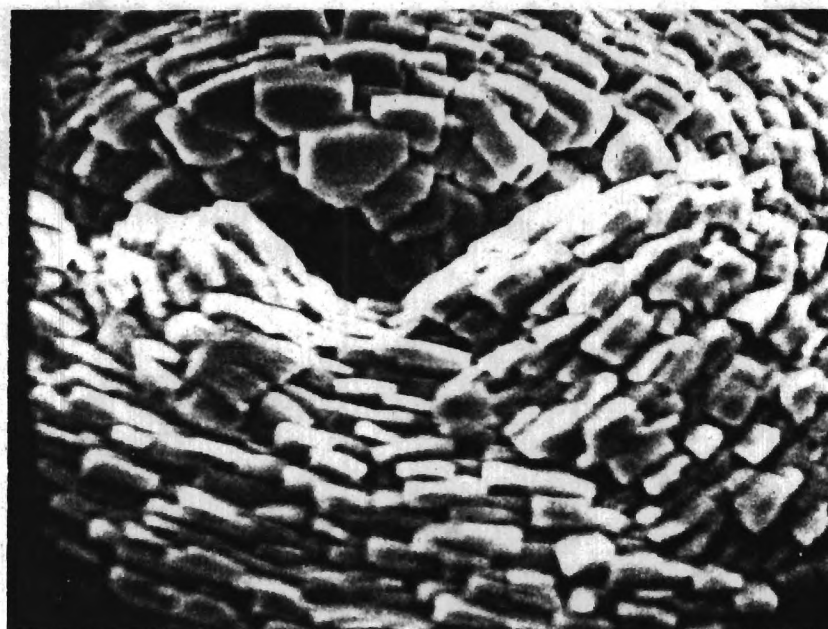


Figure 18. Plate-Like Structure Covering Surface of Grains Shown in Figure 17 (1600X).

The microstructures produced when phosphoric acid was reacted with a fine grained polycrystalline alumina was investigated by placing a drop of acid on an alumina cutting tool and then drying and firing them as described above. The average grain size of the cutting tool was $<5\mu\text{m}$. No dendritic structures were observed in the microstructure of these reaction products. The morphology consisted of a mixture of elongated, equiaxed and plate-like grains (Figures 19 and 20). These results tend to support the theory that dendrites are only formed on low index high atomic density faces since the probability of low index faces being parallel to the surface of the cutting tools is low.

Comparison of the microstructures observed during this investigation with those observed when samples were cut and polished (Ref. 16) appears to indicate that the observation of fractured surfaces instead of polished surfaces may give a better understanding of phosphoric acid - alumina reaction product morphologies. At least some of the texture shown in the micrographs of the polished samples (Ref. 16) is most likely the result of the polishing process.

Attempts were made to determine the crystal structure of aluminum phosphate grains and dendrites removed from the surface of the fired samples. Enough electron diffraction spots were not obtained to allow the phases to be identified.

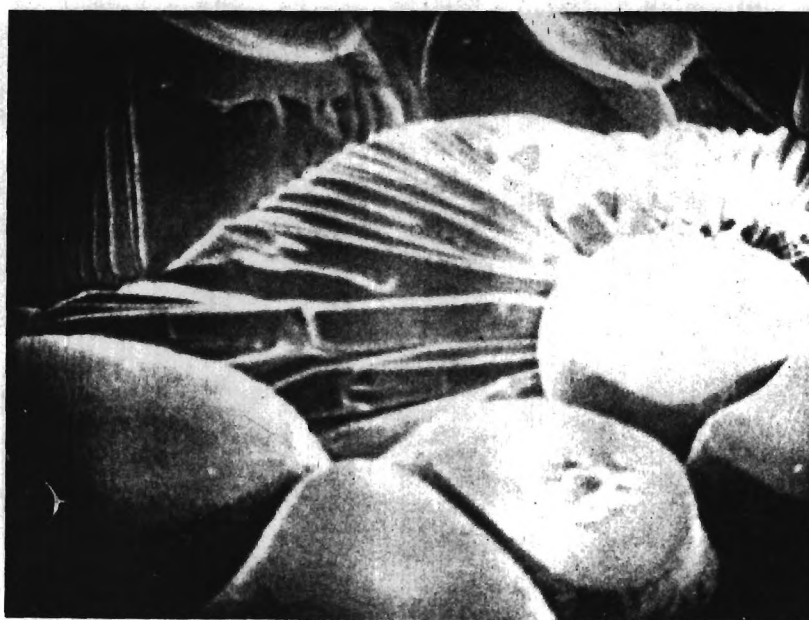


Figure 19. Surface of Reaction Product Layer Formed on the Surface of an Alumina Cutting Tool Reacted with H_3PO_4 at $1500^{\circ}F$ (500X).

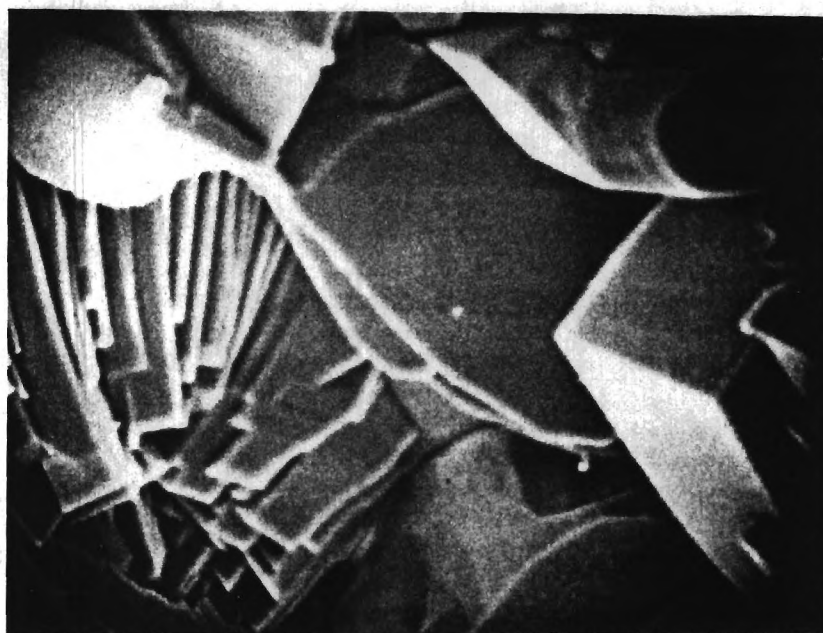


Figure 20. Plate-Like Grains on Different Area of Alumina Cutting Tool Shown in Figure 19 (900X).

C. Development of Methods to Form Phosphate Bonded Bicrystals and Tensile Testing Procedures

Preliminary experiments were carried out using on-hand alumina, magnesia and quartz single crystals. Bicrystals were produced using both phosphoric acid and sodium dihydrogen phosphate as the bonding agent. During these preliminary experiments, neither bond thickness nor crystal orientation were controlled. Samples cured at 2000°F (1093°C) for four hours were strong enough to be easily handled except for the quartz bicrystals which contained cracks which were formed due to the $\alpha \rightleftharpoons \beta$ inversion.

The sapphire single crystals used in the remainder of this study were 0.250 in. rectangular cross-section rods obtained from Saphikon Division of Tyco Laboratories, Inc. They had well oriented (0001), (11 $\bar{2}$ 0), and (1 $\bar{1}$ 00) faces exposed ($\pm 30^\circ$).

Preliminary attempts to form bicrystals using these single crystals were made using 85% H₃PO₄ (61% P₂O₅) as the bonding agent with bond thicknesses between 0.002 and 0.007" (before firing). In general, the strength of the bicrystals, bonded at 1500°F, was low and decreased as the thickness of the bond was increased. Since the separation of the bicrystals before bonding could not be accurately controlled below 0.002" (using feeler gauges), a new series of bicrystals were formed under varying loads during the heat treatment process. These bicrystals were strong enough to be easily handled. Examination of these samples in the SEM indicated that their bond thicknesses were all less than 0.002".

Three series of bicrystals were formed at 750°F, 1500°F and 2000°F. In each series, (0001) faces were bonded to (0001) faces and (11 $\bar{2}$ 0) faces

were joined to $(11\bar{2}0)$ faces using three different bonding agents and various loads. The three bonding agent solutions used were 85% H_3PO_4 (61.1% P_2O_5), $NaH_2PO_4 \cdot H_2O$ (30% P_2O_5) and Glass H $(NaPO_3)_2O$ (30% P_2O_5).

Tensile strengths were determined using an Instron Universal Testing machine and a loading jig which had a double flexible joint at the top and a reservoir of Wood's metal at the bottom. The samples were tested by super-gluing the bicrystals to two aluminum attachment rods. One of these rods was threaded into the bottom of the flexible joint. The Wood's metal was then melted with a gas torch and the cross-head lowered until the lower rod was partially submerged in the molten metal. The metal was then allowed to solidify around the bottom rod. This system was designed to minimize misalignment so the bicrystal would be loaded in pure tension. However, as the molten metal solidified and then cooled, it tended to misalign the lower rod and to also stress the bicrystal, causing some of them to fail.

The results obtained using this loading system and a cross-head speed of 0.1 cm/min. are given in Table I. These results showed that there was a positive relationship between bond strength and firing temperature. In general, the strength of the (0001) bicrystals was stronger than the $(11\bar{2}0)$ bicrystals. The samples prepared with H_3PO_4 as the bonding agent were the weakest and those prepared with Glass H were the strongest. In every case except one where a comparison was possible, the samples cured under the higher load (200 gms.) were stronger.

The bicrystals heat treated to $1500^\circ F$ were selected for morphological study after strength testing. The fracture morphologies of Glass H and $NaH_2PO_4 \cdot H_2O$ bonded bicrystals were basically the same (Figs. 21 and

Table I. Tensile Strength of Phosphate Bonded Alumina Bicrystals.

Heat Treatment Temp. (°F)	Bonding Agent	Load Applied During Firing (gms)	Bicrystal Faces Bonded	Tensile Strength (kgf/cm ²)
750	NaH ₂ PO ₄ H ₂ O	200	(0001)	20.9
750	Glass H	100	(0001)	19.3
1500	H ₃ PO ₄	200	(0001)	21.5
1500	NaH ₂ PO ₄ · H ₂ O	100	(0001)	77.0
1500	NaH ₂ PO ₄ · H ₂ O	200	(0001)	83.0
2000	NaH ₂ PO ₄ · H ₂ O	100	(0001)	65.0
2000	NaH ₂ PO ₄ · H ₂ O	200	(0001)	89.0
2000	NaH ₂ PO ₄ · H ₂ O	100	(1120)	16.5
2000	NaH ₂ PO ₄ · H ₂ O	200	(1120)	29.0
2000	Glass H	100	(0001)	64.0
2000	Glass H	200	(0001)	16.0
2000	Glass H	300	(1120)	17.5

Bicrystals that broke due to handling or during mounting in the loading jig have not been included.

22), and showed that the bond was composed of interlocking cones that join the two faces of the bicrystals together. It also can be seen that voids existed between many of the cones and that the direction of fracture was parallel to the bicrystal faces. The fracture morphology of H_3PO_4 bonded crystals was entirely different from what was observed when H_3PO_4 was fired on the surface of a crystal. In general, the H_3PO_4 bond appeared to be very porous and none of the dendritic structures seen on the crystal surfaces were observed. This porosity (similar to that in Figure 10) and the fact that aluminum was available from two crystal faces suggests that the bonding phase formed from H_3PO_4 was mono-aluminum phosphate.

In an attempt to overcome the problems associated with the first loading jig, a new loading system was developed. This system utilized two steel cables to transmit the tensile forces from the Instron to the two eyelets attached to aluminum loading blocks to which the bicrystal had been super-glued.

This new loading system was used to test a series of $(11\bar{2}0)$ bicrystals bonded with $\text{NaH}_3\text{PO}_4 \cdot \text{H}_2\text{O}$ (30% P_2O_5). These bicrystals were placed under a 100 gram weight and allowed to cure at room temperature for at least 24 hours. They were then fired at 1500°F for four hours. Their room temperature strengths are listed in Table II.

Based on the fact that all of these samples were stronger than any previously tested, our visual observation that the new system produced much better alignment during loading was confirmed. A second series of similar bicrystals was prepared (A-7 to A-8) using a 200 gram load during the 24 hour room temperature curing cycle. These bicrystals were

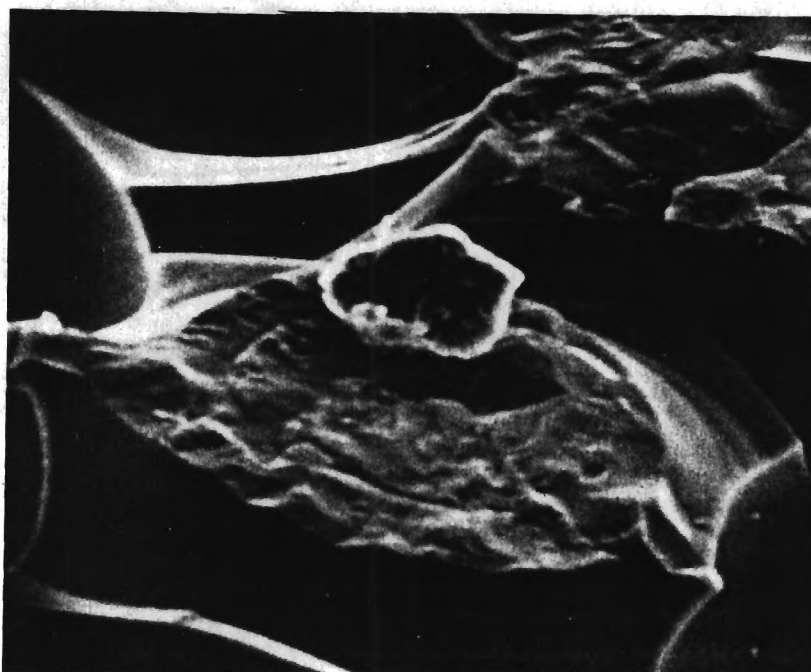


Figure 21. Fracture Morphology of $\text{NaH}_2\text{PO}_4 \cdot \text{H}_2\text{O}$ Bond Between (0001) Faces of Alumina Crystals Fired at 1500°F (1200X).

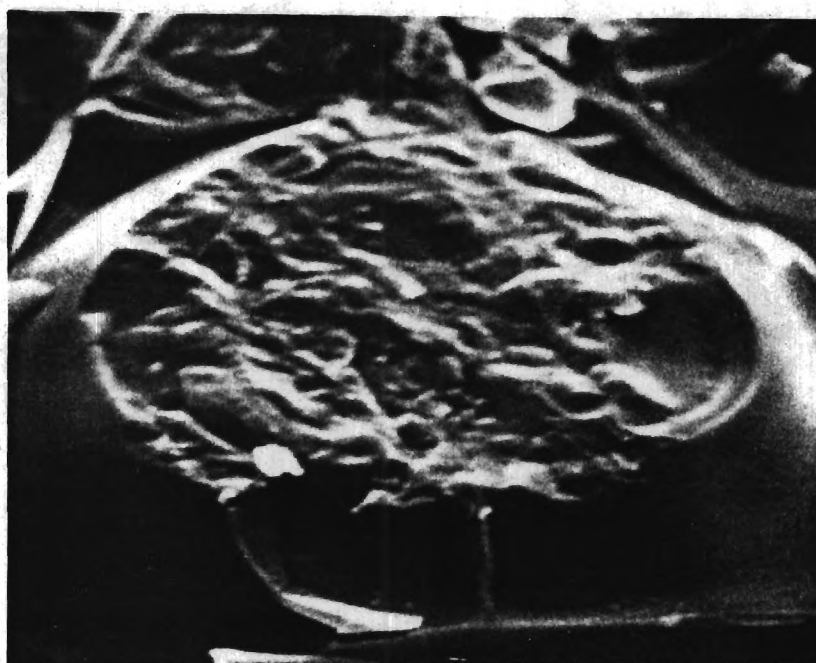


Figure 22. Fracture Morphology of Glass H Bond Between (0001) Faces of Alumina Single Crystals Fired at 1500°F (1200X).

Table II. Tensile Strength of Alumina Bicrystals Bonded with NaH_2PO_4 and Fired at 1500°F for Four Hours.

Sample Number	Load Applied During Curing (gms)	Bicrystal Faces Bonded	Crystal Condition	Tensile Strength (kgf/cm^2)
A-1	100	(11 $\bar{2}$ 0)	New	100.9
A-2	100	(11 $\bar{2}$ 0)	New	90.5
A-3	100	(11 $\bar{2}$ 0)	New	93.5
A-4	100	(11 $\bar{2}$ 0)	New	106.0
A-5	100	(11 $\bar{2}$ 0)	New	117.6
A-6	100	(11 $\bar{2}$ 0)	New	101.6
				$\bar{x} = 101.7$
				$s = 9.6$
A-7	200	(11 $\bar{2}$ 0)	Used	32.5
A-8	200	(11 $\bar{2}$ 0)	Used	33.7
A-9	200	(11 $\bar{2}$ 0)	Used	42.2
A-10	200	(11 $\bar{2}$ 0)	Used	64.0
A-11	200	(11 $\bar{2}$ 0)	Used	42.9
A-12	200	(11 $\bar{2}$ 0)	Used	40.7
				$\bar{x} = 42.7$
				$s = 11.3$
B-1	100	(0001)	Used	13.0
B-2	100	(0001)	Used	35.4
B-3	100	(0001)	Used	26.1
B-4	100	(0001)	Used	41.5
B-5	100	(0001)	Used	15.3
				$\bar{x} = 26.3$
				$s = 12.4$
B-7	100	(0001)	New	41.5
B-8	100	(0001)	New	85.3
B-9	100	(0001)	New	43.3
B-10	100	(0001)	New	66.8
B-11	100	(0001)	New	98.4
B-12	100	(0001)	New	56.2
				$\bar{x} = 65.3$
				$s = 22.9$

prepared from crystals that had been previously used. Before being re-bonded, they were lightly ground on 180, 240, 600 grit SiC paper and were then lightly polished using 1, 0.5 and 0.3 μm alumina to remove any contamination. The tensile strengths of these samples are also listed in Table II. These samples were significantly weaker than the set produced from unused crystals.

In an attempt to determine if this strength decrease was the result of reusing the alumina crystals or was due to the increased load during curing, two additional series of bicrystals bonded with $\text{NaH}_2\text{PO}_4 \cdot \text{H}_2\text{O}$ were prepared and fired. All of these samples were (0001) bicrystals cured under a 100 gram load and fired at 1500°F for four hours. The B-1 to B-5 samples were prepared from used crystals and the B-7 to B-12 samples from new crystals. Their tensile strengths are listed in Table II. Even though the new (0001) bicrystals were much weaker than the (11 $\bar{2}$ 0) bicrystals produced from unused crystals, it appears that reusing the alumina crystals decreases the strength of the alumina bicrystals.

Additional (0001) and (11 $\bar{2}$ 0) bicrystals were produced from new crystals using Glass H (30% P_2O_5) as the bonding agent. These samples were cured under 100 gram loads and fired at 1500°F. Their tensile strengths are listed in Table III. These results indicate that both (11 $\bar{2}$ 0) and (0001) bicrystals bonded with Glass H are weaker than the same type of bicrystals bonded with $\text{NaH}_2\text{PO}_4 \cdot \text{H}_2\text{O}$.

Examination of the fracture faces of the above samples suggested that the loads applied during curing may not have been uniformly distributed over the bond area. An attempt was made to improve the load distribution by curing ten samples at one time with the load being applied

Table III. Tensile Strength of Alumina Bicrystals Bonded With Glass H and Fired at 1500°F for Four Hours.

Sample Number	Load Applied During Curing (gms)	Bicrystal Faces Bonded	Tensile Strength (kgf/cm ²)
H-1	100	(11 $\bar{2}$ 0)	16.2
H-2	100	(11 $\bar{2}$ 0)	20.7
H-3	100	(11 $\bar{2}$ 0)	26.6
H-4	100	(11 $\bar{2}$ 0)	17.7
H-5	100	(11 $\bar{2}$ 0)	20.7
H-6	100	(11 $\bar{2}$ 0)	20.7
			$\bar{x} = 20.4$
			$s = 3.6$
G-2	100	(0001)	43.9
G-3	100	(0001)	34.0
G-5	100	(0001)	29.2
G-6	100	(0001)	17.2
			$\bar{x} = 31.1$
			$s = 11.1$

to the samples by a rigid one or two kilogram plate which rested on all ten specimens. These samples were cured at room temperature for 24 hours and then fired at 1500°F for 4 hours. Sodium dihydrogen phosphate and Glass H which contained 30% P_2O_5 were used as the bonding agents.

The tensile strengths of these samples are listed in Table IV. The samples whose condition is described as "polished" are used samples that were prepared in the same manner as the "used" samples in Table II, except the coarse grinding was done on 150 and 45 μm diamond wheels. The effects of crystal condition and the bicrystal faces bonded are shown in Figure 23. Figure 24 show the effect of bonding agent, curing load, and bicrystal faces bonded.

Examination of the fracture faces of these samples indicated that the distributed loading technique produced even greater nonuniformity of bond thickness. Because of this, analysis of variance calculations were not made. However, examination of the results suggests that the polishing of used samples does not produce as good a bonding surface as that present on the unused single crystals (Fig. 23). In addition, it appears that decreasing the bond thickness (increasing the curing load) may decrease the bond strength of bicrystals bonded with Glass H (Fig. 24). Since the uniformity of bond thicknesses of these samples was worse than those which were individually loaded during the curing cycle, the individual load method was used throughout the rest of this investigation.

The effect of curing time was investigated by preparing two sets of bicrystals cured at room temperature for 24 and 3 hours respectively. A 100 gm load was applied during the curing cycle and the samples fired at 1500°F

Table IV. Tensile Strength of Phosphate Bonded Alumina Bicrystals Cured Under a Distributed Load.

Bonding Agent	Load Applied During Curing (gms)	Bicrystal Faces Bonded	Crystal Condition	Tensile Strength (kgf/cm ²)
NaH ₂ PO ₄ ·H ₂ O	100	(1120)	New	40.8
NaH ₂ PO ₄ ·H ₂ O	100	(1120)	New	31.3
NaH ₂ PO ₄ ·H ₂ O	100	(1120)	New	33.0
NaH ₂ PO ₄ ·H ₂ O	100	(1120)	New	104.9
NaH ₂ PO ₄ ·H ₂ O	100	(1120)	New	64.5
				$\bar{x} = 54.9$
				$s = 30.9$
NaH ₂ PO ₄ ·H ₂ O	100	(1120)	Polished	8.1
NaH ₂ PO ₄ ·H ₂ O	100	(1120)	Polished	6.5
NaH ₂ PO ₄ ·H ₂ O	100	(1120)	Polished	9.7
NaH ₂ PO ₄ ·H ₂ O	100	(1120)	Polished	8.1
NaH ₂ PO ₄ ·H ₂ O	100	(1120)	Polished	8.1
				$\bar{x} = 8.1$
				$s = 1.1$
NaH ₂ PO ₄ ·H ₂ O	100	(0001)	New	104.9
NaH ₂ PO ₄ ·H ₂ O	100	(0001)	New	59.5
NaH ₂ PO ₄ ·H ₂ O	100	(0001)	New	15.6
NaH ₂ PO ₄ ·H ₂ O	100	(0001)	New	46.1
NaH ₂ PO ₄ ·H ₂ O	100	(0001)	New	37.5
				$\bar{x} = 52.7$
				$s = 33.2$
NaH ₂ PO ₄ ·H ₂ O	100	(0001)	Polished	31.3
NaH ₂ PO ₄ ·H ₂ O	100	(0001)	Polished	28.6
NaH ₂ PO ₄ ·H ₂ O	100	(0001)	Polished	54.8
NaH ₂ PO ₄ ·H ₂ O	100	(0001)	Polished	31.3
NaH ₂ PO ₄ ·H ₂ O	100	(0001)	Polished	31.3
				$\bar{x} = 35.5$
				$s = 10.8$
Glass H	100	(1120)	New	61.4
Glass H	100	(1120)	New	89.7
Glass H	100	(1120)	New	52.2
Glass H	100	(1120)	New	20.7
Glass H	100	(1120)	New	115.6
				$\bar{x} = 67.9$
				$s = 36.2$

Table IV. Tensile Strength of Phosphate Bonded Alumina Bicrystals Cured Under a Distributed Load (Continued).

Bonding Agent	Load Applied During Curing (gms)	Bicrystal Faces Bonded	Crystal Condition	Tensile Strength (kgf/cm ²)
Glass H	100	(0001)	New	84.2
Glass H	100	(0001)	New	30.7
Glass H	100	(0001)	New	27.4
Glass H	100	(0001)	New	47.7
Glass H	100	(0001)	New	20.7
				$\bar{x} = 42.1$
				$s = 25.5$
NaH ₂ PO ₄ • H ₂ O	200	(11 $\bar{2}$ 0)	New	63.0
NaH ₂ PO ₄ • H ₂ O	200	(11 $\bar{2}$ 0)	New	96.9
NaH ₂ PO ₄ • H ₂ O	200	(11 $\bar{2}$ 0)	New	29.0
NaH ₂ PO ₄ • H ₂ O	200	(11 $\bar{2}$ 0)	New	43.6
NaH ₂ PO ₄ • H ₂ O	200	(11 $\bar{2}$ 0)	New	80.7
				$\bar{x} = 62.6$
				$s = 27.3$
NaH ₂ PO ₄ • H ₂ O	200	(0001)	New	15.9
NaH ₂ PO ₄ • H ₂ O	200	(0001)	New	31.3
NaH ₂ PO ₄ • H ₂ O	200	(0001)	New	22.6
NaH ₂ PO ₄ • H ₂ O	200	(0001)	New	83.0
NaH ₂ PO ₄ • H ₂ O	200	(0001)	New	43.8
				$\bar{x} = 39.3$
				$s = 26.5$
Glass H	200	(11 $\bar{2}$ 0)	New	18.1
Glass H	200	(11 $\bar{2}$ 0)	New	61.3
Glass H	200	(11 $\bar{2}$ 0)	New	123.0
Glass H	200	(11 $\bar{2}$ 0)	New	28.2
Glass H	200	(11 $\bar{2}$ 0)	New	52.9
				$\bar{x} = 56.7$
				$s = 41.0$
Glass H	200	(0001)	New	28.2
Glass H	200	(0001)	New	33.3
Glass H	200	(0001)	New	17.7
Glass H	200	(0001)	New	48.5
Glass H	200	(0001)	New	15.5
				$\bar{x} = 28.6$
				$s = 13.3$

		Crystal Condition	
		New	Polished
Bicrystal Faces Bonded	(11 $\bar{2}$ 0)	54.9	8.1
	(0001)	52.7	35.5

Figure 23. Average Tensile Strength Factorial Design (2 x 2) Showing Effect of Crystal Condition and Bicrystal Faces Bonded with Sodium Dihydrogen Phosphate (30% P₂O₅) and Cured Under a Load of 100 Grams.

		Load During Curing (gms)			
		100	200		
Bicrystal Face Bonded	(11 $\bar{2}$ 0)	54.9	62.5	NaH ₂ PO ₄ •H ₂ O	Bonding Agent
		67.9	56.7	Glass H	
	(0001)	52.7	42.1	NaH ₂ PO ₄ •H ₂ O	
		39.9	28.6	Glass H	

Figure 24. Average Tensile Strength Factorial Design (2 x 2 x 2) Showing the Effect of Bonding Agent, Curing Load and Bicrystal Faces Bonded.

for 4 hours. The bonding agent used was sodium dihydrogen phosphate that had been diluted with water to reduce its P_2O_5 content to 20%. The tensile strengths of these samples are listed in Table V.

The strength of the $(11\bar{2}0)$ bicrystals decreased when the curing time was reduced from 24 to 3 hours. On the other hand, it appears the longer curing time may cause the (0001) bicrystals to be weaker, provided they are handled very carefully until after they have been fired. Thus, it appears that it takes longer for the aluminum required to form the bond to go into solution from the $(11\bar{2}0)$ faces than it does from the (0001) faces. This may be due to the fact that the (0001) face has a higher aluminum packing factor than the $(11\bar{2}0)$ face. The reason for the decrease in strength of the (0001) bicrystals with increasing curing time is unknown. However, one possibility is that after 3 hours curing, the bonding phase produces $Al(PO_4)_3$ when it is fired and that after 24 hours curing the bonding phase produces $AlPO_4$ when it is fired. These results also tend to confirm the fact that a stronger bond is formed between $(11\bar{2}0)$ faces than (0001) faces when sodium dihydrogen phosphate is used as the bonding agent (see Table II).

In a further attempt to develop a method of reusing the alumina crystals, two additional sets of samples were prepared. Both were bonded with sodium dihydrogen phosphate and cured 24 hours under a 100 gram load at room temperature. The first set was produced by cutting a used crystal in half on a Buehler Limited Isomet Low Speed Saw using a Lunzer Industrial Diamond $4 \times 0.012 \times 1/2$ " blade. The two halves were then bonded together without any further finishing treatment. The second set was prepared from used crystals that were polished on 180, 240, 320

Table V. Effect of Curing Time on the Tensile Strength of Sodium Dihydrogen Phosphate Bonded Alumina Bicrystals.

Curing Time (hrs.)	Bicrystal Faces Bonded	Tensile Strength (kgf/cm ²)
24	(11 $\bar{2}$ 0)	50.1
24	(11 $\bar{2}$ 0)	134.0
24	(11 $\bar{2}$ 0)	158.4
24	(11 $\bar{2}$ 0)	161.4
24	(11 $\bar{2}$ 0)	150.2
		$\bar{x} = 130.8$
		$s = 46.3$
24	(0001)	24.2
24	(0001)	51.7
24	(0001)	62.9
24	(0001)	35.5
		$\bar{x} = 43.6$
		$s = 17.1$
3	(11 $\bar{2}$ 0)	67.5
3	(11 $\bar{2}$ 0)	33.8
3	(11 $\bar{2}$ 0)	51.7
3	(11 $\bar{2}$ 0)	51.7
3	(11 $\bar{2}$ 0)	50.8
		$\bar{x} = 51.1$
		$s = 11.9$
3	(0001)	0*
3	(0001)	0*
3	(0001)	0*
3	(0001)	116.7
3	(0001)	95.3
		$\bar{x} = 106.0$

*Failed during handling, before firing.

and 600 grit SiC papers. The tensile strengths of these samples are listed in Table VI.

Comparison of these results with those in Table V clearly indicates the importance of surface finish on the bicrystal tensile strength. For both the $(11\bar{2}0)$ and (0001) bicrystals, the tensile strength increases (Table VII) as the surface finish is improved (diamond sawed \rightarrow polished \rightarrow new). It should also be noted that the $(11\bar{2}0)$ bicrystals were stronger than the (0001) bicrystals for equivalent surface finish (Table VII) when $\text{NaH}_2\text{PO}_4 \cdot \text{H}_2\text{O}$ (20% P_2O_5) was used as the bonding agent.

A series of bicrystals were made to investigate the effect of rotational mismatch on the strength of $(11\bar{2}0)$ bicrystals. These bicrystals were bonded with sodium dihydrogen phosphate (20% P_2O_5) and cured under a 100 gram load for 24 hours at room temperature. After curing, they were fired at 1500°F for 4 hours. The alignment jig used produced bicrystals whose mismatch angle was within $\pm 2^\circ$. The tensile strengths of these bicrystals are listed in Table VIII. The used-polished samples were prepared using the polishing technique described above. The results are also shown graphically in Figure 25.

These results indicate that the tensile strength decreases as the rotational angle is increased from 0 to 90° and then increases back to approximately its original level as the angle of rotation is further increased from 90 to 180° .

Since the load per unit area during the curing cycle varied by a factor of two as the amount of rotation was varied, an experiment was carried out to determine if the low strength of the intermediate samples

Table VI. Effect of Surface Finish on the Tensile Strength of Alumina Bicrystals Bonded with Sodium Dihydrogen Phosphate.

Bicrystal Faces Bonded	Crystal Condition	Tensile Strength (kgf/cm ²)
(11 $\bar{2}$ 0)	Diamond Sawed	56.2
(11 $\bar{2}$ 0)	Diamond Sawed	40.9
(11 $\bar{2}$ 0)	Diamond Sawed	56.2
(11 $\bar{2}$ 0)	Diamond Sawed	8.4
(11 $\bar{2}$ 0)	Diamond Sawed	60.2
(11 $\bar{2}$ 0)	Diamond Sawed	55.3
		$\bar{x} = 46.2$
		$s = 19.7$
(0001)	Diamond Sawed	21.4
(0001)	Diamond Sawed	18.4
(0001)	Diamond Sawed	17.0
(0001)	Diamond Sawed	18.0
(0001)	Diamond Sawed	17.1
(0001)	Diamond Sawed	18.0
(0001)	Diamond Sawed	21.4
(0001)	Diamond Sawed	19.4
		$\bar{x} = 18.8$
		$s = 1.7$
(11 $\bar{2}$ 0)	Polished	48.5
(11 $\bar{2}$ 0)	Polished	64.5
(11 $\bar{2}$ 0)	Polished	23.8
(11 $\bar{2}$ 0)	Polished	88.6
(11 $\bar{2}$ 0)	Polished	80.9
(11 $\bar{2}$ 0)	Polished	67.3
(11 $\bar{2}$ 0)	Polished	41.3
		$\bar{x} = 59.3$
		$s = 22.8$
(0001)	Polished	22.1
(0001)	Polished	56.5
(0001)	Polished	83.9
(0001)	Polished	17.7
(0001)	Polished	47.9
(0001)	Polished	11.0
		$\bar{x} = 39.9$
		$s = 28.0$

Table VII. Effect of Surface Finish and Crystal Faces Bonded on the Average Tensile Strength of Bicrystals Bonded with Sodium Dihydrogen Phosphate (20% P_2O_5).

Surface Finish	Average Tensile Strength (kgf)	
	Crystal Faces Bonded (11 $\bar{2}$ 0)	(0001)
Diamond Sawed	46.2	18.8
Polished	59.3	39.3
As-Received	130.8	43.6

Table VIII. Effect of Rotational Mismatch on the Tensile Strength of (11 $\bar{2}$ 0) Alumina Bicrystals Bonded with Sodium Dihydrogen Phosphate (20% P₂O₅).

Rotational Mismatch	Tensile Strength (kgf)			
	New Crystals		Used-Polished Crystals	
0	51.0	164.7	164.4	117.3
10				50.7
15	35.5	63.1		67.8
20				75.7
25				60.1
30	7.7	16.6		47.5
35				3.6
45	2.2	1.8		0*
60	1.8	0*		
75	0*	0*		
90	0*	0*		
105	0*			
120	0*			
135	0*			
150	1.8			
165	36.9			
180	113.9	84.1	96.7	

*Too weak to be tested.

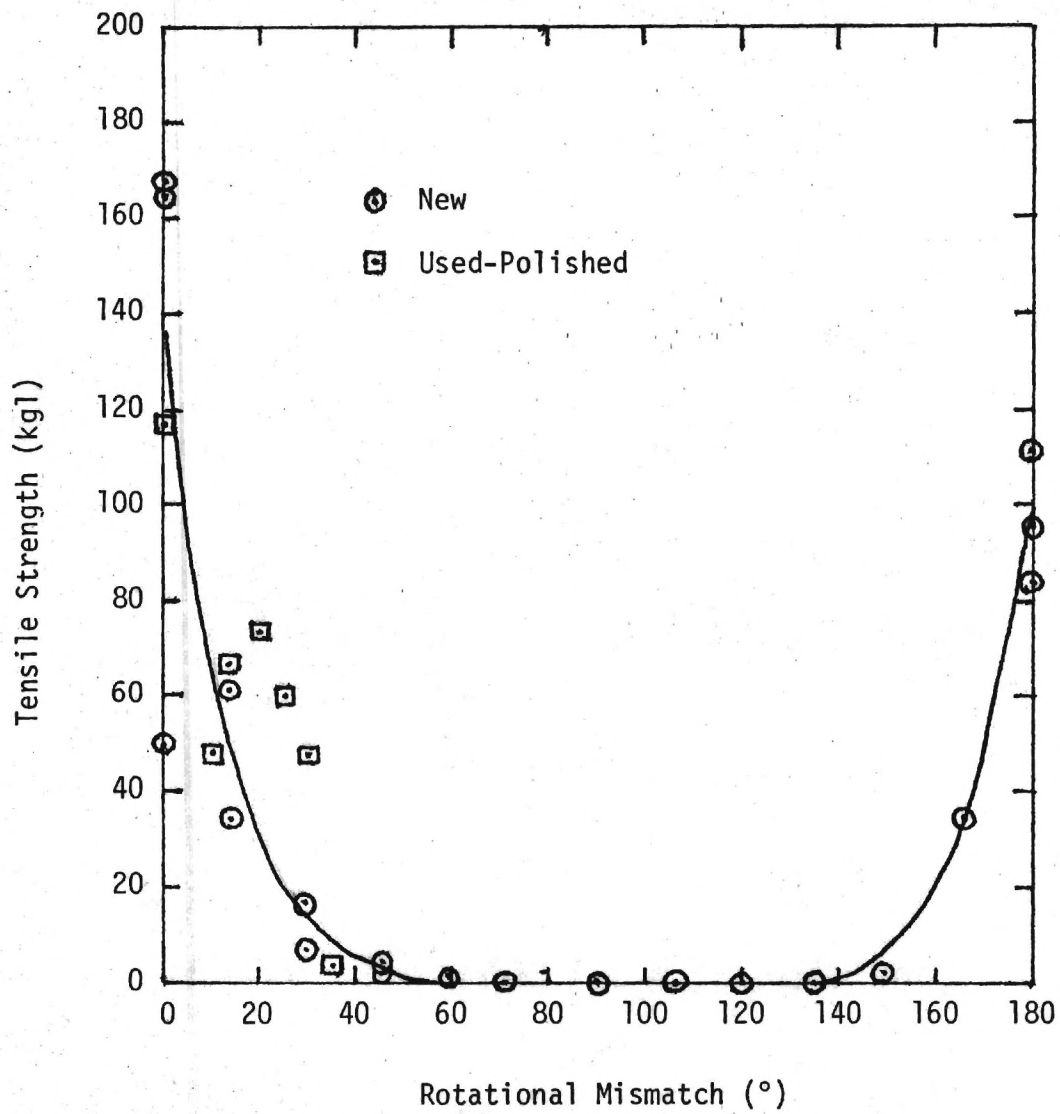


Figure 25. Effect of Rotational Mismatch on the Tensile Strength of (11 $\bar{2}$ 0) Alumina Bicrystals.

(45°- 135°) was related to the load during curing. Three 90° samples were prepared as before with loads of 100, 64, 50 grams, respectively. None of these bicrystals were strong enough to be tested.

Thus, it appears that the strength pattern observed in Figure 25 is the result of the two-fold symmetry of the $(11\bar{2}0)$ face. At this time, it is not clear whether the difference in thermal expansion with direction or bond misalignment is the cause of tensile strength minimum observed for the 90° rotational mismatch bicrystals.

The effect of a combination of both rotational and tilt mismatch was investigated by bonding the $(11\bar{2}0)$ and (0001) faces of alumina crystals together with sodium dihydrogen phosphate (20% P_2O_5) to form a bicrystal. Standard $(11\bar{2}0)$ and (0001) bicrystals were also prepared for comparison purposes. The crystals utilized for this experiment were used crystals that were repolished as described above. Each bicrystal was cured under a 100 gram load for 24 hours and then fired at 1500°F for 4 hours. The tensile strengths of these bicrystals are listed in Table IX.

The relatively high strengths of the $(11\bar{2}0)$ and (0001) bicrystals suggests that the crystals used for this experiment had a good surface finish. The combination of rotational and tilt mismatch in the $(11\bar{2}0)$ (0001) bicrystals reduced their strength to almost zero. Again, it is not known whether this decrease in strength was caused by differences in thermal expansion with direction or variations in ion density (bond misalignment).

Table IX. Effect of Rotational and Tilt Mismatch on the Tensile Strength of Alumina Bicrystals Bonded with Sodium Dihydrogen Phosphate (20% P_2O_5).

Faces Bonded	Tensile Strength (kgf/cm ²)
(11 $\bar{2}$ 0)(11 $\bar{2}$ 0)	60.5
(11 $\bar{2}$ 0)(11 $\bar{2}$ 0)	41.5
(11 $\bar{2}$ 0)(11 $\bar{2}$ 0)	145.3
(11 $\bar{2}$ 0)(11 $\bar{2}$ 0)	65.6
(11 $\bar{2}$ 0)(11 $\bar{2}$ 0)	101.7
(11 $\bar{2}$ 0)(11 $\bar{2}$ 0)	152.1
(11 $\bar{2}$ 0)(11 $\bar{2}$ 0)	172.5
(11 $\bar{2}$ 0)(11 $\bar{2}$ 0)	101.7
	$\bar{x} = 105.1$
	$s = 47.8$
(0001)(0001)	108.2
(0001)(0001)	57.4
(0001)(0001)	104.9
(0001)(0001)	113.0
(0001)(0001)	67.6
(0001)(0001)	71.7
	$\bar{x} = 87.1$
	$s = 24.2$
(11 $\bar{2}$ 0)(0001)	0*
(11 $\bar{2}$ 0)(0001)	0*
(11 $\bar{2}$ 0)(0001)	0*
(11 $\bar{2}$ 0)(0001)	21.1
(11 $\bar{2}$ 0)(0001)	0*
(11 $\bar{2}$ 0)(0001)	0*
(11 $\bar{2}$ 0)(0001)	3.2
(11 $\bar{2}$ 0)(0001)	3.0
(11 $\bar{2}$ 0)(0001)	0*
(11 $\bar{2}$ 0)(0001)	0*
	$\bar{x} = 2.7$
	$s = 6.6$

SECTION IV

Summary

When phosphoric acid is reacted with the faces of alumina single crystals (room temperature curing followed by firing at 1500°F), it appears that star-shaped dendritic crystals of $\text{Al}(\text{PO}_4)_3$ and AlPO_4 are only formed on the surface of low index relatively dense packed faces such as (0001), (1 $\bar{1}$ 00) and (11 $\bar{2}$ 0). It also appears that the whitish dendritic stars (AlPO_4) occur most frequently on the (0001) faces. This may be due to the fact that the (0001) face has a higher aluminum ion packing factor than the (1 $\bar{1}$ 00) and (11 $\bar{2}$ 0) faces. The crystals formed on the surfaces of alumina single crystal faces that did not correspond to a low index plane or on fine grained polycrystalline alumina cutting tools tended to be roughly equiaxed.

When phosphoric acid was reacted with the (0001) face of quartz at 1500°F, the reaction products appeared to be plate-like crystals. However, the reaction products formed when phosphoric acid was reacted with fused silica under the same conditions had an amorphous looking spherical morphology. The surface of the fused silica samples appeared to have been attached more severely than either the quartz or alumina samples.

These results tend to indicate that the morphology of the reaction products produced when a drop of phosphoric acid is reacted with the surface of an oxide sample are controlled by whether the sample is amorphous or crystalline. If the sample is a single crystal, the reaction product morphology appears to be related to the atomic density of the face with

which the phosphoric acid is reacted. Fine grained polycrystalline samples and single crystal faces that are not low index planes tend to produce similar reaction product morphologies.

The strength of $(11\bar{2}0)$ alumina bicrystals bonded with sodium dihydrogen phosphate (20% P_2O_5) increased when the room temperature curing time was increased from 3 to 24 hours. On the other hand, it appears the longer curing time may cause the strength of (0001) alumina bicrystals to decrease. This suggests that it takes longer for the aluminum required to form the bond to go into solution from the $(11\bar{2}0)$ faces than it does from the (0001) faces. There is also evidence that the bonding phase present in the (0001) bicrystals may change from $Al(PO_4)_3$ to $AlPO_4$ as the curing time is increased.

The tensile strength of $(11\bar{2}0)$ and (0001) alumina bicrystals bonded with $NaH_2PO_4 \cdot H_2O$ (20% P_2O_5) increased as the surface finish of the single crystal faces was improved. The tensile strength of $(11\bar{2}0)$ alumina bicrystals bonded with sodium dihydrogen phosphate or Glass H are greater than for (0001) bicrystals produced under the same conditions from crystals with equivalent surface finishes.

When the degree of rotational mismatch of $(11\bar{2}0)$ alumina bicrystals bonded with $NaH_2PO_4 \cdot H_2O$ (20% P_2O_5) was varied from 0 to 180° , the tensile strength decreased as the angle was increased from 0 to 90° and then increased back to approximately its original level when the angle was increased from 90 to 180° . It appears that this strength pattern is the result of the two fold symmetry of the $(11\bar{2}0)$ faces. At this time, it is not clear whether the difference in thermal expansion with direction or bond misalignment is the cause of these tensile strength variations.

A combination of both rotational and tilt mismatch was achieved by bonding $(11\bar{2}0)$ and (0001) alumina crystal faces together with sodium dihydrogen phosphate (20% P_2O_5). The combination of rotational and tilt mismatch in the $(11\bar{2}0)(0001)$ bicrystals reduced their tensile strength to almost zero. Again, it is not known whether this decrease in strength was caused by differences in thermal expansion with direction or variations in ion density (bond misalignment).

The production of strong phosphate bonded bicrystals requires a good surface finish on the crystal faces being bonded. The load applied during room temperature curing must also be evenly distributed over the bond area so the bond thickness will be uniform. In addition, it appears that in order to obtain maximum strengths it is necessary to minimize both rotational and tilt misalignment.

SECTION V

References

1. W. D. Kingery, "Fundamental Study of Phosphate Bonding in Refractories: I. Literature Review," J. Am. Ceram. Soc., (33) 239-41 (1950).
2. W. D. Kingery, "Fundamental Study of Phosphate Bonding in Refractories: II. Cold Setting Properties," J. Am. Ceram. Soc., (33) 242-47 (1950).
3. W. Souder and G. C. Paffenbarger, "Physical Properties of Dental Materials," Natl. Bur. Standards Circ., No. C433 (1942).
4. W. S. Crowell, "Physical Chemistry of Dental Cements," J. Am. Dental Assoc., (14) 1030-48 (1927).
5. W. Souder and I. G. Schoonover, "Probable Chemical Reactions in Silicate Cements," J. Dental Research, (18) 250 (1939).
6. W. D. Kingery, "Fundamental Study of Phosphate Bonding in Refractories: IV. Mortars Bonded with Monoaluminum and Monomagnesium Phosphate," J. Am. Ceram. Soc., (35) 61-63 (1952).
7. W. H. Gitzen, L. D. Hart, and G. MacZura, "Phosphate-Bonded Alumina Castables: Some Properties and Applications," Bull. Am. Ceram. Soc., (35) 217-23 (1956).
8. H. D. Sheets, J. V. Bulloff, and W. H. Duckworth, "Phosphate Bonding of Refractory Compositions," Brick and Clay Record, 55-57 (July 1958).
9. R. N. Rickles, "The Development of Castable Phosphate Cements, Their Chemistry, Properties, and Applications," Ph.D. Dissertation, Polytechnic Institute of Brooklyn, (June 1962).
10. J. W. Lyons, G. J. McEvan, and C. D. Siebenthal, Highway Research Bulletin Board No. 318, Highway Research Board, National Academy of Sciences - Nation Research Council, Washington, D.C., p. 318 (1957).
11. J. E. Lyon, T. U. Fox, and J. W. Lyons, "An Inhibited Phosphoric Acid for Use in High-Alumina Refractories," Bull. Am. Ceram. Soc., (45) 661-65 (1966).
12. J. E. Lyon, T. U. Fox, and J. W. Lyons, "Phosphate Bonding of Magnesia Refractories," *ibid*, 1078-81.
13. A. H. Bremser and J. A. Nelson, "Phosphate Bonding of Zirconia," *ibid*, (46) 280-82 (1967).

14. A. H. Foessel and W. S. Treffner, "Improved Phosphate-Bonded Basic Refractories," *ibid.*, (49) 652-57 (1970).
15. C. L. Venable and W. S. Treffner, "X-ray Study on Phosphate Bonding in Refractories," *ibid.*, 660-63.
16. M. J. O'Hara, J. J. Duga, and H. D. Sheets, Jr., "Studies in Phosphate Bonding," *ibid.*, (51) 590-95 (1972).
17. A. A. Chistyakova, V. A. Sivkina, V. I. Sadkov, A. P. Khashkovskaya, and L. G. Povyshiva, "Aluminophosphate Binder," *Izv. Akad. Nauk. SSSR, Neorg. Mater.*, (5) 1333-38 (1969) (English Transl.).
18. "Some Aluminum Orthophosphates," *ibid.*, 449-55.
19. I. L. Rashkovan, L. N. Kuz'minskaya and V. A. Kopeikin, "Thermal Transformations in the Aluminum Phosphate Binding Agent," *ibid.*, (2) 464-72 (1966).
20. V. M. Medvedeva, A. A. Medvedev, and I. V. Tananaw, "Thermal Transformations in an Alumino-Phosphate Binder by the Methods of Infrared Spectroscopy and X-ray Diffraction Study," *ibid.*, (1) 193-99 (1965).
21. V. A. Kopeikin, A. I. Kudryashova, L. N. Kuz'minskaya, I. L. Rashkovan and I. V. Tananaev, "Formation of an Amorphous Phase in the Cementation of Materials Based on an Aluminophosphate Binder," *ibid.*, (3) 657-69 (1967).
22. Y. V. Klyucharev and L. I. Skoblo, "Compositions of the Products Formed by Hardening of the Aluminum Phosphate Binder in Refractory Corundum Compositions," *Zh. Prikl. Khim.*, (38) 530-35 (1965) (English Translation).
23. A. V. Bromberg, A. G. Kasatkina, V. A. Kopeikin, A. I. Kuz'minskaya, I. L. Rashkovan, and I. V. Tananaev, "Aluminum-Chromium Phosphate Binders," *Izv. Akad. Nauk SSSR, Neorg. Mater.*, (5) 805-807 (1969) (English Translation).
24. A. V. Lovrov, A. A. Medvedev, N. N. Chudinova, and I. V. Tananaev, "Investigation of the Dehydration Products of Chromium Phosphate Hexahydrate," *ibid.*, (6) 503-10 (1970).
25. K. Fisher, "Chemical Bonds for Refractory Materials," *Proc. Brit. Ceram. Soc.*, 51-64 (Dec. 1969).
26. J. E. Cassidy, "Phosphate Bonding Then and Now," *Bull. Am. Ceram. Soc.*, (56) 640-43 (1977).
27. J. D. Birchall and J. E. Cassidy, "Refractory Compositions," *Brit. Pat.* 1,357,541 (19 April 1971).

28. K. Diel, "Solid Binder for Fire Proof Substances," W. German Pat. 2,412,474 (15 March 1974).
29. R. E. Fisher, "Hot Strength of Phosphate-Bonded Refractory Plastics," Bull. Am. Ceram. Soc., (56) 637-43 (1977).
30. F. J. Gonzalez and J. W. Halloran, "Reaction of Orthophosphoric Acid with Several Forms of Aluminum Oxide," *ibid.*, (59) 727-38 (1980).
31. T. Chvatal, "The Position of Refractory Phosphate Bonding Today," Sprechsaal Keram. Glas. Baustoffe, (108) 576, 78, 80, 82-89 (1975).
32. E. Preuss, B. Krahe-Urban and R. Butz, Laue Atlas, John Wiley and Sons, London, pp. 60-67 (1974).
33. B. D. Cullity, Elements of X-ray Diffraction, Addison-Wesley Publishing Co., London, pp. 239-59 (1978).
34. E. Preuss, "Plot Program for Laue Patterns and Stereographic Projections," Computer Physics Comm., (18) 261-275 (1979).
35. E. Preuss, "Calculation of Crystal Orientation Using Laue Patterns," *ibid.*, 277-80.
36. E. Preuss, "A Simplified Procedure for Orientation of Single Crystals of Any Structure," Acta Cryst., (A29) 86-90 (1978).
37. Saphikon Division of Tyco Laboratories, Inc., 51 Powers Street, Milford, NH 03055.

**A minerals and materials research contract report
NOVEMBER 1983**

FUNDAMENTAL INVESTIGATION OF PHOSPHATE BONDING

**Contract J0123041
GEORGIA INSTITUTE OF TECHNOLOGY
SCHOOL OF CERAMIC ENGINEERING**

**BUREAU OF MINES
UNITED STATES DEPARTMENT OF THE INTERIOR**



REPORT DOCUMENTATION PAGE	1. REPORT NO.	2.	3. Recipient's Accession No.
4. Title and Subtitle Fundamental Investigation of Phosphate Bonding			5. Report Date November 1983
7. Author(s) James F. Benzel			8. Performing Organization Rep. No.
9. Performing Organization Name and Address Georgia Institute of Technology School of Ceramic Engineering Atlanta, GA 30332			10. Project/Task/Work Unit No.
			11. Contract(C) or Grant(G) No. (C) (G)
12. Sponsoring Organization Name and Address United States Department of the Interior Bureau of Mines 2401 E Street, N.W. Washington, D.C. 20241			13. Type of Report & Period Covered Final Aug 82-Nov 83
15. Supplementary Notes			14.
16. Abstract (Limit 200 words) This investigation primarily utilized single crystals to study phosphate bonding. This eliminated surface area and particle shape as variables and allowed the effect of crystallographic orientation to be evaluated. The morphology of the reaction products produced when H_3PO_4 was reacted with alumina single crystals was related to the crystal face index. Star-shaped dendrites formed on low index faces and equiaxed crystals formed on faces that did not correspond to low index planes and polycrystalline samples. The tensile strength of (1120) and (0001) alumina bicrystals increased as their surface finish was improved. The tensile strength of (1120) alumina bicrystals bonded with $NaH_2PO_4 \cdot H_2O$ or Glass H are greater than (0001) bicrystals produced under the same conditions. The tensile strength of (1120) alumina bicrystals bonded with $NaH_2PO_4 \cdot H_2O$ varies with the amount of rotational mismatch between the crystals. Strength maximums occurred at 0 and 180° and a minimum at 90°. It appears this strength pattern is related to the two fold symmetry of this plane. Combination of both rotational and tilt mismatch reduced the strength of (1120)(0001) bicrystals to almost zero. The strength decreases associated with these types of bicrystal mismatches could be related to differences in thermal expansion with direction or bond misalignment.			
17. Document Analysis a. Descriptors			
b. Identifiers/Open-Ended Terms Refractory Chemical Bond Phosphate Bond Bonding Mechanism			
c. COSATI Field/Group			
18. Availability Statement Unlimited release by NTIS	19. Security Class (This Report)	21. No. of Pages 72	
	20. Security Class (This Page)	22. Price	

FOREWARD

This report was prepared by the School of Ceramic Engineering, Georgia Institute of Technology, Atlanta, Georgia 30332 under USBM Contract J0123041. The contract was initiated under the Bureau of Mines Metallurgy Program. It was administered under the technical direction of Metallurgy with Dr. Martin H. Stanczyk, acting as the Technical Project Officer. Mr. Oliver H. Snyder III was the Contract Administrator for the Bureau of Mines. This report is a summary of the work recently completed on this contract during the period 20 August 1982 to 20 October 1983. This report was submitted by the authors on 20 November 1983.

Portions of this report will be used as part of a Ph.D. dissertation to be submitted during 1984. Note that in our opinion, no patentable features of phosphate bonding are disclosed herein. Reference to specific brands, equipment or trade names in this report is made to facilitate understanding and does not imply endorsement by the Bureau of Mines or the authors.

CONTENTS

	<u>Page</u>
Foreward	4
Illustrations	6
Tables	8
Unit of measure abbreviations	9
Abstract	10
Introduction	11
Background	13
Experimental program	28
Single crystal orientation	28
Reaction of phosphate bonding agent with different crystallographic faces of single crystals and fused bicrystals and tensile testing procesures	29
Development of Methods to Form Phosphate Bonded Bicrystals and Tensile Testing Procedures	45
Conclusions	67
References	70

ILLUSTRATIONS

	<u>Page</u>
1. Dendrite Crystals on Surface of Alumina Crystal Reacted with H_3PO_4 at 1500°F	31
2. Reaction Product Layer Below Dendrites	31
3. Reaction Product Layer Formed on Surface of Alumina Crystal Reacted with Chromic Phosphoric Acid Mixture at 1500°F	32
4. Top Surface of Reaction Products on (0001) Face of Quartz Crystal Reacted with Phosphoric Acid at 1500°F	32
5. Reaction Product Layer Formed on Surface of a Fused Silica Rod Reacted with Phosphoric Acid at 1500°F	34
6. Plate-Like Crystals Growing Out of Spheres Shown in Figure 5	34
7. Whitish Star-Shaped Dendritic Crystals on Surface of Reaction Products Produced by Reacting H_3PO_4 with (0001) Face of Alumina at 1500°F	35
8. Whitish and Grayish-Shaped Dendritic Crystals Produced by Reacting H_3PO_4 with (0001) Face of Alumina Crystal at 1500°F	35
9. Structure of Aluminum Meta Phosphate $[Al(PO_4)_3]$ Dendrites	37
10. Porous Morphology of Monoaluminum Phosphate ($AlPO_4$) Dendritic Structure	37
11. Nearly Equiaxed Crystals Covering ($\bar{1}\bar{1}00$) Face of Alumina Crystal Reacted with H_3PO_4	39
12. Fractured Alumina Crystal with Equiaxed Crystals on ($\bar{1}\bar{1}00$) Face	39
13. Dendritic Structure on Face of ($\bar{1}\bar{1}02$) Alumina Crystal Reacted with H_3PO_4 at 1500°F	40
14. Aluminum Phosphate Reaction Products on Surface of ($\bar{1}\bar{1}\bar{2}2$) Face of Alumina Crystal Reacted with H_3PO_4 at 1500°F	40

ILLUSTRATIONS (Continued)

	<u>Page</u>
15. Higher Magnification of Surface Shown in Figure 14 . . .	41
16. Surface of Reaction Products on a Random Plane of an Alumina Crystal Reacted with H_3PO_4 at 1500°F	41
17. Same as Figure 16 Except Random Plane was Different	42
18. Plate-Like Structure Covering Surface of Grains Shown in Figure 17	42
19. Surface of Reaction Product Layer Formed on the Surface of an Alumina Cutting Tool Reacted with H_3PO_4 at 1500°F	44
20. Plate-Like Grains on Different Area of Alumina Cutting Tool Shown in Figure 19	44
21. Fracture Morphology of $NaH_2PO_4 \cdot H_2O$ Bond Between (0001) Faces of Alumina Crystals Fired at 1500°F	48
22. Fracture Morphology of Glass H Bond Between (0001) Faces of Alumina Single Crystals Fired at 1500°F	48
23. Average Tensile Strength Factorial Design (2 x 2) Showing Effect of Crystal Condition and Bicrystal Faces Bonded with Sodium Dihydrogen Phosphate (30% P_2O_5) and Cured Under a Load of 100 Grams	56
24. Average Tensile Strength Factorial Design (2 x 2 x 2) Showing the Effect of Bonding Agent, Curing Load and Bicrystal Faces Bonded.	57
25. Effect of Rotational Mismatch on the Tensile Strength of (1120) Alumina Bicrystals	64

TABLES

	<u>Page</u>
1. Tensile Strength of Phosphate Bonded Alumina Bicrystals . . .	47
2. Tensile Strength of Alumina Bicrystals Bonded with NaH_2PO_4 and Fired at 1500°F for Four Hours	50
3. Tensile Strength of Alumina Bicrystals Bonded with Glass H and Fired at 1500°F for Four Hours	52
4. Tensile Strength of Phosphate Bonded Alumina Bicrystals Cured Under a Distributed Load	54
5. Effect of Curing Time on the Tensile Strength of Sodium Dihydrogen Phosphate Bonded Alumina Bicrystals	55
6. Effect of Surface Finish on the Tensile Strength of Alumina Bicrystals Bonded with Sodium Dihydrogen Phosphate	59
7. Effect of Surface Finish and Crystal Faces Bonded on the Average Tensile Strength of Bicrystals Bonded with Sodium Dihydrogen Phosphate (20% P_2O_5)	61
8. Effect of Rotational Mismatch on the Tensile Strength of (1120) Alumina Bicrystals with Sodium Dihydrogen Phosphate (20% P_2O_5)	62
9. Effect of Rotational and Tilt Mismatch on the Tensile Strength of Alumina Bicrystals Bonded with Sodium Phosphate (20% P_2O_5)	63

UNIT OF MEASURE ABBREVIATIONS USED IN THIS REPORT

°	angular degree
'	angular minute
gm	gram
hr	hour
"	inch
kgf/cm ²	kilogram of force per centimeter square
kV	kilovolt
μm	micrometer
mA	milliampere
w/o	weight percent

FUNDAMENTAL INVESTIGATION OF PHOSPHATE BONDING

By Morteza Soltani¹ and James F. Benzel²

ABSTRACT

This investigation primarily utilized single crystals to study phosphate bonding. This eliminated surface area and particle shape as variables and allowed the effect of crystallographic orientation to be evaluated. The morphology of the reaction products produced when H_3PO_4 was reacted with alumina single crystals was related to the crystal face index. Star-shaped dendrites formed on low index faces and equiaxed crystals formed on faces that did not correspond to low index planes and polycrystalline samples. The tensile strength of $(11\bar{2}0)$ and (0001) alumina bicrystals increased as their surface finish was improved. The tensile strength of $(11\bar{2}0)$ alumina bicrystals bonded with $NaH_2PO_4 \cdot H_2O$ or Glass H are greater than (0001) bicrystals produced under the same conditions. The tensile strength of $(11\bar{2}0)$ alumina bicrystals bonded with $NaH_2PO_4 \cdot H_2O$ varies with the amount of rotational mismatch between the crystals. Strength maximums occurred at 0 and 180° and a minimum at 90°. It appears this strength pattern is related to the two fold symmetry of this plane. Combination of both rotational and tilt mismatch reduced the strength of $(11\bar{2}0)(0001)$ bicrystals to almost zero. The strength decreases associated with these types of bicrystal mismatches could be related to differences in thermal expansion with direction or bond misalignment.

¹Graduate Research Assistant

²Professor of Ceramic Engineering

School of Ceramic Engineering, Georgia Institute of Technology,
Atlanta, Georgia

INTRODUCTION

Phosphoric acid and acid phosphate compounds were first used as binders for dental materials and refractories shortly after the turn of the century. In addition to a wide variety of oxides and silicates, a number of other materials such as glasses, metal halides, metal hydrates and metals have been formed into shapes using phosphate binders.

Almost all of the phosphate bonding investigations reported to date utilized finely powdered materials or mixtures of fine grained materials and polycrystalline aggregates. The only known exception has been the use of a phosphate binder system to join moderately large mica single crystals to produce larger and thicker mica sheets for electronic applications.

The objective of this investigation was to achieve a better understanding of the mechanisms of phosphate bonding. The uniqueness of the experiments is that they were based on studying the joining together of two single crystals by phosphate bonding rather than studying the properties of polycrystalline masses held together by phosphate bonds. The use of single crystals in these experiments allowed the elimination of variables such as surface area and particle shape and also permitted the investigation of the effect crystallographic orientation plays in phosphate bonding.

The availability of this type of fundamental information could lead to the production of better and longer-lasting refractories. Since many of the currently used phosphate bonded refractories contain alumina, chrome oxide and zirconia, improving their service life would reduce the necessity for importation of bauxite, chrome ore and zirconia-bearing minerals.

BACKGROUND

In 1950, Kingery published a comprehensive literature review (1) and a fundamental study (2) on the phosphate bonding of refractories. The purpose of this section is to summarize the fundamental information cited or reported in these two papers and to outline subsequent progress that has been made toward understanding phosphate bonding.

Kingery's literature search (1) indicated that three major methods of forming phosphate bonds had been identified. They were: (1) reaction of phosphoric acid with siliceous materials, (2) reaction of phosphoric acid with oxides, and (3) the direct addition or formation in situ of acid phosphates. Cold setting (room temperature) as well as heat setting refractory bonds were described but very little fundamental information about these materials was found in the pre-1950 patent or general literature.

Dental literature indicated that zinc oxide based cements were crystalline (3 - 4) and that the bond was primarily dibasic zinc phosphate ($\text{ZnHPO}_4 \cdot 3\text{H}_2\text{O}$). A hard white dental cement formed from powdered alumina-lime-silica glass and phosphoric acid (3 - 5) was reported to be bonded by an amorphous silica gel formed by a solution of about 30% of the glass.

Kingery's systematic study (2) of a large number of metal oxide-phosphoric acid reactions at room temperature indicated three distinct classes of reactions: (1) acidic and chemically inert oxides do not react,

(2) strongly basic oxides react violently to form porous friable structures, and (3) weakly basic and amphoteric oxides react but not all of them form bonded structures.

All of the reactions in the third classification which produced cement-like materials contained mono- and di-basic phosphates [$M_x(H_2PO_4)_y$ and $M_x(HPO_4)_y$], whereas no acid phosphates were detected in the similar non-cohesive mixtures. This led Kingery to conclude that acid phosphates act as the bonding media in cold-setting phosphate cements. He also concluded, because of the number of different oxides involved, that this was a general property of hydrogen phosphates rather than one particular chemical compound.

Comparison of bars (90 w/o fused Al_2O_3 and 10 w/o kaolin) bonded with phosphoric acid or phosphoric acid containing one of a number of cation additions (3) indicated that small weakly basic or amphoteric ions such as Al^{+++} , Be^{++} , Fe^{+++} and Mg^{++} increased the bonding power of phosphoric acid and that large or strongly basic ions such as Ba^{++} , Ca^{++} and Th^{+++} decrease its effectiveness. Based on these results, Kingery concluded that weakly basic cations having a moderately small ionic radii were necessary to optimize the bond strength by allowing the formation of a somewhat variable and flexible partially non-ordered or glassy structure. The larger more basic cations tend to have higher coordination numbers which prevent the formation of flexible connected polyhedra structures, resulting in more ordered structures which results in lower bond strengths.

Heat treatment of bars (92.85 w/o fused Al_2O_3 and 7.15 w/o ball clay) bonded with 7.15 w/o mono-aluminum phosphate (2) to various temperatures

produced the unusual result that all of their room temperature MOR's were greater than their dried strength. This lack of a temperature zone of weakness was attributed to the gradual loss of combined water and the gradual crystallization of the hydration products over a wide temperature range with no sharp rupturing effects.

The first step in this process is the loss of combined water, which leads to the formation of an amorphous phase containing three moles of water ($\text{Al}_2\text{O}_3 \cdot \text{P}_2\text{O}_5 \cdot 3\text{H}_2\text{O}$). This material crystallizes over a fairly wide temperature range (260-500°C) as additional water is lost. The resulting compound [aluminum metaphosphate, $\text{Al}(\text{PO}_3)_3$] also forms a bond with the aggregate.

When Kingery (2) reacted aluminum hydrate ($\text{Al}_2\text{O}_3 \cdot x\text{H}_2\text{O}$) with phosphoric acid no crystalline reaction products were detected. Thus, at room temperature, the bonding phase must have been amorphous. However, continuous rate of weight loss measurements on heating clearly showed the characteristic peaks for mono-aluminum phosphate. This suggests that the amorphous bonding phase may contain more water of hydration than mono-aluminum phosphate and that it crystallizes below 200°C as the result of a gradual dehydration process which results in the formation of mono-aluminum phosphate.

In 1952, Kingery (6) demonstrated that mortars formed from fire clay grog, kaolin, and either mono-aluminum or mono-magnesium phosphate bonds produced excellent joints between half fire bricks fired at temperatures between 105°C and 1500°C for five hours. The transverse strength of neat mortar bars bonded with mono-aluminum phosphate and cured at 105°C increased almost linearly as the percent phosphate bond was increased from 2 to 12 w/o.

Gitzen et al. (7) in studying the phosphate bonding of sintered alumina grog found that higher bond strength was obtained with phosphoric acid than with the various forms of aluminum phosphate. Forming the acid in place by adding water to dry mixes containing phosphorous pentoxide (P_2O_5) also produced excellent bonding. The use of dry diammonium phosphate $(HN_4)_2HPO_4$ to produce phosphoric acid *in situ* resulted in weaker bond strength and production of ammonia during the casting operation.

When castables were prepared using tabular alumina and phosphoric acid, it was necessary to heat-set them by heating at 600 to 800°F. These authors (7) thought the bonding process consisted of dehydration of orthophosphoric acid (H_3PO_4) at 416°F to form pyrophosphoric acid ($H_4P_2O_7$) which on continued heating at 600 to 800°F reacts with the alumina to form aluminum phosphate ($AlPO_4$). They attributed the loss of strength observed between 2000 and 2800°F to decomposition of aluminum phosphate to alumina and P_2O_5 . By substituting Bayer alumina for some of the tabular alumina, they produced castables which developed an initial cold-set at room temperature.

To investigate the effect of the inversion of the α - β cristobalite form of aluminum phosphate, test bars of an alumina ramming mix bonded with phosphoric acid were heat treated 20 hours at 2400°F (7). No decrease in strength occurred even after the bars were cycled through the inversion temperature 300 times.

Sheets et al. (8) suggested the following scenario for the phosphate bonding of alumina:

"Initially, a trivalent phosphate anion is present. As the acid reacts with the alumina, covalent polymerization occurs.

This results in bivalent PO_4 units which will become 'ends' in chain polymerizations. Two of these can fuse to form a tetravalent pyrophosphate.

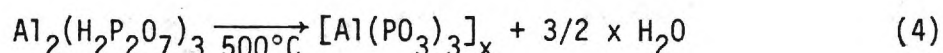
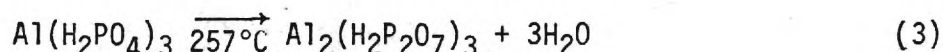
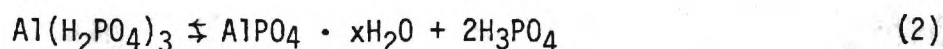
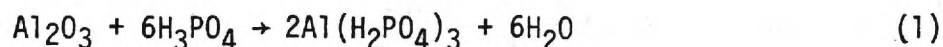
As the reaction proceeds, PO_4 units form with only one formal charge remaining. These units may be called 'middles.' One unit, terminated by two of the previously formed 'ends' gives a family of linear polyphosphates.

The next step in the development of the bond comes from PO_4 groups having no formal charge but capable of forming 'branches.' Branching, such as is proposed here, could give rise to a sheet structure.

The foregoing, 'ends,' 'middles,' and 'branches' involve only the phosphorous and oxygen atoms. To explain the unusual properties of phosphated-bonded alumina, one would expect the Al atom to become involved in these reactions. Structural chemists believe in the formation of 'super branches' which are capable of 3 dimensional growth. Thus, phosphate bonding can be viewed as a heteropolyanionization process leading to the formation of a strong oxygen polyhedral structure."

Rickles' (9) investigation of the reaction between aluminum hydroxide and phosphoric acid (25-90°C) determined that the reaction products of this system were a mixture of amorphous mono-aluminum phosphate and a crystalline solid having the chemical composition $3\text{Al}_2\text{O}_3 \cdot 2\text{P}_2\text{O}_5 \cdot 8\text{H}_2\text{O}$. A direct correlation between the amount of amorphous mono-aluminum phosphate and bond strength was found. This was attributed to its non-uniform structure and bonding. When the molar ratio of $\text{Al}(\text{OH})_3$ to H_3PO_4 was 1:3 only amorphous mono-aluminum phosphate was formed. The addition of alumina to the reaction mixture in the ratio of 3:7 with respect to aluminum hydroxide [$\text{Al}_2\text{O}_3:\text{Al}(\text{OH})_3$] produced the highest tensile strength and decreased porosity. He also determined that the reaction between zirconium oxide and phosphoric acid produced zirconium pyrophosphate which maintained high strength at 1300°C.

Lyons et al. (10) suggested the following reaction sequence for phosphoric acid with high-alumina refractory mixes:



The $\text{Al}(\text{H}_2\text{PO}_4)_3$ is water soluble and is the bonding phase (11) in two senses: (1) its sticky, viscous nature at room temperature, and (2) as a precursor to $\text{Al}_2(\text{H}_2\text{P}_2\text{O}_7)_3$ and $[\text{Al}(\text{PO}_3)_3]_x$ in the cured refractory.

If the reaction can be slowed or stopped after the first reaction the refractory mixes would remain workable over a long period of time and would provide a large amount of $\text{Al}(\text{H}_2\text{PO}_4)_3$ that is the precursor to the binding material $[\text{Al}(\text{PO}_3)_3]_x$. Addition of oxalic acid to act as a sequestering agent to hold aluminum in a soluble form extended the storage life of ramming and plastic mixes to six months and longer (11). These experiments confirmed the theory that the setting of phosphate-bonded alumina refractories is caused by the precipitation of insoluble aluminum phosphates.

Lyon et al. (12) investigated the bonding of magnesia refractories with sodium phosphate glasses cured at 250°F. They found that as the average chain length (6-50) of the glass and the amount of bond added

were increased, room temperature MOR's increased and hot MOR's decreased. The shorter chain length (1-3) crystalline sodium phosphates gave poorer cold and hot MOR's than the glassy phosphates.

It was believed (12) that glassy phosphate bonding was the result of degrading these materials to orthophosphoric acid or to ortho-salts during the curing cycle. The acid component then reacts with the magnesia to form the bond.

Samples of MgO mixed with the phosphate glasses and sufficient water to form a paste were heat treated and x-ray diffraction patterns run. Similar patterns were obtained for samples heat treated at the same temperature irrespective of the glass chain length. The 125°F patterns contained lines for magnesium orthophosphate, which confirmed the degradation of the glasses. The 950°F material was composed mainly of amorphous material and the 2200°F samples showed strong crystalline orthophosphate lines plus a large amount of noncrystalline material. These results suggest that the bonding of MgO between 500 and 2200°F is the result of amorphous phosphate glasses. As 2200-2300°F is reached the glasses begin crystallizing to form $\text{Mg}_3(\text{PO}_4)_2$. Lyon et al. (12) concluded that the loss of strength observed in this temperature range indicated that $\text{Mg}_3(\text{PO}_4)_2$ is not a bonding agent.

Bremser and Nelson (13) used a mixture of ammonium dihydrogen phosphate and monofluorophosphoric acid to produce low temperature bonding (260°C) of stabilized and unstabilized zirconia. The MOR's of the calcia stabilized bars were higher than those of unstabilized bars from room temperature to ~1200°C where a liquid formed in the stabilized bars.

X-ray diffraction indicated that after being heated to 1240°C the unstabilized bars contained only monoclinic zirconia and zirconium pyrophosphate. However, analysis of the stabilized zirconia bars indicated that most of the cubic zirconia had reverted to the monoclinic form and that $\text{CaZr}(\text{PO}_3)_2$ was present in addition to zirconium pyrophosphate.

A sharp decrease in the MOR of the stabilized bars was observed between 200 and 400°C but between 400 and 600°C the strength returned to about its original value (3500 psi). A second decrease in strength occurred between 600 and 900°C; however, the strength again recovered (3000 psi) at 1000°C. Above 1000°C the strength decreased with increasing temperature until liquid formed at about 1200°C. The strength of the unstabilized bars remained fairly constant (1500-1900 psi) from room temperature to 1100°C. Between 1100 and 1240°C there was some decrease in strength; however, the specimens showed brittle fracture. The irregular nature of the MOR - temperature curve for the calcia stabilized zirconia bars was attributed to the formation of one or more intermediate calcium compounds which result in the formation of a double phosphate of calcium and zirconium $[\text{CaZr}(\text{PO}_4)_2]$ at about 1200°C.

Reaction studies (13) showed the following reaction series for unstabilized zirconia reacted with monofluorophosphoric acid alone or in the presence of ammonium dihydrogen phosphate: the acid dissociates releasing fluorine, which leads to the formation of an intermediate zirconium pyrophosphate. Zirconium pyrophosphate (ZrP_2O_7) is stable to 1380°C where it begins to lose P_2O_5 forming zirconyl pyrophosphate $[(\text{ZrO})_2\cdot\text{P}_2\text{O}_7]$, which is stable to 1600°C.

Foessel and Treffner (14) using a glassy sodium polyphosphate

(chain length of 21), a lime-bearing addition as a second binder, and selected magnesite aggregates produced refractories having 2700°F MOR's greater than 2000 psi. By adjusting the $\text{CaO}:(\text{P}_2\text{O}_5 + \text{SiO}_2)$ ratio of a mix composition containing an aggregate which had low strength at 2700°F, they produced brick with hot MOR's above 3500 psi at 2700°F. The optimum $\text{CaO}:(\text{P}_2\text{O}_5 + \text{SiO}_2)$ ratio was around 1:1. Bricks of this type were at least twice as strong as direct bonded magnesite-chrome bricks up to 2850°F.

Similar results were obtained in magnesite-chrome refractories. However, it was found that as the MgO content decreased the optimum $\text{CaO}:(\text{P}_2\text{O}_5 + \text{SiO}_2)$ ratio increased from about 1:1 to about 1.25:1 for 60% MgO class brick. Conventional and high fired phosphate-bonded compositions were also superior to phosphate-free equivalents.

The rather narrow limits of the $\text{CaO}:(\text{P}_2\text{O}_5 + \text{SiO}_2)$ ratio for maximum hot MOR (14) in magnesite refractories suggested that the bond might consist of a single well-defined compound. Venable and Treffner (15) investigated this theory by reacting a glassy long-chain sodium polyphosphate polymer with the various components present in these magnesite refractories. They concluded that sodium dicalcium orthophosphate ($\text{Na}_2\text{O} \cdot 2\text{CaO} \cdot \text{P}_2\text{O}_5$) was the major high temperature bonding complex in these compositions.

Exploratory experiments (15) showed that $\text{Na}_2\text{O} \cdot 2\text{CaO} \cdot \text{P}_2\text{O}_5$ softened to a viscous liquid between 1500 and 1600°C. However, before complete melting occurred sodium was lost and the bond composition shifted toward highly refractory whitlockite ($3\text{CaO} \cdot \text{P}_2\text{O}_5$), melting point 1775°C. The presence of silica results in the formation of calcium silicophosphates

at the expense of the sodium calcium phosphate bonding phase. Therefore, for high hot strengths in unburned magnesite brick the silica content should be kept low and the $\text{CaO}:\text{P}_2\text{O}_5$ should be approximately equal to unity.

O'Hara et al. (16) summarized the phase conversions reported (17 - 22) for an aluminum-phosphate binder with a $\text{P}_2\text{O}_5:\text{Al}_2\text{O}_3$ molar ratio of ≈ 2.3 . It was generally agreed that the major phase in this binder system is $\text{AlH}_3(\text{PO}_4)_2 \cdot 3\text{H}_2\text{O}$, which on heat treatment is converted to the berlinite and cristobalite forms of AlPO_4 and variscite $[\text{Al}(\text{H}_2\text{PO}_4)_3]$. Variscite is a highly hygroscopic phase which becomes amorphous above 570°F . Hydrated aluminum phosphates crystallize from the amorphous phase and gradually dehydrate between 930 and 1470°F to form $\text{Al}(\text{PO}_3)_3$ which in turn forms a metaphosphate glass between 2000 and 2370°F . The glass decomposes above 2370°F to form AlPO_4 with vaporization of P_2O_5 . Aluminum orthophosphate is isostructural with silica and its common polymorphs.

The physiochemical changes produced by heat treatment of chromium phosphates and chromium aluminum phosphate binders indicate that they differ from aluminum phosphate binders by retaining an amorphous phase over a larger temperature range (23 - 24). They also may produce stronger bonds (25).

The diametral tensile strength of alumina specimens bonded with phosphoric acid or a mixture of phosphoric acid and chromic acid (16) were similar and increased with acid content for curing temperatures of 700 and 1500°F . The strength of specimens fired at 2000°F did not vary with acid content but those containing chromium were ≈ 2.5 times stronger.

Chromic acid containing specimens that had been cured at 700°F had lower overall thermal expansion when heated to 1500 or 2000°F than specimens bonded only with phosphoric acid. The isothermal expansion (1500°F for 4 hours) of the chromium containing specimen was also much lower. The sluggish isothermal expansion was attributed to the transformation of the berlinite to the tridymite form of AlPO_4 (1470°F). Cooling curves for specimens not containing chromic acid showed inversions corresponding to the β to α inversions of the tridymite and cristobalite forms of AlPO_4 for specimens heated to 1500 and 2000°F, respectively.

These findings suggest that the reason phosphoric acid bonded alumina specimens fired to 2000°F are weaker than ones bonded with a mixture of chromic and phosphoric acids is that the presence of chromium ions reduce the amount of AlPO_4 formed which prevents the structure from being disrupted when it is cooled through the β to α inversions.

O'Hara and his coworkers (16) investigated the microstructure of these types of bonds by placing a drop of phosphoric acid or a mixture of phosphoric and chromic acid on the polished surface of polycrystalline alumina specimens which were then cured or fired. Sections of these specimens were then examined using a scanning electron microscope.

Their micrographs indicate that the aluminum-phosphate bond material developed at 700°F consisted of three distinct types: (1) a fine particle crystalline material at the bond-substrate interface and at phase boundaries, (2) an intermediate phase of larger particle size, and (3) an outer phase which appeared to be amorphous.

The specimen heated to 2000°F showed only two distinct phases (1) a fine particle crystalline phase at the bond-substrate interface and

(2) an outer layer that appeared to be glassy. There was a large separation between the bond and the substrate. They suggest that the devitrification of the bond near the substrate interface is due to a gradient in the bond composition. The higher alumina content of the bond material near the interface would most likely form AlPO_4 , whereas, bond material farther away from the substrate might form $\text{Al}(\text{PO}_3)_3$.

The specimen produced by heating a mixture of the two acids (1:1 weight ratio of P_2O_5 to CrO_3) on a substrate to 2000°F produced a different reaction product morphology. Only one phase was observed. It consisted of a uniform agglomerate of small, most likely crystalline, particulate material. No attempt was made to identify any of the observed phases.

In a review, Cassidy (26) discussed several of the new phosphate bonds that have been developed. Aluminum chlorophosphate hydrate (27) is a dry powder developed especially for use in castable refractories. It is highly soluble in water and decomposes to form AlPO_4 on heating without formation of any intermediate metaphosphates. The simple thermochemistry of aluminum chlorophosphate hydrate allows it to be used in refractories which are subjected to rapid heating. Mixtures of aluminum phosphate and urea phosphate (28) have been used as a dry bond for heat setting alumina castables.

Fisher (29) found that at temperatures up to 2000°F increasing the level of phosphate binder present in high alumina plastics produced increases in their hot MOR's. At higher test temperatures this trend was still measurable but was much less pronounced. He also determined

that bauxite based phosphate bonded plastics were as strong at 2000°F and stronger at 2500°F than similar tabular alumina plastics.

The type of phosphate binder used did not have a significant effect on the level of hot MOR achieved between 1500 and 2500°F. This was unexpected in view of the different way in which they form the bond during the curing process. The hydrated aluminum phosphate $[\text{AlH}_3(\text{PO}_4)_2 \cdot 3\text{H}_2\text{O}]$ was formed with all three types of binder, but its mode of formation varied. In the phosphoric-acid-bonded plastics, the alumina required to form this compound is supplied by solution of fine grained alumina. In the plastics bonded with stoichiometric aluminum phosphate this compound can be formed directly from the binder so there is essentially no reaction between the binder and the alumina. The acid-rich aluminum phosphate should react mildly with the alumina since it contains the ingredients for both the hydrated aluminum phosphate and free phosphoric acid.

Gonzalez and Halloran (30) determined that the reaction products of orthophosphoric acid and alumina at temperatures up to 500°C consisted of a mixture of aluminum phosphates that vary depending on the type of alumina, concentration, reactions time and temperature. The extent of the reaction and the relative yield of each aluminum phosphate were shown to be related to the relative activity of the system. The relative activity (S_R) is given by the total surface area of the alumina per mole of P_2O_5 in the system. The fraction of alumina reacted increased with increasing relative activity and temperature.

Mixes with low relative activity values tend to yield aluminum phosphates with low Al:P ratios [i.e., $\text{Al}(\text{H}_2\text{PO}_4)_3$, $\text{AlH}_2\text{P}_3\text{O}_{10} \cdot 2\text{H}_2\text{O}$ and $\text{Al}(\text{PO}_3)_3$]. In contrast, phosphates with high Al:P ratios (i.e., the

polymorphs of AlPO_4) are formed in mixes of high relative activity.

Condensed phosphates such as $\text{Al}(\text{PO}_3)_3$ were shown to react with excess alumina at temperatures between 500 and 700°C. Thus, reaction products in the vicinity of alumina particles would be expected to form AlPO_4 by solidstate reaction.

Alum-derived alumina containing metastable $\gamma\text{-Al}_2\text{O}_3$ reacted in high $\text{Al}_2\text{O}_3:\text{P}_2\text{O}_5$ ratio mixes to form large amounts of the cristobalite form of AlPO_4 at 150°C. In contrast, mixes of identical composition prepared from alum-derived $\alpha\text{-Al}_2\text{O}_3$ reacted at a slower rate and produced only amorphous reaction products.

Since Kingery's (1) literature review in 1950 the amount of published information on phosphate bonding has been greatly expanded. Chvatal's (31) 1975 review which concentrated primarily on the 1965-1975 literature contained 222 references. Most of the effort represented by these publications has been devoted towards empirically investigating phosphate bonding materials and development of useful refractory products.

The effect of variables such as temperature, particle size, concentration, source of raw materials and time on the form and relative abundance of the reaction products present in a number of phosphate bonded systems have been investigated. However, there is still little fundamental physiochemical information about phosphate bonding in the literature. This is not surprising when the complexity of the multistep reactions, the difficulty in differentiation between the many possible reaction products and the fine grain sized polycrystalline nature of materials being bonded are taken into consideration.

Thus it appears that fundamental investigations on phosphate bonding should be performed on simple model systems. This investigation involves the use of single crystals to accomplish this goal.

EXPERIMENTAL PROGRAM

This section describes the methods developed to orient single crystals; the experiments carried out to investigate the reaction of phosphate bonding agents with fused silica and different crystallographic faces of single crystals; the development of methods to form phosphate bonded bicrystals and tensile testing procedures, the formation and testing of aligned bicrystals of alumina and the investigation of the effect of rotational mismatch on the fired tensile strength of alumina bicrystals.

Single Crystal Orientation

Many of the experiments carried out during this investigation required the determination of the crystal faces which were to be bonded together or reacted with phosphate bonding agents. Preuss (32) developed two Fortran IV computer programs designed to reduce the time required to accomplish single crystal orientations, using the conventional Laue back reflection method (33). A program called PLOMAX (34) was used to plot the back reflection Laue pattern for any desired orientation. The unknown orientation was then determined using a program named COL (35) to analyze the Laue data. The two programs then allow the calculation of the amount of rotation necessary to translate the crystal to the desired orientation (36). These two programs were modified so they would run on our Cyber 730 computer system. Crystals of alumina, magnesia, and quartz were successfully oriented using this technique.

The optimum time for producing the required back reflection Laue patterns using CuK_α radiation (35 kV and 20 mA) and 3000 speed, Type 57 Polaroid film was found to be between 10 and 20 minutes.

The crystal faces referred to in the remainder of this report were all determined or checked using the above procedure. The sapphire single crystals (37) were purchased in the form of square rods with the sides consisting of (0001) and $(11\bar{2}0)$ faces and the ends being $(1\bar{1}00)$ faces. The back reflection Laue patterns for at least one face from each rod was determined to make sure that the orientation was the one desired.

Reaction of Phosphate Bonding Agents with Different Crystallographic Faces of Single Crystals and Fused Silica

O'Hara et al (16) investigated the microstructures formed when a drop of phosphoric acid or a mixture of phosphoric and chromic acid was placed on the polished surface of polycrystalline alumina specimens and fired (see the Background Section for a summary of their work). Similar experiments utilizing single crystals and fused silica rods were carried out during this investigation.

A drop of phosphoric acid (61 % P_2O_5) or a 1:1 mixture of phosphoric acid (61 % P_2O_5) and chromic acid (61 % CrO_3) was placed on lapped surfaces of alumina, fused silica and quartz specimens. The alumina and quartz specimens were single crystals. The acid solutions were placed on the (0001) face of the quartz crystals. The orientation of the alumina crystals were not determined, but was perpendicular to the surface of the grown rod (1/4" diameter).

The acid solutions were dried at about 80°C for at least six hours and then fired at 1500°F (815°C). After cooling, a diamond saw cut was made about two-thirds of the way through the sample in the face opposite from the one on which the reaction had taken place. The reaction face was then fractured by gently tapping a wedge placed in the cut.

The alumina, fused silica and quartz samples reacted with phosphoric acid at 1500°F and the alumina crystal reacted with the chromic-phosphoric acid mixture at 1500°F were coated with gold and examined with an SEM. The surface of the alumina-phosphoric acid reaction area was made up primarily of dendrites (fig. 1), which appeared to be crystalline. Below the dendrites, there was a layer that contained a small amount of porosity (fig. 2). Beneath this layer, there may be another very thin layer of material. However, the structure observed could also have been the result of acid roughening of the surface of the alumina crystal. In some locations, a crack between the porous layer and the thin layer or the roughened alumina crystal were observed (fig. 2).

The reaction products formed when the chromic acid mixture was reacted with an alumina crystal were friable and appeared to be very porous. The top surface of these reaction products consisted of many small, needle-like crystals. It also appeared that some of the reaction layer was either broken off or crushed during the cutting and mounting procedure. Below this surface, a very porous amorphous appearing layer was present (fig. 3). This layer appeared to be tightly adherent to the surface of the alumina crystal as no cracks were observed.

The top surface of the phosphoric acid-quartz reaction products appeared to be composed primarily of plate-like crystals (fig. 4). The

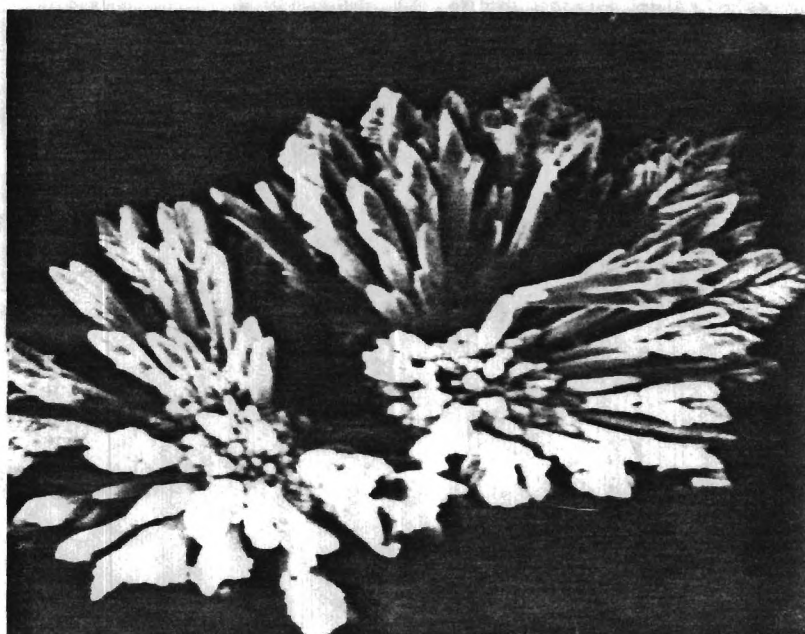


FIGURE 1. Dendrite crystals on surface of alumina crystal reacted with H_3PO_4 at 1500°F (400X).

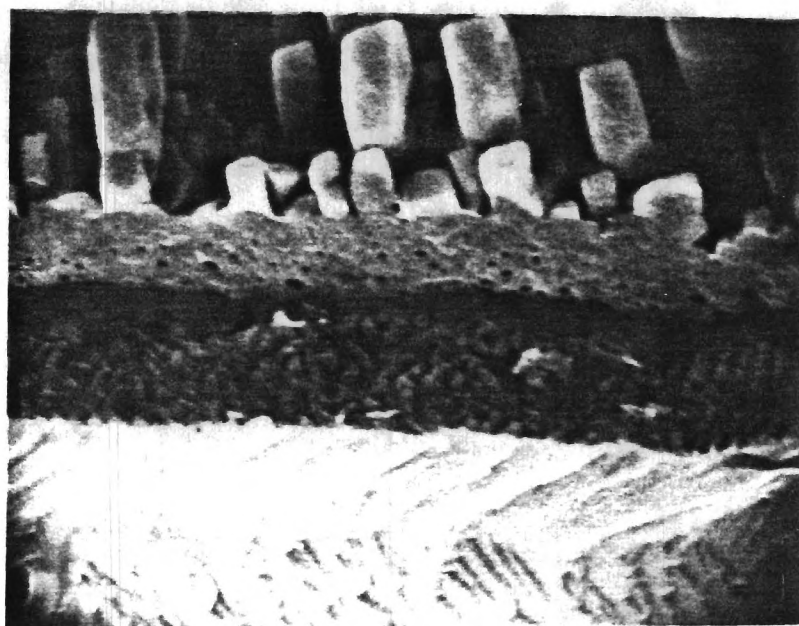


FIGURE 2. Reaction product layer below dendrites (2500X).



FIGURE 3. Reaction product layer formed on surface of alumina crystal reacted with chromic phosphoric acid mixture at 1500°F (3500X).



FIGURE 4. Top surface of reaction products on (0001) face of quartz crystal reacted with phosphoric acid at 1500°F (2500X).

material below this surface was granular in nature and appeared to be tightly bonded to the surface of the quartz.

Some cracks developed in the quartz crystal when it was cooled through the β to α transition. The surface of the phosphoric acid-fused silica reaction products was composed of amorphous looking spheres (fig. 5) and plate-like crystals that appeared to have grown out of the spheres (fig. 6). Below the surface, the coating was made up of the amorphous spheres with voids between the spheres. The surface of the fused silica sample appeared to have been attacked much more severely than either the quartz or the alumina single crystals.

After the square alumina rods that were to be used for forming the phosphate bonded bicrystals were received, additional reaction experiments were performed. The surfaces of these rods contained (0001), ($11\bar{2}0$), and (1T00) faces. Drops of phosphoric acid were reacted with samples of each face at 1500°F in the same manner as described above. After cooling in the furnace to room temperature, the reaction face was fractured by gently tapping a wedge placed in a diamond saw cut made in the back face before firing. The fractured samples were then mounted on SEM stubs and sputtered with gold.

The morphology of these alumina samples were examined with the SEM. At 100X, the (0001) face appeared to be primarily covered with whitish, star-shaped crystals on a gray crystalline background. A few grayish, star-shaped crystals were also observed to be composed of dendrites (see figures 7 and 8). These types of crystal morphologies were also seen on ($11\bar{2}0$) and (1T00) faces. However, a smaller percentage of these surfaces were covered with the star-shaped crystals.



FIGURE 5. Reaction product layer formed on surface of a fused silica rod reacted with phosphoric acid at 1500°F (1500X).

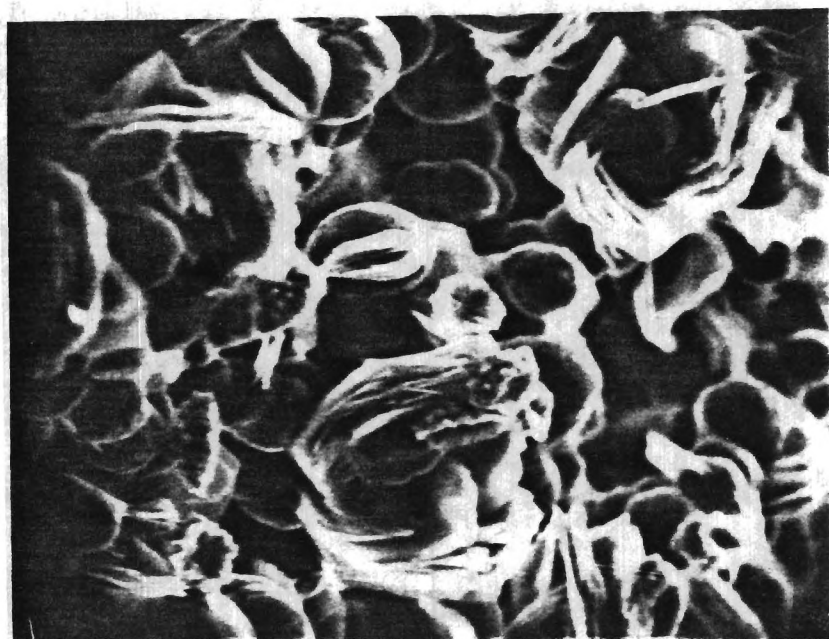


FIGURE 6. Plate-like crystals growing out of spheres shown in figure 5 (1500X).



FIGURE 7. Whitish star-shaped dendritic crystals on surface of reaction products produced by reacting H_3PO_4 with (0001) face of alumina at 1500°F (610X).

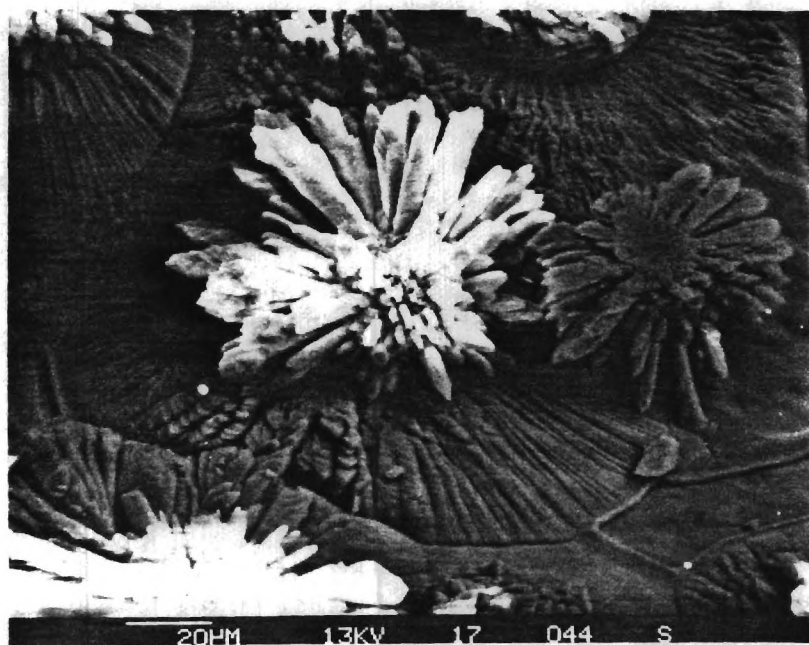


FIGURE 8. Whitish and grayish-shaped dendritic crystals produced by reacting H_3PO_4 with (0001) face of alumina crystal at 1500°F (600X).

EDAX analysis of the whitish star-shaped crystals indicated that their Al:P ratio was 1:3. This suggests that they are composed of aluminum meta phosphate ($\text{Al}(\text{PO}_4)_3$). This phase is reported to be the major phase present on the surfaces of the alumina (1) that had been heat treated above 500°C (932°F).

EDAX analysis of the grayish star-shaped crystals and the grayish crystalline background material indicated an Al:P ratio of approximately 1:1 (1:1.07), which suggests they are composed of monoaluminum phosphate (AlPO_4). This compound can exist in several polymorphic forms (berlinite, cristobalite, or tridymite forms). The different growth morphologies of the gray MAP may indicate the presence of two of these polymorphs. In addition to the slightly different growth morphologies of the $\text{Al}(\text{PO}_4)_3$ and AlPO_4 (MAP) dendritic structures, at higher magnifications (figures 9 and 10) it can clearly be seen that the MAP crystals contain much higher porosity. The flat interlocking MAP crystals covering the surface of the alumina appear to have nucleated at a central location and then to have grown outward until they encountered another group of crystals growing in a different direction.

Similar morphologies were seen on the $(1\bar{1}00)$ and $(11\bar{2}0)$ faces. However, it appeared that the whitish dendritic stars occurred much less frequently than on the (0001) face. This may be due to the fact that the (0001) face has a higher aluminum packing factor than the $(1\bar{1}00)$ and $(11\bar{2}0)$ faces.

The higher concentration of aluminum ions on the (0001) face appears to increase the amount of aluminum in the reaction products so that more AlPO_4 and less $\text{Al}(\text{PO}_4)_3$ is produced. Whereas, the elongated MAP crystals covering the (0001) surface appear to be grown out from a central



FIGURE 9. Structure of aluminum meta phosphate $[Al(PO_4)_3]$ dendrites (3200X).

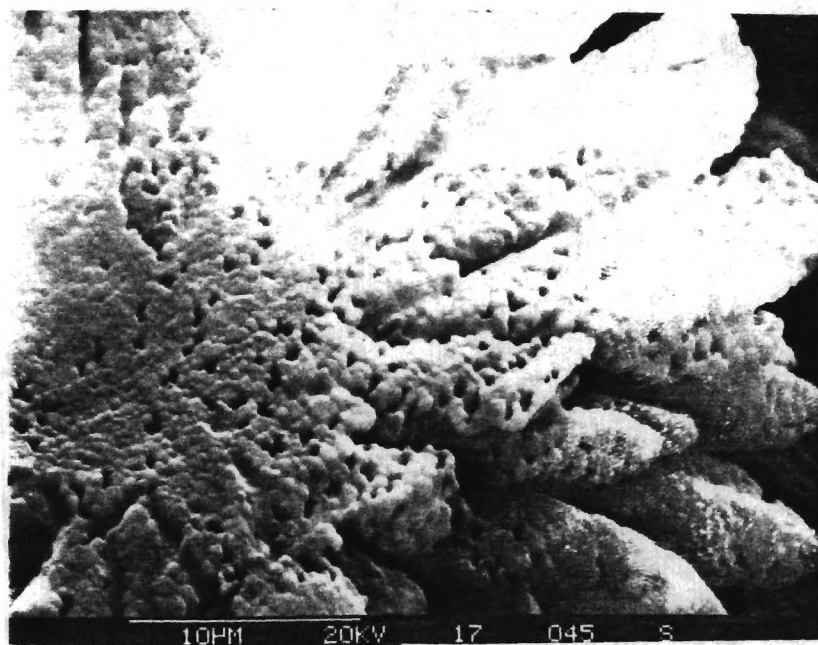


FIGURE 10. Porous morphology of monoaluminum phosphate $(AlPO_4)$ dendritic structure (3200X).

location (figures 7 and 8), those covering the $(1\bar{1}00)$ surface appeared to be more nearly equiaxed (figures 11 and 12).

Alumina samples were cut from the sapphire rods so that $(1\bar{1}02)$, $(11\bar{2}2)$ and two random faces were exposed. The random faces were cut in such a manner that it is unlikely they correspond to any low index face. A drop of phosphoric acid was placed on each of these faces and they were then dried and fired at 1500°F as described above. The reaction products on the $(1\bar{1}02)$ faces had morphologies similar to those observed on the (0001) faces, except that the star-like dendritic structures (fig. 13) appeared to contain more branching (less needle like). The aluminum phosphate structure formed on the $(11\bar{2}2)$ face did not contain any of the star-like dendritic structures. This face was covered with roughly equiaxed grains (fig. 14) that had a plate-like or even cubic substructure on portions of its surface (fig. 15).

The structures formed on the two randomly oriented faces did not contain any of the large star-like dendritic structures (figures 16 and 17). However, a few small dendrites were observed on one of them (fig. 16). Since these faces were prepared so that they most likely do not correspond to any low index face, it is reasonable to assume that they have relatively low aluminum packing densities. The fact that no large dendrite structures were formed suggests that large dendritic structures most likely only form on faces with high aluminum packing densities. The roughly equiaxed major grains shown in figure 17 are also covered with a plate-like substructure (fig. 18).

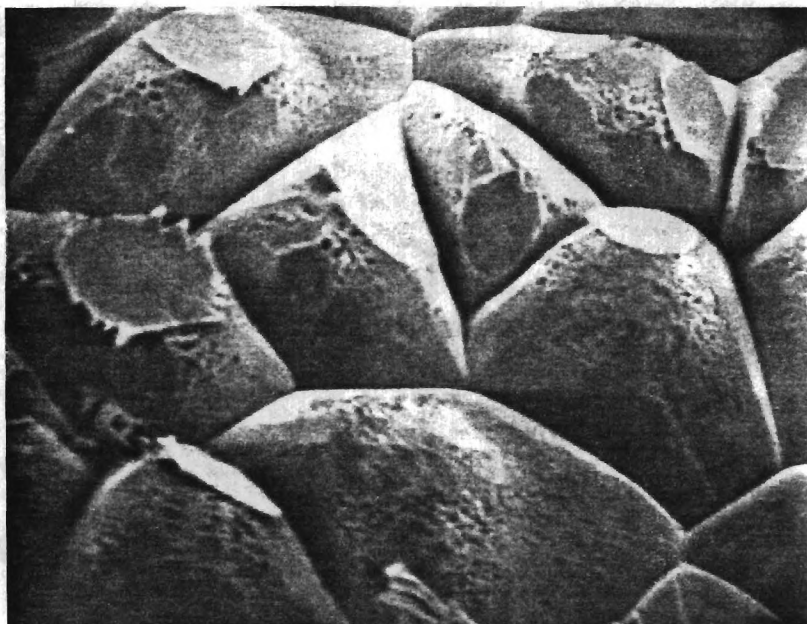


FIGURE 11. Nearly equiaxed crystals covering $(1\bar{1}00)$ face of alumina crystal reacted with H_3PO_4 (1000X).



FIGURE 12. Fractured alumina crystal with equiaxed crystals on $(1\bar{1}00)$ face (250X).

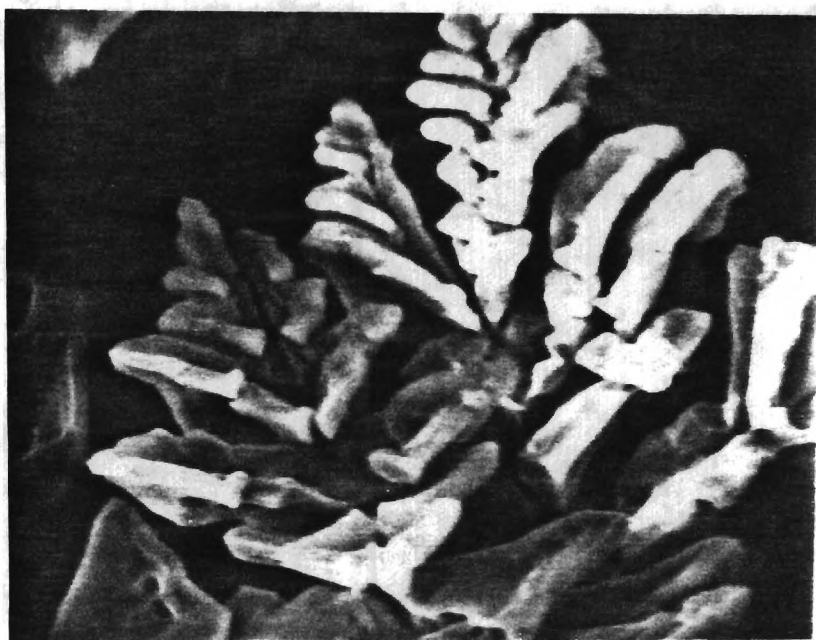


FIGURE 13. Dendritic structure on face of $(1\bar{1}02)$ alumina crystal reacted with H_3PO_4 at 1500°F (1250X).



FIGURE 14. Aluminum phosphate reaction products on surface of $(11\bar{2}2)$ face of alumina crystal reacted with H_3PO_4 at 1500°F (250X).

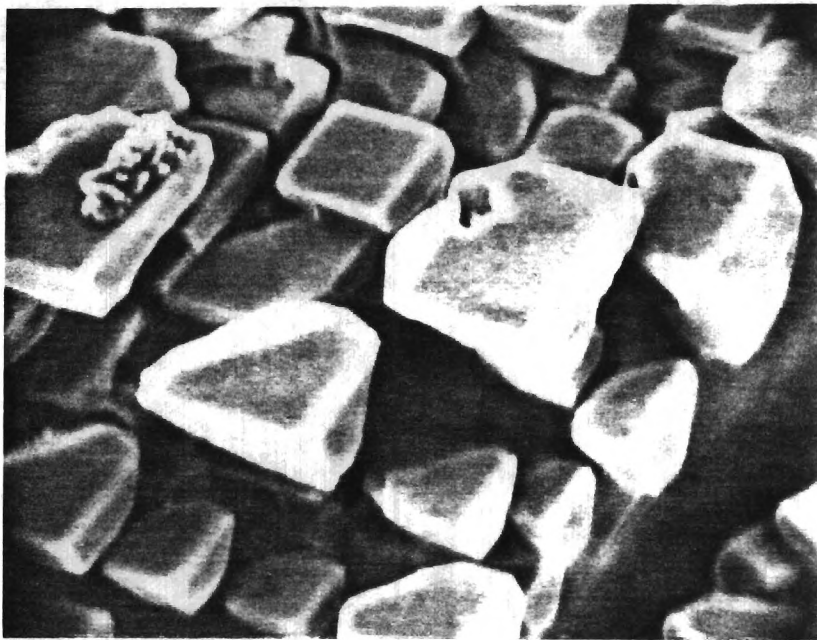


FIGURE 15. Higher magnification of surface shown in figure 14 (1100X).

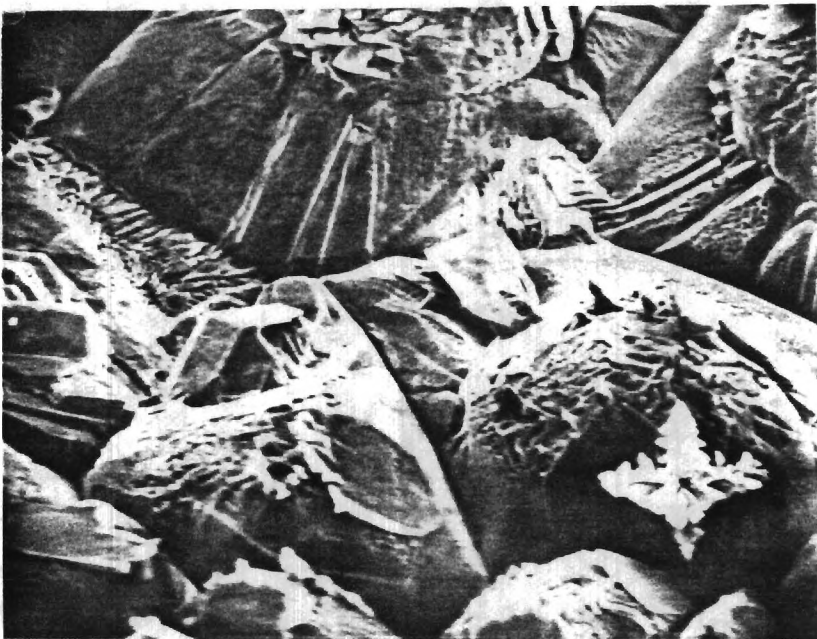


FIGURE 16. Surface of reaction products on a random plane of an alumina crystal reacted with H_3PO_4 at 1500°F (250X).

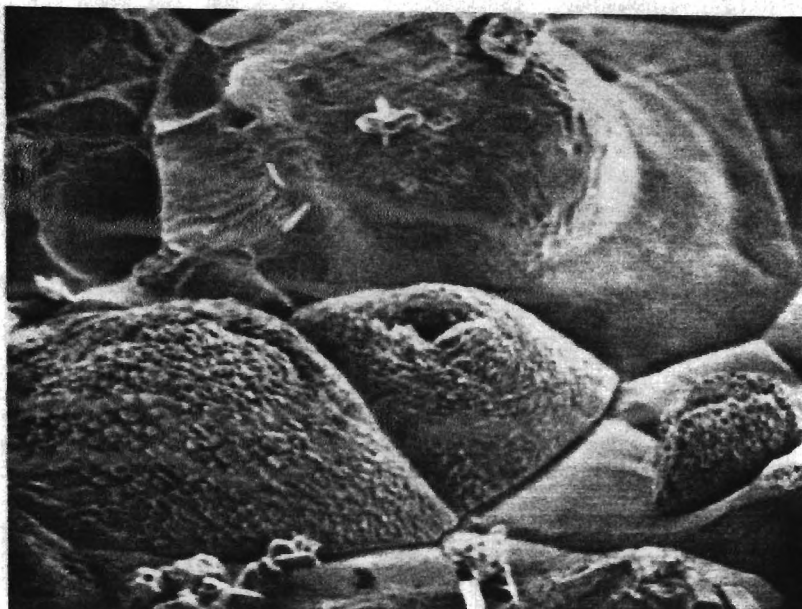


FIGURE 17. Same as figure 16 except random plane was different (250X).

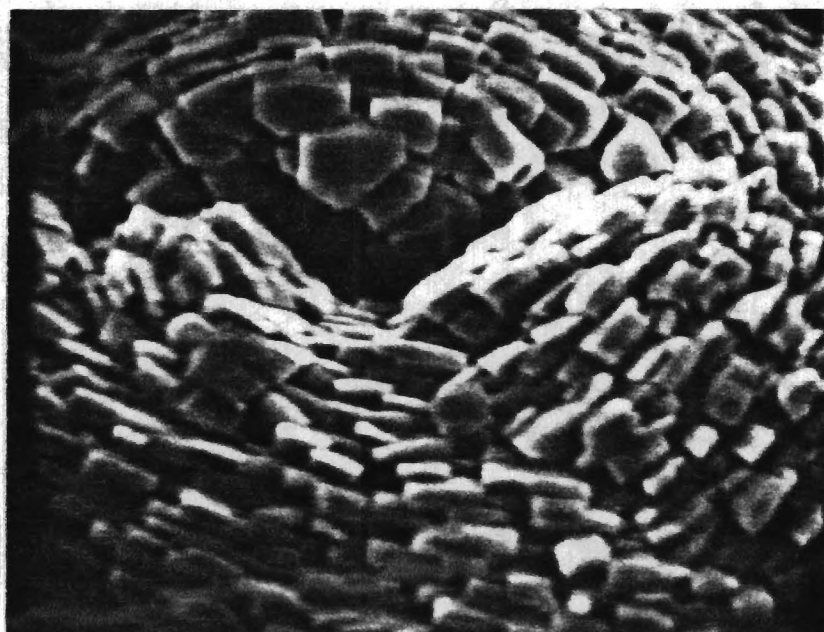


FIGURE 18. Plate-like structure covering surface of grains shown in figure 17 (1600X).

The microstructures produced when phosphoric acid was reacted with a fine grained polycrystalline alumina was investigated by placing a drop of acid on an alumina cutting tool and then drying and firing them as described above. The average grain size of the cutting tool was $<5\mu\text{m}$. No dendritic structures were observed in the microstructure of these reaction products. The morphology consisted of a mixture of elongated, equiaxed and plate-like grains (figures 19 and 20). These results tend to support the theory that dendrites are only formed on low index high atomic density faces since the probability of low index faces being parallel to the surface of the cutting tools is low.

Comparison of the microstructures observed during this investigation with those observed when samples were cut and polished (16) appears to indicate that the observation of fractured surfaces instead of polished surfaces may give a better understanding of phosphoric acid - alumina reaction product morphologies. At least some of the texture shown in the micrographs of the polished samples (16) is most likely the result of the polishing process.

Attempts were made to determine the crystal structure of aluminum phosphate grains and dendrites removed from the surface of the fired samples. Enough electron diffraction spots were not obtained to allow the phases to be identified.

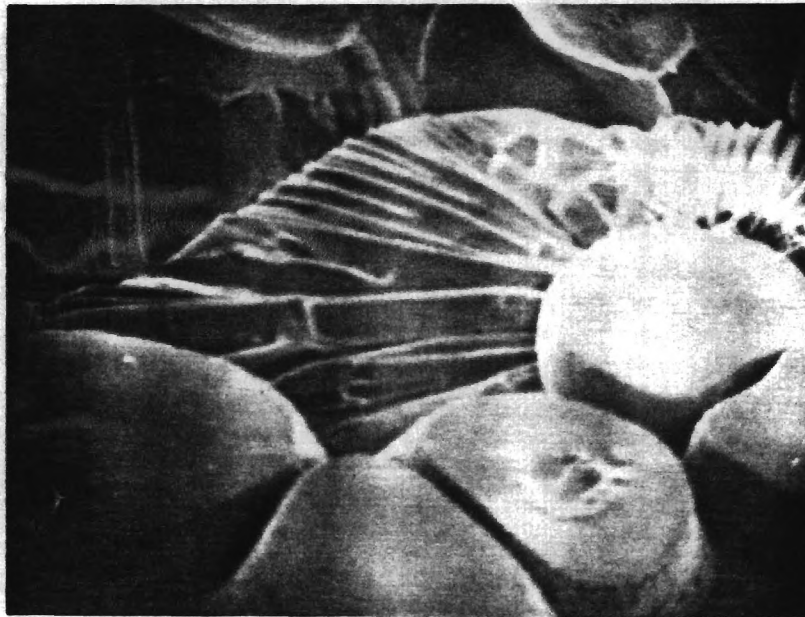


FIGURE 19. Surface of reaction product layer formed on the surface of an alumina cutting tool reacted with H_3PO_4 at 1500°F (500X).

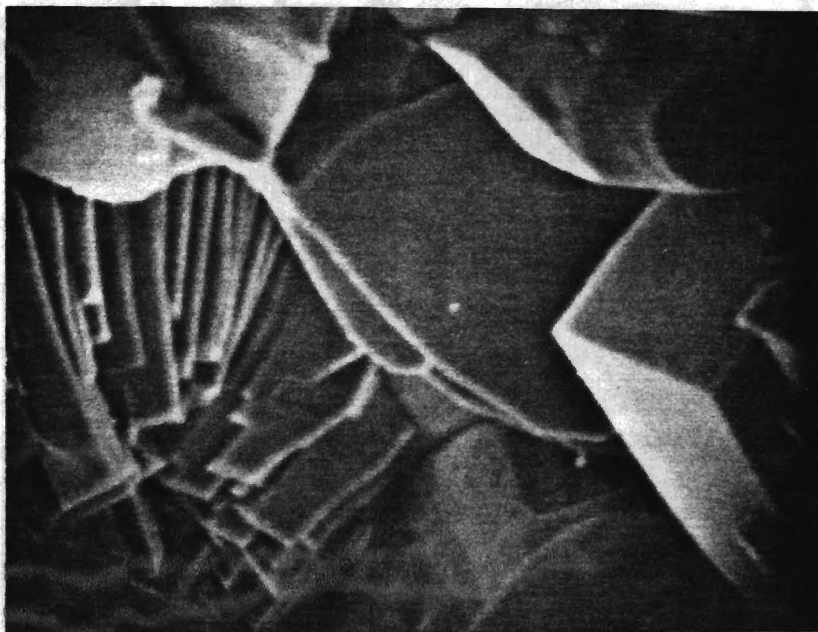


FIGURE 20. Plate-like grains on different area of alumina cutting tool shown in figure 19 (900X).

Development of Methods to Form Phosphate Bonded Bicrystals and Tensile Testing Procedures

Preliminary experiments were carried out using on-hand alumina, magnesia and quartz single crystals. Bicrystals were produced using both phosphoric acid and sodium dihydrogen phosphate as the bonding agent. During these preliminary experiments, neither bond thickness nor crystal orientation were controlled. Samples cured at 2000°F (1093°C) for four hours were strong enough to be easily handled except for the quartz bicrystals which contained cracks which were formed due to the $\alpha \rightleftharpoons \beta$ inversion.

The sapphire single crystals used in the remainder of this study were 0.250 in. rectangular cross-section rods obtained from Saphikon Division of Tyco Laboratories, Inc. They had well oriented (0001), (11 $\bar{2}$ 0), and (1 $\bar{1}$ 00) faces exposed ($\pm 30'$).

Preliminary attempts to form bicrystals using these single crystals were made using 85% H₃PO₄ (61% P₂O₅) as the bonding agent with bond thicknesses between 0.002 and 0.007" (before firing). In general, the strength of the bicrystals, bonded at 1500°F, was low and decreased as the thickness of the bond was increased. Since the separation of the bicrystals before bonding could not be accurately controlled below 0.002" (using feeler gauges), a new series of bicrystals were formed under varying loads during the heat treatment process. These bicrystals were strong enough to be easily handled. Examination of these samples in the SEM indicated that their bond thicknesses were all less than 0.002".

Three series of bicrystals were formed at 750°F, 1500°F and 2000°F. In each series, (0001) faces were bonded to (0001) faces and (11 $\bar{2}$ 0) faces

were joined to $(11\bar{2}0)$ faces using three different bonding agents and various loads. The three bonding agent solutions used were 85% H_3PO_4 (61.1% P_2O_5), $NaH_2PO_4 \cdot H_2O$ (30% P_2O_5) and Glass H $(NaPO_3)_2O$ (30% P_2O_5).

Tensile strengths were determined using an Instron Universal Testing machine and a loading jig which had a double flexible joint at the top and a reservoir of Wood's metal at the bottom. The samples were tested by super-gluing the bicrystals to two aluminum attachment rods. One of these rods was threaded into the bottom of the flexible joint. The Wood's metal was then melted with a gas torch and the cross-head lowered until the lower rod was partially submerged in the molten metal. The metal was then allowed to solidify around the bottom rod. This system was designed to minimize misalignment so the bicrystal would be loaded in pure tension. However, as the molten metal solidified and then cooled, it tended to misalign the lower rod and to also stress the bicrystal, causing some of them to fail.

The results obtained using this loading system and a cross-head speed of 0.1 cm/min. are given in table 1. These results showed that there was a positive relationship between bond strength and firing temperature. In general, the strength of the (0001) bicrystals was stronger than the $(11\bar{2}0)$ bicrystals. The samples prepared with H_3PO_4 as the bonding agent were the weakest and those prepared with Glass H were the strongest. In every case except one where a comparison was possible, the samples cured under the higher load (200 gms.) were stronger.

The bicrystals heat treated to $1500^\circ F$ were selected for morphological study after strength testing. The fracture morphologies of Glass H and $NaH_2PO_4 \cdot H_2O$ bonded bicrystals were basically the same (figures 21 and

Table 1. - Tensile strength of phosphate bonded alumina bicrystals.

Heat treatment temp. (°F)	Bonding agent	Load applied during firing (gms)	Bicrystal faces bonded	Tensile strength (kgf/cm ²)
750	NaH ₂ PO ₄ · H ₂ O	200	(0001)	20.9
750	Glass H	100	(0001)	19.3
1500	H ₃ PO ₄	200	(0001)	21.5
1500	NaH ₂ PO ₄ · H ₂ O	100	(0001)	77.0
1500	NaH ₂ PO ₄ · H ₂ O	200	(0001)	83.0
2000	NaH ₂ PO ₄ · H ₂ O	100	(0001)	65.0
2000	NaH ₂ PO ₄ · H ₂ O	200	(0001)	89.0
2000	NaH ₂ PO ₄ · H ₂ O	100	(1120)	16.5
2000	NaH ₂ PO ₄ · H ₂ O	200	(1120)	29.0
2000	Glass H	100	(0001)	64.0
2000	Glass H	200	(0001)	16.0
2000	Glass H	300	(1120)	17.5

Bicrystals that broke due to handling or during mounting in the loading jig have not been included.

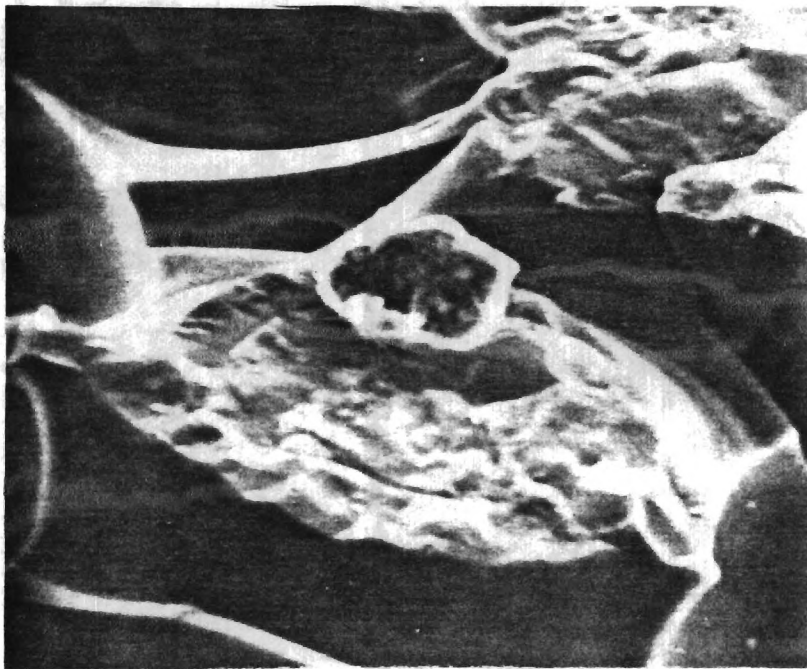


FIGURE 21. Fracture morphology of $\text{NaH}_2\text{PO}_4 \cdot \text{H}_2\text{O}$ bond between (0001) faces of alumina crystals fired at 1500°F (1200X).

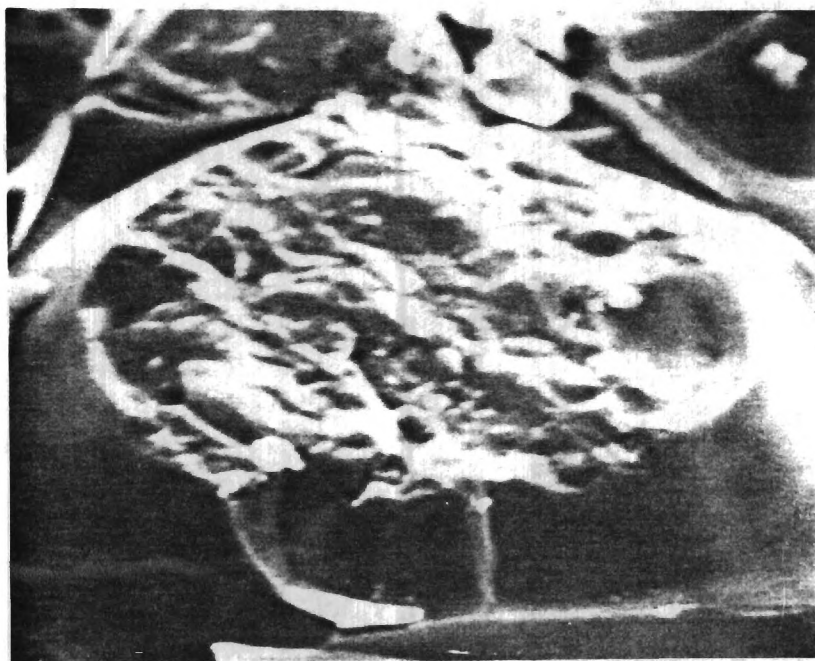


FIGURE 22. Fracture morphology of glass H bond between (0001) faces of alumina single crystals fired at 1500°F (1200X).

22), and showed that the bond was composed of interlocking cones that join the two faces of the bicrystals together. It also can be seen that voids existed between many of the cones and that the direction of fracture was parallel to the bicrystal faces. The fracture morphology of H_3PO_4 bonded crystals was entirely different from what was observed when H_3PO_4 was fired on the surface of a crystal. In general, the H_3PO_4 bond appeared to be very porous and none of the dendritic structures seen on the crystal surfaces were observed. This porosity (similar to that in figure 10 and the fact that aluminum was available from two crystal faces suggests that the bonding phase formed from H_3PO_4 was mono-aluminum phosphate.

In an attempt to overcome the problems associated with the first loading jig, a new loading system was developed. This system utilized two steel cables to transmit the tensile forces from the Instron to the two eyelets attached to aluminum loading blocks to which the bicrystal had been super-glued.

This new loading system was used to test a series of $(11\bar{2}0)$ bicrystals bonded with $NaH_3PO_4 \cdot H_2O$ (30% P_2O_5). These bicrystals were placed under a 100 gram weight and allowed to cure at room temperature for at least 24 hours. They were then fired at $1500^\circ F$ for four hours. Their room temperature strengths are listed in table 2.

Based on the fact that all of these samples were stronger than any previously tested, our visual observation that the new system produced much better alignment during loading was confirmed. A second series of similar bicrystals was prepared (A-7 to A-8) using a 200 gram load during the 24 hour room temperature curing cycle. These bicrystals were

Table 2. - Tensile strength of alumina bicrystals bonded with NaH_2PO_4 and fired at 1500°F for four hours.

Sample number	Load applied during curing (gms)	Bicrystal faces bonded	Crystal condition	Tensile strength (kgf/cm ²)
A-1	100	(11 $\bar{2}$ 0)	New	100.9
A-2	100	(11 $\bar{2}$ 0)	New	90.5
A-3	100	(11 $\bar{2}$ 0)	New	93.5
A-4	100	(11 $\bar{2}$ 0)	New	106.0
A-5	100	(11 $\bar{2}$ 0)	New	117.6
A-6	100	(11 $\bar{2}$ 0)	New	101.6
				$\bar{x} = 101.7$
				$s = 9.6$
A-7	200	(11 $\bar{2}$ 0)	Used	32.5
A-8	200	(11 $\bar{2}$ 0)	Used	33.7
A-9	200	(11 $\bar{2}$ 0)	Used	42.2
A-10	200	(11 $\bar{2}$ 0)	Used	64.0
A-11	200	(11 $\bar{2}$ 0)	Used	42.9
A-12	200	(11 $\bar{2}$ 0)	Used	40.7
				$\bar{x} = 42.7$
				$s = 11.3$
B-1	100	(0001)	Used	13.0
B-2	100	(0001)	Used	35.4
B-3	100	(0001)	Used	26.1
B-4	100	(0001)	Used	41.5
B-5	100	(0001)	Used	15.3
				$\bar{x} = 26.3$
				$s = 12.4$
B-7	100	(0001)	New	41.5
B-8	100	(0001)	New	85.3
B-9	100	(0001)	New	43.3
B-10	100	(0001)	New	66.8
B-11	100	(0001)	New	98.4
B-12	100	(0001)	New	56.2
				$\bar{x} = 65.3$
				$s = 22.9$

prepared from crystals that had been previously used. Before being re-bonded, they were lightly ground on 180, 240, 600 grit SiC paper and were then lightly polished using 1, 0.5 and 0.3 μm alumina to remove any contamination. The tensile strengths of these samples are also listed in table 2. These samples were significantly weaker than the set produced from unused crystals.

In an attempt to determine if this strength decrease was the result of reusing the alumina crystals or was due to the increased load during curing, two additional series of bicrystals bonded with $\text{NaH}_2\text{PO}_4 \cdot \text{H}_2\text{O}$ were prepared and fired. All of these samples were (0001) bicrystals cured under a 100 gram load and fired at 1500°F for four hours. The B-1 to B-5 samples were prepared from used crystals and the B-7 to B-12 samples from new crystals. Their tensile strengths are listed in table 2. Even though the new (0001) bicrystals were much weaker than the (11 $\bar{2}$ 0) bicrystals produced from unused crystals, it appears that reusing the alumina crystals decreases the strength of the alumina bicrystals.

Additional (0001) and (11 $\bar{2}$ 0) bicrystals were produced from new crystals using Glass H (30% P_2O_5) as the bonding agent. These samples were cured under 100 gram loads and fired at 1500°F. Their tensile strengths are listed in table 3. These results indicate that both (11 $\bar{2}$ 0) and (0001) bicrystals bonded with Glass H are weaker than the same type of bicrystals bonded with $\text{NaH}_2\text{PO}_4 \cdot \text{H}_2\text{O}$.

Examination of the fracture faces of the above samples suggested that the loads applied during curing may not have been uniformly distributed over the bond area. An attempt was made to improve the load distribution by curing ten samples at one time with the load being applied

Table 3. - Tensile strength of alumina bicrystals bonded with glass H and fired at 1500°F for four hours.

Sample number	Load applied during curing (gms)	Bicrystal faces bonded	Tensile strength (kgf/cm ²)
H-1	100	(11 $\bar{2}$ 0)	16.2
H-2	100	(11 $\bar{2}$ 0)	20.7
H-3	100	(11 $\bar{2}$ 0)	26.6
H-4	100	(11 $\bar{2}$ 0)	17.7
H-5	100	(11 $\bar{2}$ 0)	20.7
H-6	100	(11 $\bar{2}$ 0)	20.7
			$\bar{x} = 20.4$
			$s = 3.6$
G-2	100	(0001)	43.9
G-3	100	(0001)	34.0
G-5	100	(0001)	29.2
G-6	100	(0001)	17.2
			$\bar{x} = 31.1$
			$s = 11.1$

to the samples by a rigid one or two kilogram plate which rested on all ten specimens. These samples were cured at room temperature for 24 hours and then fired at 1500°F for 4 hours. Sodium dihydrogen phosphate and Glass H which contained 30% P_2O_5 were used as the bonding agents.

The tensile strengths of these samples are listed in table 4. The samples whose condition is described as "polished" are used samples that were prepared in the same manner as the "used" samples in table 2, except the coarse grinding was done on 150 and 45 μ m diamond wheels. The effects of crystal condition and the bicrystal faces bonded are shown in figure 23. Figure 24 shows the effect of bonding agent, curing load, and bicrystal faces bonded.

Examination of the fracture faces of these samples indicated that the distributed loading technique produced even greater nonuniformity of bond thickness. Because of this, analysis of variance calculations were not made. However, examination of the results suggests that the polishing of used samples does not produce as good a bonding surface as that present on the unused single crystals (fig. 23). In addition, it appears that decreasing the bond thickness (increasing the curing load) may decrease the bond strength of bicrystals bonded with Glass H (fig. 24). Since the uniformity of bond thicknesses of these samples was worse than those which were individually loaded during the curing cycle, the individual load method was used throughout the rest of this investigation.

The effect of curing time was investigated by preparing two sets of bicrystals cured at room temperature for 24 and 3 hours respectively. A 100 gm load was applied during the curing cycle and the samples fired at 1500°F

Table 4. - Tensile strength of phosphate bonded alumina bicrystals cured under a distributed load.

Bonding agent	Load applied during curing (gms)	Bicrystal faces bonded	Crystal condition	Tensile strength (kgf/cm ²)
NaH ₂ PO ₄ ·H ₂ O	100	(11 $\bar{2}$ 0)	New	40.8
NaH ₂ PO ₄ ·H ₂ O	100	(11 $\bar{2}$ 0)	New	31.3
NaH ₂ PO ₄ ·H ₂ O	100	(11 $\bar{2}$ 0)	New	33.0
NaH ₂ PO ₄ ·H ₂ O	100	(11 $\bar{2}$ 0)	New	104.9
NaH ₂ PO ₄ ·H ₂ O	100	(11 $\bar{2}$ 0)	New	64.5
				$\bar{x} = 54.9$
				$s = 30.9$
NaH ₂ PO ₄ ·H ₂ O	100	(11 $\bar{2}$ 0)	Polished	8.1
NaH ₂ PO ₄ ·H ₂ O	100	(11 $\bar{2}$ 0)	Polished	6.5
NaH ₂ PO ₄ ·H ₂ O	100	(11 $\bar{2}$ 0)	Polished	9.7
NaH ₂ PO ₄ ·H ₂ O	100	(11 $\bar{2}$ 0)	Polished	8.1
NaH ₂ PO ₄ ·H ₂ O	100	(11 $\bar{2}$ 0)	Polished	8.1
				$\bar{x} = 8.1$
				$s = 1.1$
NaH ₂ PO ₄ ·H ₂ O	100	(0001)	New	104.9
NaH ₂ PO ₄ ·H ₂ O	100	(0001)	New	59.5
NaH ₂ PO ₄ ·H ₂ O	100	(0001)	New	15.6
NaH ₂ PO ₄ ·H ₂ O	100	(0001)	New	46.1
NaH ₂ PO ₄ ·H ₂ O	100	(0001)	New	37.5
				$\bar{x} = 52.7$
				$s = 33.2$
NaH ₂ PO ₄ ·H ₂ O	100	(0001)	Polished	31.3
NaH ₂ PO ₄ ·H ₂ O	100	(0001)	Polished	28.6
NaH ₂ PO ₄ ·H ₂ O	100	(0001)	Polished	54.8
NaH ₂ PO ₄ ·H ₂ O	100	(0001)	Polished	31.3
NaH ₂ PO ₄ ·H ₂ O	100	(0001)	Polished	31.3
				$\bar{x} = 35.5$
				$s = 10.8$
Glass H	100	(11 $\bar{2}$ 0)	New	61.4
Glass H	100	(11 $\bar{2}$ 0)	New	89.7
Glass H	100	(11 $\bar{2}$ 0)	New	52.2
Glass H	100	(11 $\bar{2}$ 0)	New	20.7
Glass H	100	(11 $\bar{2}$ 0)	New	115.6
				$\bar{x} = 67.9$
				$s = 36.2$

Table 4. - Tensile strength of phosphate bonded alumina bicrystals cured under a distributed load (continued).

Bonding agent	Load applied during curing (gms)	Bicrystal faces bonded	Crystal condition	Tensile strength (kgf/cm ²)
Glass H	100	(0001)	New	84.2
Glass H	100	(0001)	New	30.7
Glass H	100	(0001)	New	27.4
Glass H	100	(0001)	New	47.7
Glass H	100	(0001)	New	20.7
				$\bar{x} = 42.1$
				$s = 25.5$
NaH ₂ PO ₄ • H ₂ O	200	(11 $\bar{2}$ 0)	New	63.0
NaH ₂ PO ₄ • H ₂ O	200	(11 $\bar{2}$ 0)	New	96.9
NaH ₂ PO ₄ • H ₂ O	200	(11 $\bar{2}$ 0)	New	29.0
NaH ₂ PO ₄ • H ₂ O	200	(11 $\bar{2}$ 0)	New	43.6
NaH ₂ PO ₄ • H ₂ O	200	(11 $\bar{2}$ 0)	New	80.7
				$\bar{x} = 62.6$
				$s = 27.3$
NaH ₂ PO ₄ • H ₂ O	200	(0001)	New	15.9
NaH ₂ PO ₄ • H ₂ O	200	(0001)	New	31.3
NaH ₂ PO ₄ • H ₂ O	200	(0001)	New	22.6
NaH ₂ PO ₄ • H ₂ O	200	(0001)	New	83.0
NaH ₂ PO ₄ • H ₂ O	200	(0001)	New	43.8
				$\bar{x} = 39.3$
				$s = 26.5$
Glass H	200	(11 $\bar{2}$ 0)	New	18.1
Glass H	200	(11 $\bar{2}$ 0)	New	61.3
Glass H	200	(11 $\bar{2}$ 0)	New	123.0
Glass H	200	(11 $\bar{2}$ 0)	New	28.2
Glass H	200	(11 $\bar{2}$ 0)	New	52.9
				$\bar{x} = 56.7$
				$s = 41.0$
Glass H	200	(0001)	New	28.2
Glass H	200	(0001)	New	33.3
Glass H	200	(0001)	New	17.7
Glass H	200	(0001)	New	48.5
Glass H	200	(0001)	New	15.5
				$\bar{x} = 28.6$
				$s = 13.3$

		Average Tensile Strengths (kgf/cm ²)	
		Crystal Condition	
		New	Polished
Bicrystal Faces Bonded	(11 $\bar{2}$ 0)	54.9	8.1
	(0001)	52.7	35.5

FIGURE 23. Average tensile strength factorial design (2 x 2) showing effect of crystal condition and bicrystal faces bonded with sodium dihydrogen phosphate (30% P₂O₅) and cured under a load of 100 grams.

		Average Tensile Strength (kgfcm ²)		
		Load During Curing (gms)		
		100	200	
Bicrystal Face Bonded	(11 $\bar{2}$ 0)	54.9	62.5	NaH ₂ PO ₄ ·H ₂ O
		67.9	56.7	Glass H
	(0001)	52.7	42.1	NaH ₂ PO ₄ ·H ₂ O
		39.9	28.6	Glass H
Bonding Agent				

FIGURE 24. Average tensile strength factorial design (2 x 2 x 2) showing the effect of bonding agent, curing load and bicrystal faces bonded.

for 4 hours. The bonding agent used was sodium dihydrogen phosphate that had been diluted with water to reduce its P_2O_5 content to 20%. The tensile strengths of these samples are listed in table 5.

The strength of the $(11\bar{2}0)$ bicrystals decreased when the curing time was reduced from 24 to 3 hours. On the other hand, it appears the longer curing time may cause the (0001) bicrystals to be weaker, provided they are handled very carefully until after they have been fired. Thus, it appears that it takes longer for the aluminum required to form the bond to go into solution from the $(11\bar{2}0)$ faces than it does from the (0001) faces. This may be due to the fact that the (0001) face has a higher aluminum packing factor than the $(11\bar{2}0)$ face. The reason for the decrease in strength of the (0001) bicrystals with increasing curing time is unknown. However, one possibility is that after 3 hours curing, the bonding phase produces $Al(PO_4)_3$ when it is fired and that after 24 hours curing the bonding phase produces $AlPO_4$ when it is fired. These results also tend to confirm the fact that a stronger bond is formed between $(11\bar{2}0)$ faces than (0001) faces when sodium dihydrogen phosphate is used as the bonding agent (see table 2).

In a further attempt to develop a method of reusing the alumina crystals, two additional sets of samples were prepared. Both were bonded with sodium dihydrogen phosphate and cured 24 hours under a 100 gram load at room temperature. The first set was produced by cutting a used crystal in half on a Buehler Limited Isomet Low Speed Saw using a Lunzer Industrial Diamond 4 x 0.012 x 1/2" blade. The two halves were then bonded together without any further finishing treatment. The second set was prepared from used crystals that were polished on 180, 240, 320

Table 5. - Effect of curing time on the tensile strength of sodium dihydrogen phosphate bonded alumina bicrystals.

Curing time (hrs)	Bicrystal faces bonded	Tensile strength (kgf/cm ²)
24	(11 $\bar{2}$ 0)	50.1
24	(11 $\bar{2}$ 0)	134.0
24	(11 $\bar{2}$ 0)	158.4
24	(11 $\bar{2}$ 0)	161.4
24	(11 $\bar{2}$ 0)	150.2
		$\bar{x} = 130.8$
		$s = 46.3$
24	(0001)	24.2
24	(0001)	51.7
24	(0001)	62.9
24	(0001)	35.5
		$\bar{x} = 43.6$
		$s = 17.1$
3	(11 $\bar{2}$ 0)	67.5
3	(11 $\bar{2}$ 0)	33.8
3	(11 $\bar{2}$ 0)	51.7
3	(11 $\bar{2}$ 0)	51.7
3	(11 $\bar{2}$ 0)	50.8
		$\bar{x} = 51.1$
		$s = 11.9$
3	(0001)	0*
3	(0001)	0*
3	(0001)	0*
3	(0001)	116.7
3	(0001)	95.3
		$\bar{x} = 106.0$

*Failed during handling, before firing.

and 600 grit SiC papers. The tensile strengths of these samples are listed in table 6.

Comparison of these results with those in table 5 clearly indicates the importance of surface finish on the bicrystal tensile strength. For both the $(11\bar{2}0)$ and (0001) bicrystals, the tensile strength increases (table 7) as the surface finish is improved (diamond sawed \rightarrow polished \rightarrow new). It should also be noted that the $(11\bar{2}0)$ bicrystals were stronger than the (0001) bicrystals for equivalent surface finish (table 7) when $\text{NaH}_2\text{PO}_4 \cdot \text{H}_2\text{O}$ (20% P_2O_5) was used as the bonding agent.

A series of bicrystals were made to investigate the effect of rotational mismatch on the strength of $(11\bar{2}0)$ bicrystals. These bicrystals were bonded with sodium dihydrogen phosphate (20% P_2O_5) and cured under a 100 gram load for 24 hours at room temperature. After curing, they were fired at 1500°F for 4 hours. The alignment jig used produced bicrystals whose mismatch angle was within $\pm 2^\circ$. The tensile strengths of these bicrystals are listed in table 8. The used-polished samples were prepared using the polishing technique described above. The results are also shown graphically in figure 25.

These results indicate that the tensile strength decreases as the rotational angle is increased from 0 to 90° and then increases back to approximately its original level as the angle of rotation is further increased from 90 to 180° .

Since the load per unit area during the curing cycle varied by a factor of two as the amount of rotation was varied, an experiment was carried out to determine if the low strength of the intermediate samples

Table 6. - Effect of surface finish on the tensile strength of alumina bicrystals bonded with sodium dihydrogen phosphate.

Bicrystal faces bonded	Crystal condition	Tensile strength (kgf/cm ²)
(11 $\bar{2}$ 0)	Diamond Sawed	56.2
(11 $\bar{2}$ 0)	Diamond Sawed	40.9
(11 $\bar{2}$ 0)	Diamond Sawed	56.2
(11 $\bar{2}$ 0)	Diamond Sawed	8.4
(11 $\bar{2}$ 0)	Diamond Sawed	60.2
(11 $\bar{2}$ 0)	Diamond Sawed	55.3
		$\bar{x} = 46.2$
		$s = 19.7$
(0001)	Diamond Sawed	21.4
(0001)	Diamond Sawed	18.4
(0001)	Diamond Sawed	17.0
(0001)	Diamond Sawed	18.0
(0001)	Diamond Sawed	17.1
(0001)	Diamond Sawed	18.0
(0001)	Diamond Sawed	21.4
(0001)	Diamond Sawed	19.4
		$\bar{x} = 18.8$
		$s = 1.7$
(11 $\bar{2}$ 0)	Polished	48.5
(11 $\bar{2}$ 0)	Polished	64.5
(11 $\bar{2}$ 0)	Polished	23.8
(11 $\bar{2}$ 0)	Polished	88.6
(11 $\bar{2}$ 0)	Polished	80.9
(11 $\bar{2}$ 0)	Polished	67.3
(11 $\bar{2}$ 0)	Polished	41.3
		$\bar{x} = 59.3$
		$s = 22.8$
(0001)	Polished	22.1
(0001)	Polished	56.5
(0001)	Polished	83.9
(0001)	Polished	17.7
(0001)	Polished	47.9
(0001)	Polished	11.0
		$\bar{x} = 39.9$
		$s = 28.0$

Table 7. - Effect of surface finish and crystal faces bonded on the average tensile strength of bicrystals bonded with sodium dihydrogen phosphate (20% P_2O_5).

Surface finish	Average tensile strength (kgf/cm ²)	
	Crystal faces bonded	
	(11 $\bar{2}$ 0)	(0001)
Diamond Sawed	46.2	18.8
Polished	59.3	39.3
As-Received	130.8	43.6

Table 8. - Effect of rotational mismatch on the tensile strength of (11 $\bar{2}$ 0) alumina bicrystals bonded with sodium dihydrogen phosphate (20% P₂O₅).

Rotational mismatch	Tensile strength (kgf/cm ²)			
	New crystals			Used-polished crystals
0	51.0	164.7	164.4	117.3
10	-	-	-	50.7
15	35.5	63.1	-	67.8
20	-	-	-	75.7
25	-	-	-	60.1
30	7.7	16.6	-	47.5
35	-	-	-	3.6
45	2.2	1.8	-	0*
60	1.8	0*	-	-
75	0*	0*	-	-
90	0*	0*	-	-
105	0*	-	-	-
120	0*	-	-	-
135	0*	-	-	-
150	1.8	-	-	-
165	36.9	-	-	-
180	113.9	84.1	96.7	-

*Too weak to be tested.

-Not prepared.

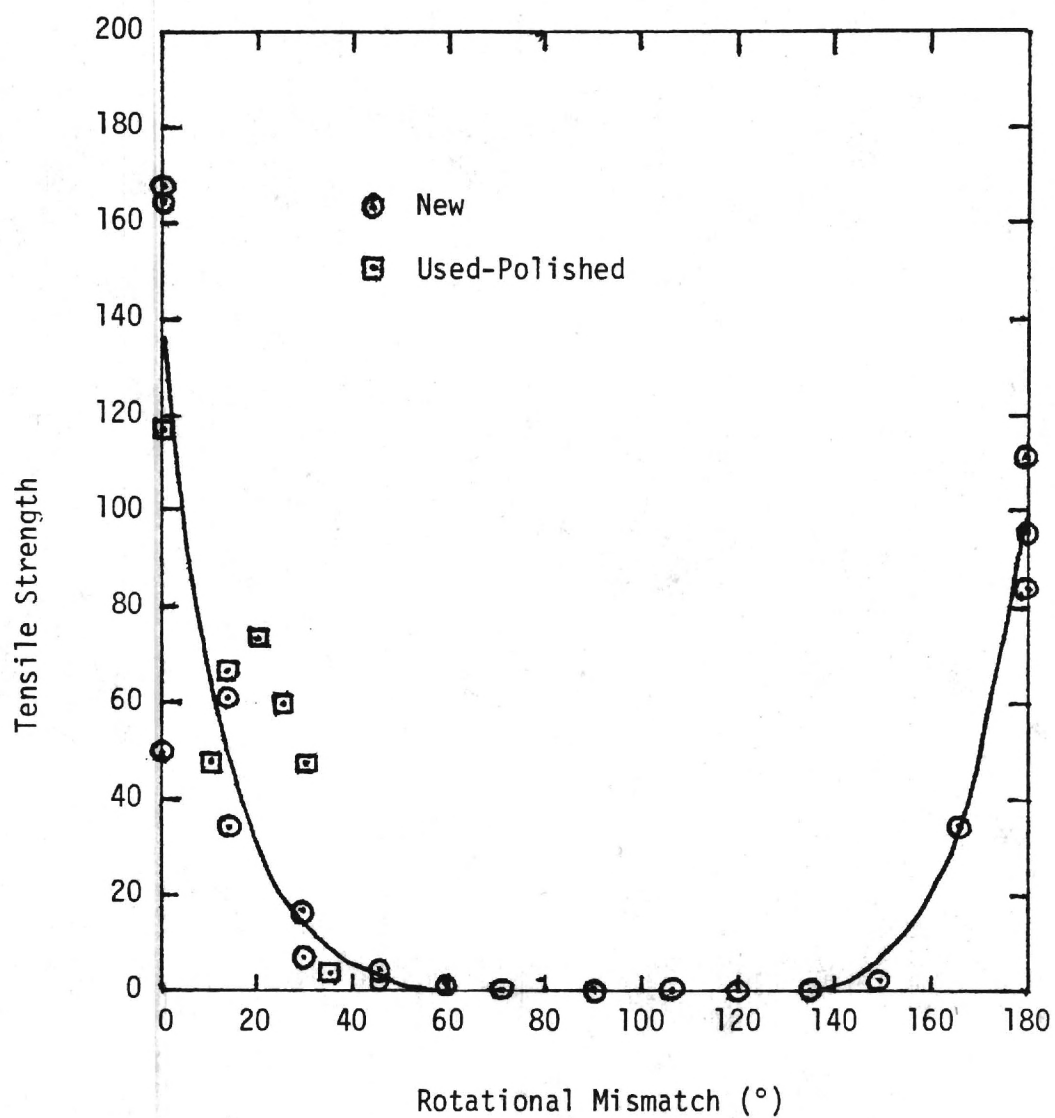


FIGURE 25. Effect of rotational mismatch on the tensile strength of (11 $\bar{2}$ 0) alumina bicrystals.

(45°- 135°) was related to the load during curing. Three 90° samples were prepared as before with loads of 100, 64, 50 grams, respectively. None of these bicrystals were strong enough to be tested.

Thus, it appears that the strength pattern observed in figure 25 is the result of the two-fold symmetry of the $(11\bar{2}0)$ face. At this time, it is not clear whether the difference in thermal expansion with direction or bond misalignment is the cause of tensile strength minimum observed for the 90° rotational mismatch bicrystals.

The effect of a combination of both rotational and tilt mismatch was investigated by bonding the $(11\bar{2}0)$ and (0001) faces of alumina crystals together with sodium dihydrogen phosphate (20% P_2O_5) to form a bicrystal. Standard $(11\bar{2}0)$ and (0001) bicrystals were also prepared for comparison purposes. The crystals utilized for this experiment were used crystals that were repolished as described above. Each bicrystal was cured under a 100 gram load for 24 hours and then fired at 1500°F for 4 hours. The tensile strengths of these bicrystals are listed in table 9.

The relatively high strengths of the $(11\bar{2}0)$ and (0001) bicrystals suggests that the crystals used for this experiment had a good surface finish. The combination of rotational and tilt mismatch in the $(11\bar{2}0)$ (0001) bicrystals reduced their strength to almost zero. Again, it is not known whether this decrease in strength was caused by differences in thermal expansion with direction or variations in ion density (bond misalignment).

Table 9. - Effect of rotational and tilt mismatch on the tensile strength of alumina bicrystals bonded with sodium dihydrogen phosphate (20% P_2O_5).

Faces bonded	Tensile strength (kgf/cm ²)
$(11\bar{2}0)(11\bar{2}0)$ $(11\bar{2}0)(11\bar{2}0)$ $(11\bar{2}0)(11\bar{2}0)$ $(11\bar{2}0)(11\bar{2}0)$ $(11\bar{2}0)(11\bar{2}0)$ $(11\bar{2}0)(11\bar{2}0)$ $(11\bar{2}0)(11\bar{2}0)$ $(11\bar{2}0)(11\bar{2}0)$	60.5 41.5 145.3 65.6 101.7 152.1 172.5 101.7 <hr/> $\bar{x} = 105.1$ $s = 47.8$
$(0001)(0001)$ $(0001)(0001)$ $(0001)(0001)$ $(0001)(0001)$ $(0001)(0001)$ $(0001)(0001)$	108.2 57.4 104.9 113.0 67.6 71.7 <hr/> $\bar{x} = 87.1$ $s = 24.2$
$(11\bar{2}0)(0001)$ $(11\bar{2}0)(0001)$ $(11\bar{2}0)(0001)$ $(11\bar{2}0)(0001)$ $(11\bar{2}0)(0001)$ $(11\bar{2}0)(0001)$ $(11\bar{2}0)(0001)$ $(11\bar{2}0)(0001)$ $(11\bar{2}0)(0001)$ $(11\bar{2}0)(0001)$	0* 0* 0* 21.1 0* 0* 3.2 3.0 0* 0* <hr/> $\bar{x} = 2.7$ $s = 6.6$

*Too weak to be tested.

CONCLUSIONS

When phosphoric acid is reacted with alumina single crystals (room temperature curing followed by firing at 1500°F) the morphology of the reaction products are related to the index of the crystal face. Star-shaped dendritic crystals of $\text{Al}(\text{PO}_4)_3$ and AlPO_4 only formed on the surface of low index relatively dense packed faces such as (0001), $(1\bar{1}00)$ and $(11\bar{2}0)$. The crystals formed on the surfaces of alumina single crystal faces that did not correspond to a low index plane and those formed on fine grained polycrystalline alumina cutting tools were roughly equiaxed. When phosphoric acid was reacted with the (0001) face of quartz at 1500°F, the reaction products appeared to be plate-like crystals. However, the reaction products formed when phosphoric acid was reacted with fused silica under the same conditions had an amorphous looking spherical morphology. The surface of the fused silica samples appeared to have been attacked more severely than either the quartz or alumina samples.

These results support the conclusions that the morphology of the reaction products produced when phosphoric acid is reacted with the surface of oxide samples is controlled by the crystallinity of the sample. If the sample is a single crystal, the reaction product morphology is related to the atomic density of the crystal face with which the phosphoric acid reacted. Fine grained polycrystalline samples and single crystal faces with low atomic densities tend to produce similar reaction product morphologies.

The strength of $(11\bar{2}0)$ alumina bicrystals bonded with sodium dihydrogen phosphate increased when the room temperature curing time was

increased from 3 to 24 hours. On the other hand, longer curing time caused the strength of (0001) alumina bicrystals to decrease. This suggests that it takes longer for the aluminum required to form the bond to go into solution from the $(11\bar{2}0)$ faces than it does from the (0001) faces. There is also evidence that the bonding phase present in the (0001) bicrystals may change from $\text{Al}(\text{PO}_4)_3$ to AlPO_4 as the curing time is increased.

The tensile strength of $(11\bar{2}0)$ and (0001) alumina bicrystals bonded with $\text{NaH}_2\text{PO}_4 \cdot \text{H}_2\text{O}$ increased as the surface finish of the single crystal faces was improved. The tensile strength of $(11\bar{2}0)$ alumina bicrystals bonded with sodium hydrogen phosphate or Glass H are greater than for (0001) bicrystals produced under the same conditions from crystals with equivalent surface finishes.

The tensile strength of $(11\bar{2}0)$ alumina bicrystals bonded with $\text{NaH}_2\text{PO}_4 \cdot \text{H}_2\text{O}$ varies with the amount of rotational mismatch between the crystals. The tensile strength decreased as the rotational mismatch was increased from 0 to 90° and then increased back to approximately its original level when the mismatch angle was increased from 90 to 180° . It appears that this strength pattern is related to the two fold symmetry of the $(11\bar{2}0)$ faces. The combination of both rotational and tilt mismatch reduced the tensile strength of $(11\bar{2}0)$ (0001) bicrystals to almost zero. The strength decreases associated with these types of bicrystal mismatches could be related to differences in thermal expansion with direction or bond misalignment.

The production of strong phosphate bonded bicrystals requires a good surface finish on the crystal faces being bonded. The load applied during room temperature curing must also be evenly distributed over the bond area

so the bond thickness will be uniform. In addition, in order to obtain maximum strengths it is necessary to minimize both rotational and tilt misalignment.

REFERENCES

1. Kingery, W. D. Fundamental Study of Phosphate Bonding in Refractories: I. Literature Review. J. Am. Ceram. Soc. v. 33, 1950, pp. 239-41.
2. Kingery, W.D. Fundamental Study of Phosphate Bonding in Refractories: II. Cold Setting Properties. *ibid*, pp. 242-47.
3. Souder, W. and Paffenbarger, G. C. Physical Properties of Dental Materials. Natl. Bur. Standards Cir. C433, 1942.
4. Crowell, W. S. Physical Chemistry of Dental Cements. J. Am. Dental Assoc. v. 14, 1927, pp. 1030-48.
5. Souder, W. and Schoonover, I. G. Probable Chemical Reactions in Silicate Cements. J. Dental Research. v. 18, 1939, p. 250.
6. Kingery, W. D. Fundamental Study of Phosphate Bonding in Refractories: IV. Mortars Bonded with Monoaluminum and Monomagnesium Phosphate. J. Am. Ceram. Soc. v. 35, 1952, pp. 61-63.
7. Gitzen, W. H., Hart, L. D., and MacZura, G. Phosphate-Bonded Alumina Castables: Some Properties and Applications. Bull. Am. Ceram. Soc. v. 35, 1956, pp. 217-23.
8. Sheets, H. D., Bulloff, J. V., and Duckworth, W. H. Phosphate Bonding of Refractory Compositions. Brick and Clay Record. No. 7, 1958, pp. 55-57.
9. Rickles, R. N. The Development of Castable Phosphate Cements, Their Chemistry, Properties, and Applications. Ph.D. Dissertation, Polytechnic Institute of Brooklyn, 1962.
10. Lyons, J. W., McEvan, G. J., and Siebenthal, C. D., Highway Research Bulletin Board No. 318, Highway Research Board, National Academy of Sciences - Nation Research Council, Washington, D.C., 1957, p. 318.
11. Lyon, J. E., Fox, T. U., and Lyons, J. W. An Inhabited Phosphoric Acid for Use in High-Alumina Refractories. Bull. Am. Ceram. Soc. v. 45, 1966, pp. 661-65.
12. Lyon, J. E., Fox, T. U., and Lyons, J.W. Phosphate Bonding of Magnesite Refractories. *ibid*, pp. 1078-81.
13. Bremser, A. H. and Nelson, J. A. Phosphate Bonding of Zirconia. *ibid*, v. 46, 1967, pp. 280-82.

14. Foessel, A. H. and Treffner, W. S. Improved Phosphate-Bonded Basic Refractories. *ibid*, v. 49, 1970, pp. 652-57.
15. Venable, C. L. and Treffner, W. S. X-ray Study on Phosphate Bonding in Refractories. *ibid*, pp. 660-63.
16. O'Hara, M. J., Duga, J. J., and Sheets, H.D. Jr. Studies in Phosphate Bonding. *ibid*, v. 51, 1972, pp. 590-95.
17. Chistyakova, A. A., Sivkina, V. A., Sadkov, V. I., Khashkovskaya, A. P., and Povyshiva, L. G. Aluminophosphate Binder. *Izv. Okad. Nauk. SSSR, Neorg. Mater., English Transl.* v. 5, 1969, pp. 1333-38.
18. Some Aluminum Orthophosphates. *ibid*, pp. 449-55.
19. Rashkovan, I. L., Kuz'minskaya, L. N., and Kopeikin, V. A. Thermal Transformations in the Aluminum Phosphate Binding Agent. *ibid*, v. 2, 1966, 464-72.
20. Medvedeva, V. M., Medvedev, A. A., and Tananaw, I. V. Thermal Transformations in an Alumino-Phosphate Binder by the Methods of Infrared Spectroscopy and X-ray Diffraction Study. *ibid*, v. 1, 1965, 193-99.
21. Kopeikin, V. A., Kudryashova, A. I., Kuz'minshaya, L. N., Rashkovan, I. L., and Tananaev, I. V. Formation of an Amorphous Phase in the Cementation of Materials Based on an Aluminophosphate Binder. *ibid*, v. 3, 1967, pp. 657-69.
22. Klyucharev, Y. V. and Skoblo, L. I. Compositions of the Products Formed by Hardening of the Aluminum Phosphate Binder in Refractory Corundum Compositions. *Zh. Prikl. Khim. English Translation.* v. 38, 1965, pp. 530-35.
23. Bromberg, A. V., Kasatkina, A. G., Kopeikin, V. A., Kuz'minskaya, A. I., Rashkovan, I. L., and Tananaev, I. V. Aluminum-Chromium Phosphate Binders. *Izv. Akad. Nauk SSSR, Neorg. Mater. English Translation.* v. 5, 1969, 805-807.
24. Lovrov, A. B., Medvedev, A. A., Chudinova, N. N., and Tananaev, I. V. Investigation of the Dehydration Products of Chromium Phosphate Hexahydrate. *ibid*, v. 6, 1970, pp. 503-10.
25. Fisher, K. Chemical Bonds for Refractory Materials. *Proc. Brit. Ceram. Soc.* No. 12, 1969, pp. 51-64.
26. Cassidy, J. E. Phosphate Bonding Then and Now. *Bull. Am. Ceram. Soc.* v. 56, 1977, 640-43.

27. Birchall, J. D. and Cassidy, J. E. Refractory Compositions. Brit. Pat. 1,357,541, 19 April 1971.
28. Diel, K. Solid Binder for Fire Proof Substances. W. German Pat. 2,412,474, 15 March 1974.
29. Fisher, R. E. Hot Strength of Phosphate-Bonded Refractory Plastics. Bull. Am. Ceram. Soc. v. 56, 1977, 637-43.
30. Gonzalez, F. J., and Halloran, J. W. Reaction of Orthophosphoric Acid with Several Forms of Aluminum Oxide. *ibid*, v. 59, 1980, 727-38.
31. Chvatal, T. The Position of Refractory Phosphate Bonding Today. Sprechsaal Keram. Glas. Baustoffe. v. 108, 1975, pp. 576, 78, 80, 82-89.
32. Preuss, E., Krahe-Urban, B., and Butz, R. Laue Atlas. John Wiley and Sons, London, 1974, pp. 60-67.
33. Cullity, B. D. Elements of X-ray Diffraction. Addison-Wesley Publishing Co., London, 1978, pp. 239-59.
34. Preuss, E. Plot Program for Laue Patterns and Stereographic Projections. Computer Physics Comm. v. 18, 1979, pp. 261-75.
35. Preuss, E. Calculation of Crystal Orientation Using Laue Patterns. *ibid*, 277-80.
36. Preuss, E. A Simplified Procedure for Orientation of Single Crystals of Any Structure. Acta Cryst. v. A29, 1978, pp. 86-90.
37. Saphikon Division of Tyco Laboratories, Inc., 51 Powers Street, Milford, NH 03055.